Vol. 59 • No. 2

February 2016

Microwave Journal .com

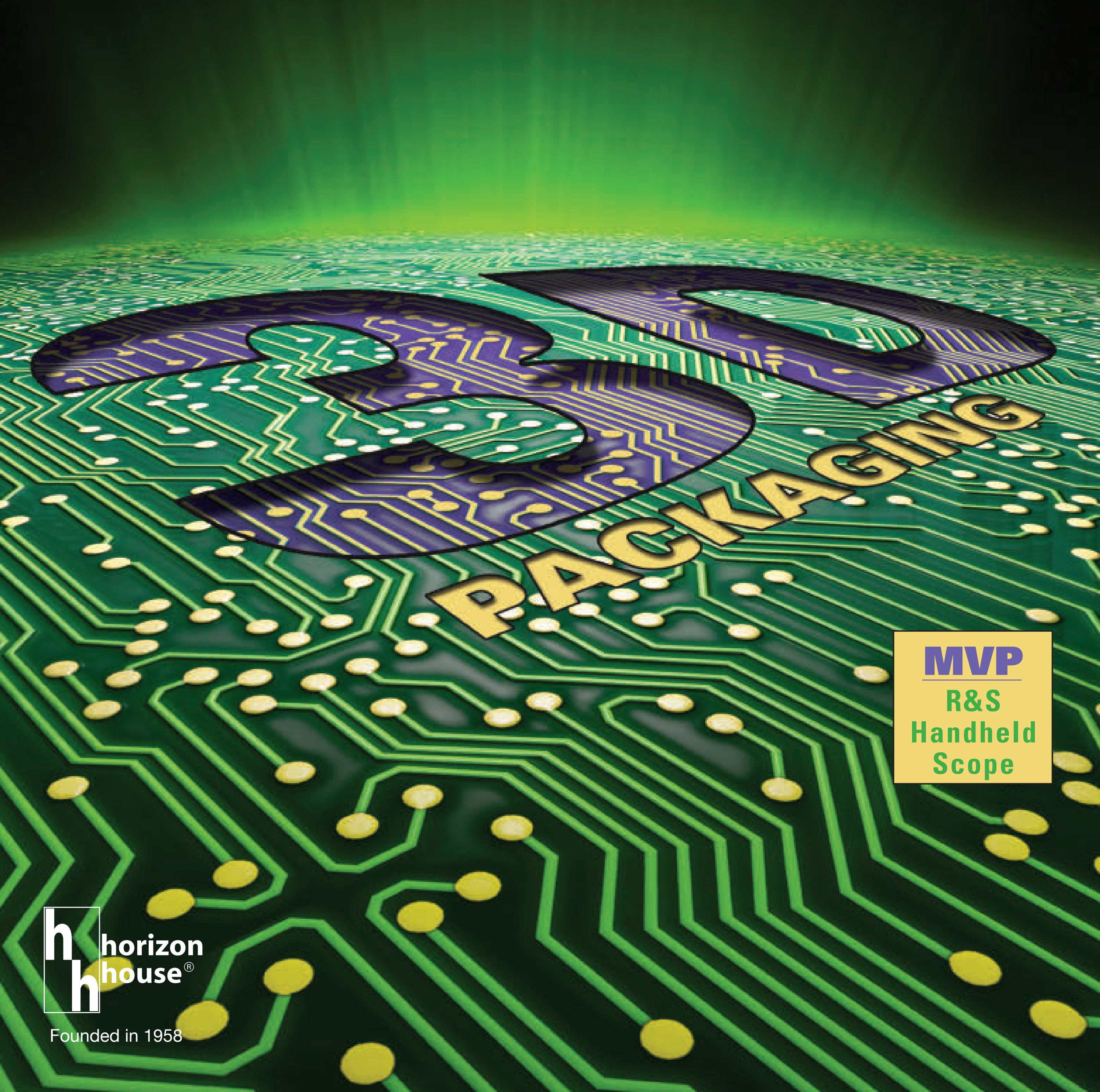

MVP
R&S Handheld Scope

horizon house®
Founded in 1958

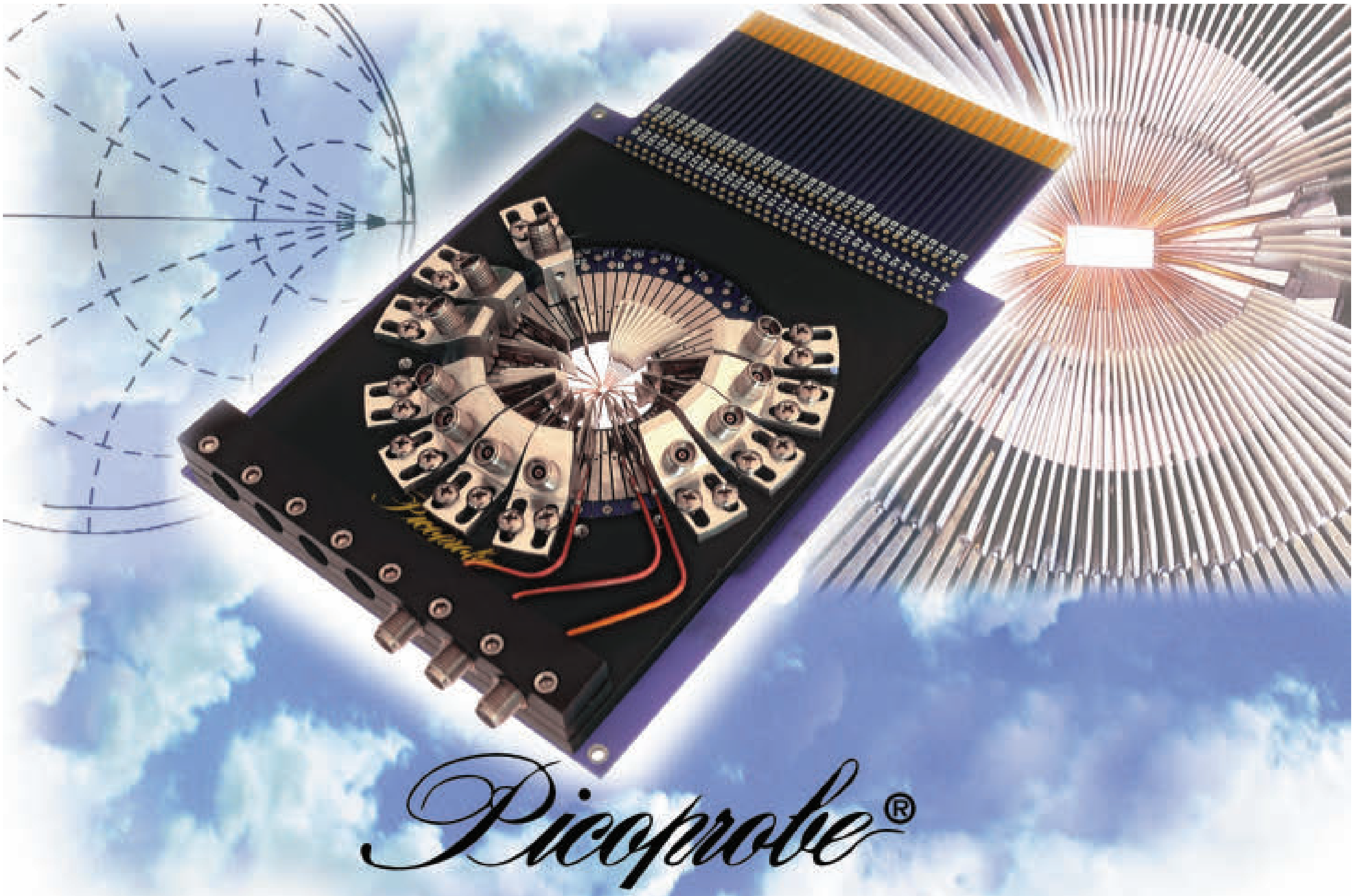

Picoprobe elevates probe cards to a higher level…

(…110 GHz to be exact.)

Since 1981, GGB Industries, Inc., has blazed the on-chip measurement trail with innovative designs, quality craftsmanship, and highly reliable products. Our line of custom microwave probe cards continues our tradition of manufacturing exceptional testing instruments.

Through unique modular design techniques, hundreds of low frequency probe needles and a variety of microwave probes with operating frequencies from DC to 40, 67, or even 110 GHz can be custom configured to your layout.

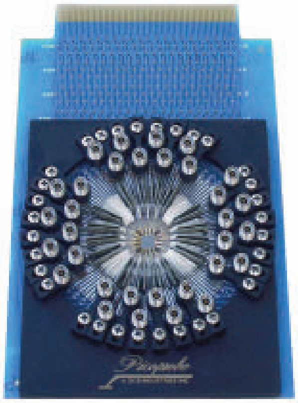

Our patented probe structures provide the precision and ruggedness you require for both production and characterization testing. And only Picoprobe® offers the lowest loss, best match, low inductance power supplies, and current sources on a single probe card.

Our proven probe card design technology allows full visibility with inking capability and ensures reliable contacts, even when probing non-planar structures.

Not only do you get all the attractive features mentioned, but you get personal, professional service, rapid response, and continuous product support--all at an affordable price so your project can be completed on time and within budget.

Typical Specs	10GHz	20GHz	40GHz
Insertion Loss	0.6 dB	0.8 dB	1.3 dB
Return Loss	22 dB	18 dB	15 dB

For technical assistance, custom product designs, or off-the-shelf delivery,call GGB Industries, Inc., at (239) 643-4400.

GGB INDUSTRIES, INC. • P.O. BOX 10958 • NAPLES, FL 34101

Telephone (239) 643-4400 • Fax (239) 643-4403 • E-mail email@ggb.com • www.picoprobe.com

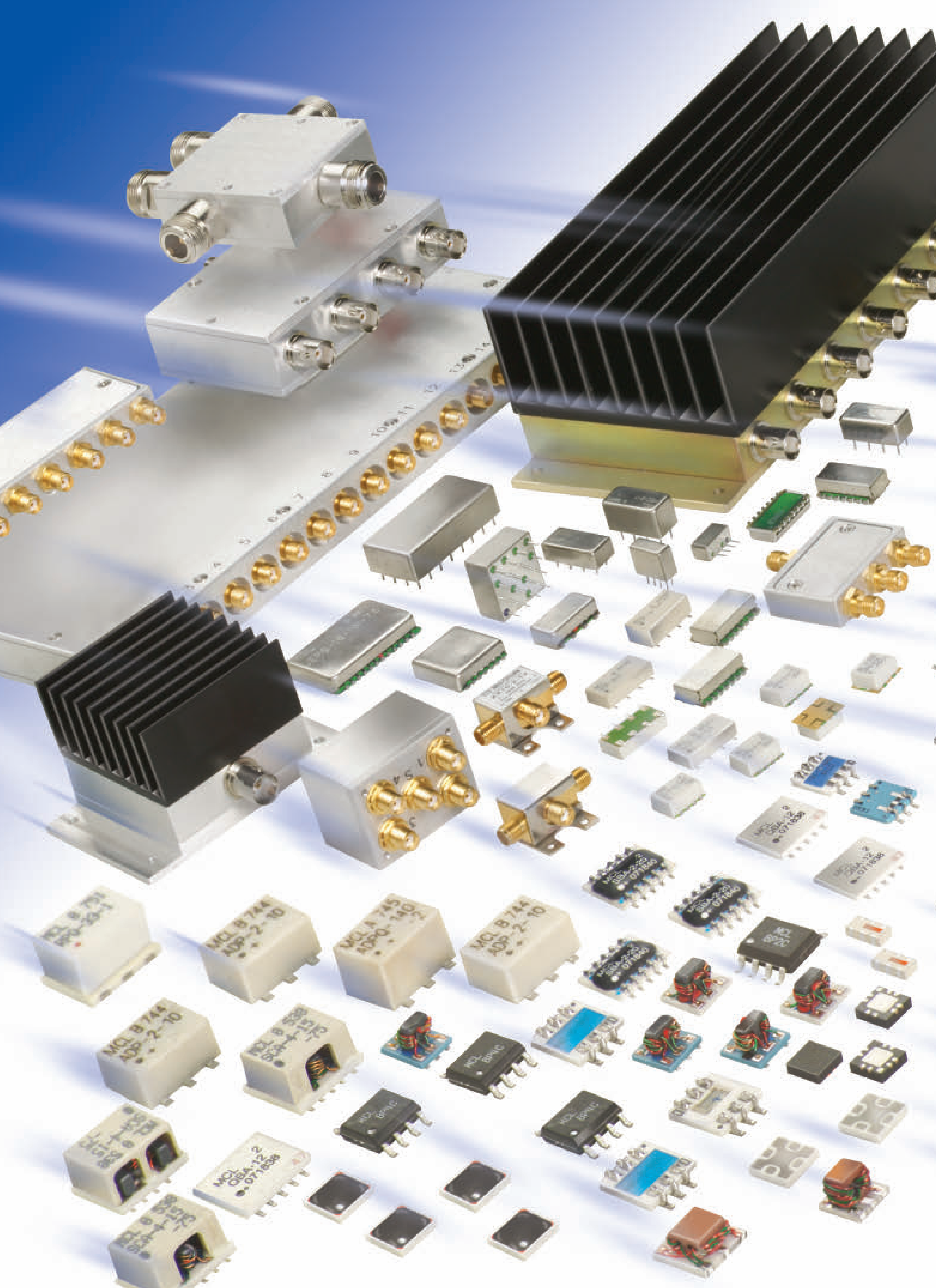
MCL B 744
ADP-2-10
MCL
QBA-12
071836

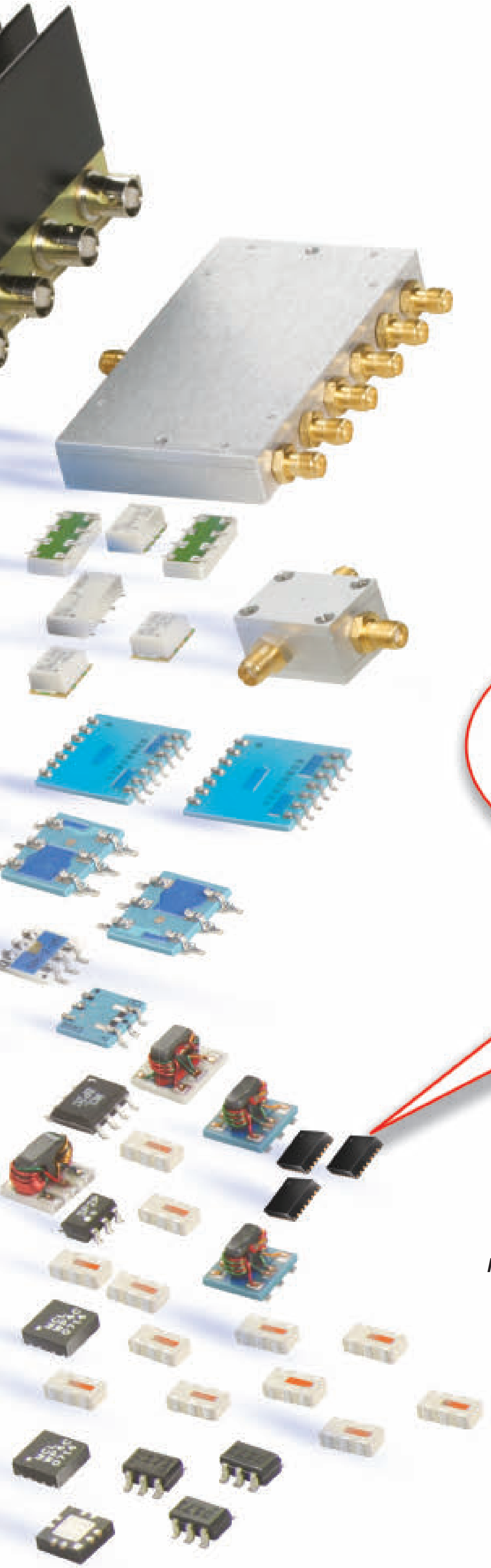

POWER SPLITTERS/ COMBINERS

from **2 kHz to 26.5 GHz** as low as 94¢ ea. (qty. 1000)

NEW!

THE WIDEST BANDWIDTH IN THE INDUSTRY IN A SINGLE MODEL!

EP2K1+ 2 to 26.5 GHz
EP2K+ 5 to 20 GHz
EP2C+ 1.8 to 12.5 GHz

The industry's largest selection includes THOUSANDS of models from 2 kHz to 26.5 GHz, with up to 300 W power handling, in coaxial, flat-pack, surface mount and rack mount housings for 50 and 75Ω systems.

From 2-way through 48-way designs, with 0°, 90°, or 180° phase configurations, Mini-Circuits' power splitter/combiners offer a vast selection of features and capabilities to meet your needs from high power and low insertion loss to ultra-tiny LTCC units and much more.

Need to find the right models fast? Visit minicircuits.com and use Yoni2®! It's our patented search engine that searches actual test data for the models that meet your specific requirements! You'll find test data, S-parameters, PCB layouts, pricing, real-time availability, and everything you need to make a smart decision fast!

All Mini-Circuits' catalog models are available off the shelf for immediate shipment, so check out our website today for delivery as soon as tomorrow!

RoHS Compliant
Product availability is listed on our website.

Mini-Circuits®

www.minicircuits.com P.O. Box 350166, Brooklyn, NY 11235-0003 (718) 934-4500 sales@minicircuits.com

448 rev Q

Technology On the Move™

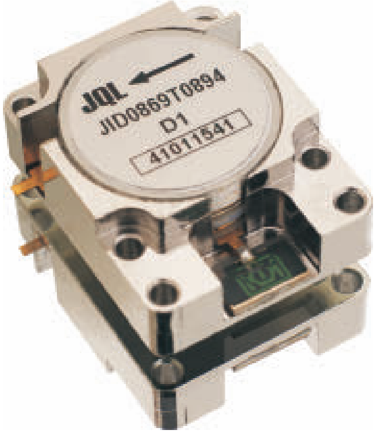

Drop-in Isolators

Cavity Filters

Surface Mount Circulators

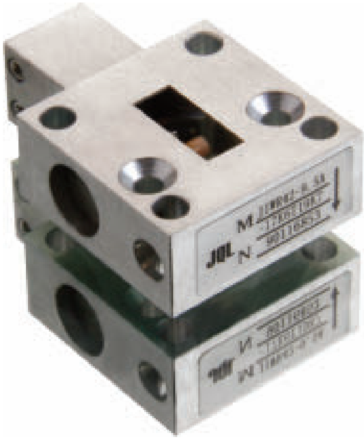

Waveguide Isolators

Power Combiners

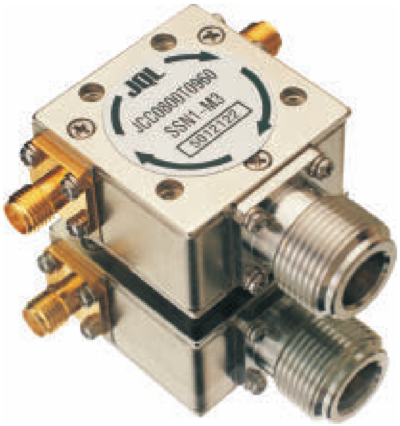

Coaxial Circulators

JQL

Tel:1(888)236-9828(US&Canada)
1(630)930-9917(Worldwide)
www.jqlelectronics.com sales@jqlelectronics.com

Microwave Journal
February 2016
Vol. 59 • No. 2
High Frequency Components and PCBs
mwjournal.com

CONTENTS

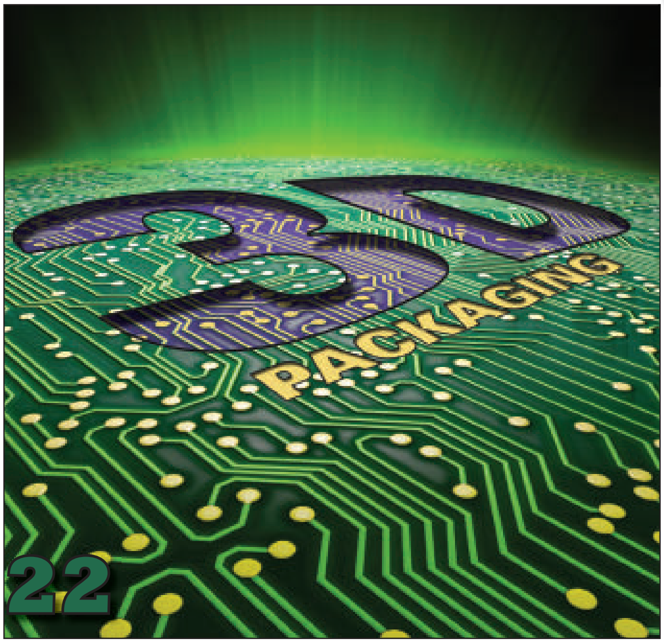

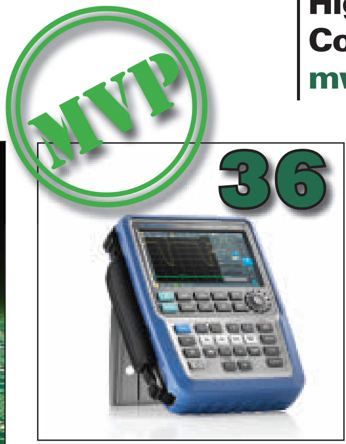

AUGMENTED REALITY: HOW IT WORKS

STEP 1	STEP 2	STEP 3
Download the free Layar app from the iTunes (iOS) or Google Play (Android) store.	Launch the app to view enhanced content on any page with the layar logo.	Frame the entire page in the screen and tap to experience enhancements (tap screen again for full screen view).

Look for the Layar logo on participating pages. **AR pages may expire after 30 days.**

59 YEARS OF PUBLISHING EXCELLENCE

Microwave Journal

CONTENTS

mwjournal.com

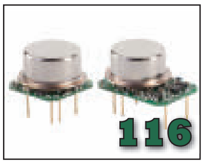

Microwave Journal (USPS 396-250) (ISSN 0192-6225) is published monthly by Horizon House Publications Inc., 685 Canton St., Norwood, MA 02062. Periodicals postage paid at Norwood, MA 02062 and additional mailing offices.

POSTMASTER: Send address corrections to *Microwave Journal*, PO Box 1143, Skokie, IL 60076 or e-mail mwj@halldata.com. Subscription information: (847) 763-4943. This journal is issued without charge upon written request to qualified persons working in the RF & microwave industry. Other subscriptions are: domestic, $120.00 per year, two-year subscriptions, $185.00; foreign, $200.00 per year, two-year subscriptions, $370.00; back issues (if available) and single copies, $10.00 domestic and $20.00 foreign. Claims for missing issues must be filed within 90 days of date of issue for complimentary replacement.

STAFF

Publisher: Carl Sheffres
Editor: Patrick Hindle
Technical Editor: Gary Lerude
Managing Editor: Jennifer DiMarco
Associate Technical Editor: Cliff Drubin
Multimedia Staff Editor: Leslie Nikou
Multimedia Staff Editor: Barbara Walsh
Consulting Editor: Harlan Howe, Jr.
Consulting Editor: Frank Bashore
Consulting Editor: David Vye
Consulting Editor: Raymond Pengelly
Electronic Marketing Manager: Chris Stanfa
Digital Content Production Specialist: Lauren Tully
Event Coordinator: Jacqueline Williams
Audience Development Manager: Carol Spach
Traffic Manager: Edward Kiessling
Director of Production & Distribution: Robert Bass
Art Director: Janice Levenson
Graphic Designer: Sachiko Stiglitz

EUROPE

International Editor: Richard Mumford
Office Manager: Nina Plesu

CORPORATE STAFF

CEO: William M. Bazzy
President: Ivar Bazzy
Vice President: Jared Bazzy

EXECUTIVE EDITORIAL OFFICE
685 Canton Street, Norwood, MA 02062
Tel: (781) 769-9750
FAX: (781) 769-5037
e-mail: mwj@mwjournal.com

EUROPEAN EDITORIAL OFFICE
16 Sussex Street, London SW1V 4RW, England
Tel: Editorial: +44 207 596 8730 Sales: +44 207 596 8740
FAX: +44 207 596 8749

SUBSCRIPTION SERVICES
Send subscription inquiries and address changes to:
Tel: (847) 763-4943
e-mail: mwj@halldata.com

BPA WORLDWIDE

www.mwjournal.com

Printed in the USA

Microwave Journal Online

Scan page using layar app

Visit us @ mwjournal.com

eLEARNING free webinars

5G Physical Layer Modeling: A Communication System Architect's Guide
Presented by: Keysight Technologies 2/4

RF and Microwave Heating Simulation and Application Design
Sponsored by: COMSOL 2/18

Large Signal Device Characterization for RF Power Amplifier Design
Sponsored by: National Instruments 2/23

Web Survey

What new packaging technology will take off in 2016?

Look for our multiple choice survey online at mwjournal.com

December Survey
Which ISM market will be the "next big app" for solid-state PAs?

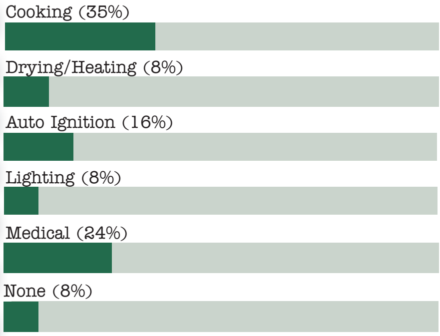

Executive Interviews

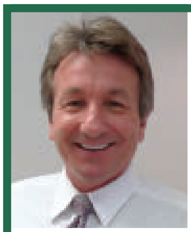

Mario Narduzzi, marketing manager for Communications Measurement Solutions at **Keysight Technologies**, discusses the modular test and measurement instrument market growth within Keysight in addition to overall market trends toward modular technologies and integrated solutions.

Thorsten Chmielus, founder and CEO of **Aaronia AG** explains his motivation and approach to technological development and product promotion, as well as his vision for the future.

WHITE PAPERS

Altair — *Electromagnetic Design in the Electronics Industry*

KEYSIGHT TECHNOLOGIES — *The Communication System Architect's Guide to 5G Physical Layer Modeling*

Catch *Frequency Matters*, the industry update from *Microwave Journal*, www.microwavejournal.com/FrequencyMatters

COM

MARCH

MARK YOUR CALENDAR

2/29–3/2 Arlington, Va.

9th Annual Military Radar Summit

As the only event in the United States that focuses exclusively on Military Radar, the summit again will bring together experts and thought leaders responsible for advancing critical discussion on this narrow and deep subject. Whether by land, sea, or air, military radar is used everywhere and requires consistent reexamination to achieve maximum performance. Come ready to learn and engage as this community works towards developing the next generation of capabilities for this essential technology.
www.militaryradarsummit.com

2

WEBINAR

Millimeter Wave and E-Band Vector Network Analyzer Solutions

Sponsored by:

Anritsu
envision : ensure

10

WEBINAR

Sponsored by:

KEYSIGHT TECHNOLOGIES

7-10

SATELLITE 2016

National Harbor, Md.

SATELLITE is the conduit for innovation in satellite technology — bringing the leaders, and market leading companies and brands behind this transformation together in one place. SATELLITE is one of the most important global satellite communications event of the year, and largest gathering of ALL markets in the satellite community. This year's program is built around focusing on these issues and much more.
www.satshow.com/conference

14-17 Orlando, Fla.

GOMACTech

GOMACTech was established primarily to review developments in microcircuit applications for government systems. Established in 1968, the conference has focused on advances in systems being developed by the Department of Defense and other government agencies and has been used to announce major government microelectronics initiatives such as VHSIC and MIMIC, and provides a forum for government reviews.
www.gomactech.net

16

WEBINAR

Sponsored by:

NATIONAL INSTRUMENTS

21-25 Las Vegas, Nev.

IWCE International Wireless Communications Expo

Since 1977, the International Wireless Communications Expo (IWCE) has been the authoritative annual event for communications technology professionals in the working world. IWCE features over 370 exhibitors showcasing the latest products and trends in the industry. Over 7,000 individuals attend from a diverse group of industry professionals including government/military, public safety (law enforcement, fire service, emergency medical & 911), utility, transportation and business enterprise. **www.iwceexpo.com**

23-24 Paris, France

Microwave & RF

Microwave & RF 2016 is dedicated to radio frequencies, microwave, wireless, EMC and optical fiber solutions. In its 5th year, the event will be held with two other complementary exhibitions: MtoM & Connected Objects and Embedded Systems. Session topics will include EMC, photonics and microwave, RFID, non-standard antennas, wireless solutions for automotive applications and active antennas.
www.microwave-rf.com

FOR DETAILS, VISIT MWJOURNAL.COM/EVENTS

Coming**Events**

CALL FOR PAPERS

EDI CON USA
February 28, 2016

RFIT
April 1, 2016

IEEE CSICS 2016
April 22, 2016

mwjournal.com

MARCH

IDGA Military Radar Summit
February 29–March 2, 2016 • Arlington, Va.
www.militaryradarsummit.com

Satellite 2016
March 7–10, 2016 • National Harbor, Md.
www.satshow.com

GOMACTech
March 14–17, 2016 • Orlando, Fla.
www.gomactech.net

IWCE
March 21–25, 2016 • Las Vegas, Nev.
www.iwceexpo.com

Microwave & RF
March 23–24, 2016 • Paris, France
www.microwave-rf.com

APRIL

WAMICON 2016
April 11–13, 2016 • Clearwater Beach, Fla.
www.wamicon.org

ARMMS RF & Microwave Society Conference
April 18–19, 2016 • Oxfordshire, UK
www.armms.org

EDI CON China 2016
April 19–21, 2016 • Beijing, China
www.ediconchina.com

MAY

AUVSI Xponential 2016
May 2–5, 2016 • New Orleans, La.
www.xponential.org

EW Europe
May 10–12, 2016 • Rotterdam, Netherlands
www.eweurope.com

DAS & Small Cells Congress
May 16–18, 2016 • Las Vegas, Nev.
www.dascongress.com

CS Mantech 2016
May 16–19, 2016 • Miami, Fla.
www.csmantech.org

RFIC 2016
May 22–24, 2016 • San Francisco, Calif.
www.rfic-ieee.org

IMS 2016
May 22–27, 2016 • San Francisco, Calif.
http://ims2016.mtt.org

Space Tech Expo
May 24–26, 2016 • Pasadena, Calif.
www.spacetechexpo.com

Aerospace Electrical Systems Expo
May 24–26, 2016 • Pasadena, Calif.
www.aesexpo.com

87th ARFTG Microwave Measurement Symposium
May 27, 2016 • San Francisco, Calif.
www.arftg.org

JUNE

Sensors Expo & Conference
June 21–23, 2016 • San Jose, Calif.
www.sensorsexpo.com

JULY

IEEE EMC
July 25–29, 2016 • Ottawa, Ontario
www.emc2016.emcss.org

NEMO 2016
July 27–29, 2016 • Beijing, China
www.nemo-ieee.org

AUGUST

RFIT 2016
August 24–26, 2016 • Taipei, Taiwan
www.rfit2016.org

SEPTEMBER

CTIA Super Mobility
September 7–9, 2016 • Las Vegas, Nev.
www.ctiasupermobility2016.com

EDI CON USA
September 20–22, 2016 • Boston, Mass.
www.ediconusa.com

OCTOBER

EuMW 2016
October 3–7, 2016 • London, UK
www.eumweek.com

Phased Array 2016
October 18–21, 2016 • Waltham, Mass.
www.array2016.org

EDI CON 2016 Electronic Design Innovation Conference 电子设计创新会议

Major Expansion for EDI CON China 2016

Patrick Hindle, Microwave Journal *Editor*

Exciting new developments are in store for EDI CON China in 2016, the Chinese year of the monkey. Key partnerships with industry leading events EMC China, sponsored by the China Electrotechnical Society (CES), and the China Radar Industry Association (CRIA) conference will greatly expand the overall technical program and audience. Both events will co-locate their conferences at the China National Convention Center (CNCC) in Beijing, April 19-21, 2016, forming a powerhouse event that is the largest high frequency/high speed design conference and exhibition in Beijing. EDI CON China aims to bring together the smartest minds in the industry while fulfilling the attributes of the monkey in Chinese culture — intelligence and power.

The China Electrotechnical Society's Electromagnetic Technology Conference & Exhibition (EMC China) is a natural extension of the EDI CON China event that already covers EMC/EMI topics but will now feature a comprehensive parallel conference and expanded exhibition. This will bring additional delegates to the event with a strong interest in EMC/EMI applications and products plus more exhibitors on the show floor. The China Radar Industry Association conference extends EDI CON China's coverage of radar topics with planned keynote talks addressing the latest advances in radar, phased arrays and space-based radar given by high-profile experts in the industry from China and the U.S. Dr. Eli Brookner, a leading radar expert who worked for Raytheon for more than 50 years, will give an update on advances in radar and phased array technology and Dr. Ben De from Nanjing Research Institute of Electronics Technology will discuss space-based radar topics.

Also new this year to the EDI CON China conference program is a full day track on silicon on insulator (SOI) and GaN semiconductor technology, as well as a full day track on radar measurement and modeling. The semiconductor track will feature a keynote talk by Peter Rabbeni Sr., director of the RF business development and product marketing at GLOBALFOUNDRIES, who will discuss the emergence of SOI in the RF/microwave industry. The conference will also provide a new program for the full day track on 5G technologies that will kick off with featured speakers from China Mobile and Ericsson, plus a panel session about the latest accomplishments in 5G research. There will also be featured tracks on amplifier modeling/measurement, IoT design, mmWave applications, high speed digital design, EMC/EMI measurement/modeling and system level measurement (LTE, Wi-Fi/802.11xx, radar, satellite communications and GNSS).

Dr. Wai Chen, chief scientist and general manager, Internet of Things Research Institute at China Mobile, will serve as Chairman for EDI CON China 2016 and participate in the plenary session discussing the latest developments in IoT.

The new partnerships allow for increased participation from companies involved in radar and EMC activities. Organized by the China Council for the Promotion of International Trade (CCPIT), a group of government laboratories and institutions will be representing the local aerospace and defense industry. In addition, a variety of companies will be demonstrating 5G test and measurement technologies, IoT applications, radar measurement and modeling, EMC testing and compliance, high speed design techniques and many other related technologies. Similar to last year's event, at least 15 participants are slated for the poster session on the exhibition floor.

EDI CON China 2016 will also debut educational courses. Zhancang Wang, author of the book, "Envelope Tracking Power Amplifiers for Wireless Communications," and former employee of Microsoft/Nokia, will teach "Doherty and High Efficiency Amplifier Design Techniques." Eli Brookner will cover "Advancements in MIMO and Phased Array Radar Technology." Each course will be two hours in length. Reserve your seat early for these classes as space is limited (go to www.ediconchina.com/registration to sign up).

In only its fourth year, EDI CON China has grown quickly by consistently adding relevant content, securing key partnerships and speakers, and attracting companies with worldwide reach. Please join us in Beijing, April 19-21, 2016 at the CNCC for this exciting three-day event. Visit www.ediconchina.com for the most up-to-date information. ■

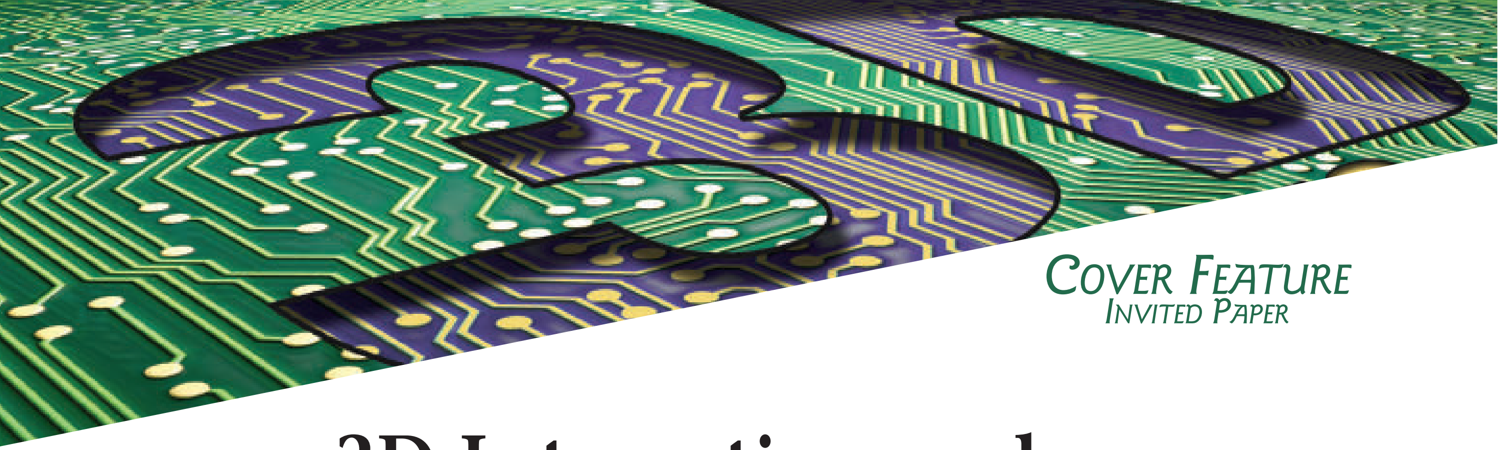

3D Integration and Packaging of mmWave Circuits and Antennas: Opportunities and Challenges

Ossama El Bouayadi, Yann Lamy, Laurent Dussopt and Gilles Simon
CEA-Leti, Grenoble, France

3D integration came as a response to the requirements of high performance and small footprint electronic devices. Today, the need for more heterogeneous integration schemes with increased functionalities becomes more obvious as the three worlds of digital, analog/mixed-signal (AMS) and RF electronics are converging. High performance computing, military, aerospace and medical devices stand among the market drivers for 3D integration technologies. While these niche applications can afford the relatively high cost of low volume customization, efforts are now focused on bringing vertical stacking and packaging solutions to mainstream and high volume applications for portable devices, entertainment and automobiles.

The underexploited millimeter wave (mmWave) frequency range (30 to 300 GHz) was restricted to niche applications, such as spectroscopy and military radar, until the late 70s. The front-end complexity and the need for nonstandard fabrication techniques kept the cost of mmWave modules out of reach of high volume and consumer markets. Since the early 80s, major advances have been demonstrated by R&D institutes[1] and achieved in the semiconductor industry, opening new horizons for a wide range of applications: high data rate communications, automotive radar, airborne and missile tracking systems, space spectrometry and imaging. Global revenue of the mmWave components market was estimated to be around $116 million in 2013 and is expected to reach $1.1 billion by 2018, which would be a compound annual growth rate (CAGR) of about 59 percent.[2] While this can be viewed by the industry as a great economic opportunity, the emerging applications are bringing specific challenges in terms of electrical performance, compactness, integration possibilities and system reliability. This article focuses on short to mid-range

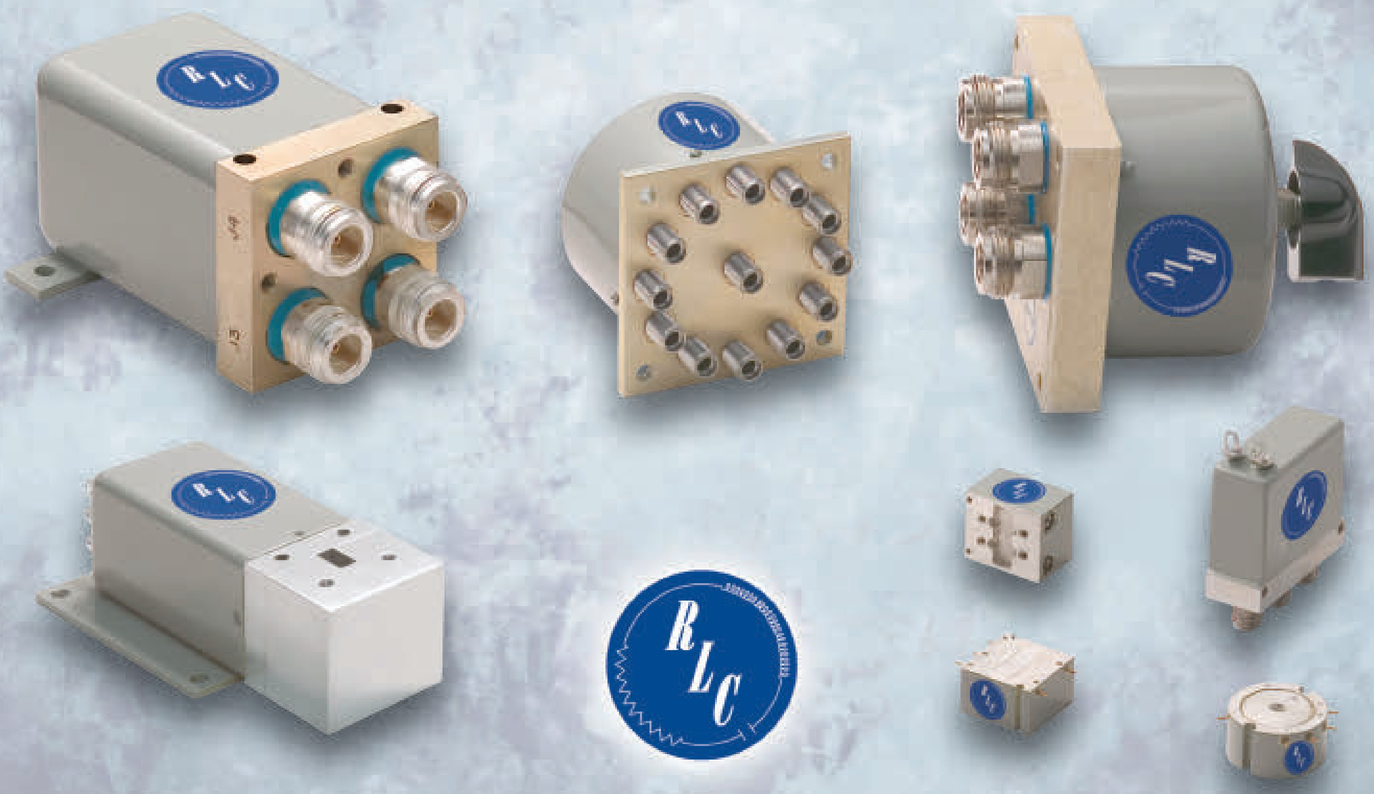

communication devices that illustrate some of the technical challenges related to the integration of wireless transceivers and their coexistence with other components. The short wavelengths at mmWave frequencies can be seen as an opportunity to integrate passive components whose typical dimensions become compatible with standard electronic packages. For some of the applications, bulky elements such as waveguides, connectors, nonplanar filters and large antenna arrays still slow the progress towards fully integrated and miniaturized systems. In the case of short-range, 60 GHz communications, portable devices are expected to be the main market driver for the coming decade — hence the need for fully integrated, compact and yet high performance transceivers. Regarding antennas, the miniaturization process is limited by the fundamental relation between the radiator's area and the achievable gain; this is often seen as the bottleneck for full integration of wireless transceivers.

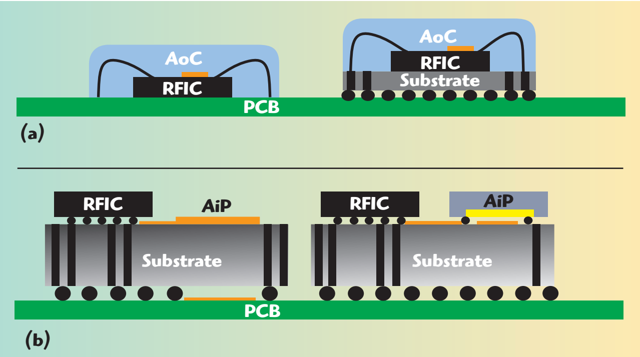

Fig. 1 AoC (a) and AiP (b) integration schemes.

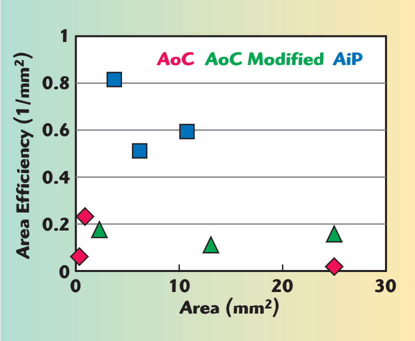

Fig. 2 Typical area efficiency for integrated antennas.

INTEGRATING TRANSCEIVERS WITH ANTENNAS

The antenna-on-chip (AoC) approach consists of integrating the radiating elements directly into the back-end stack of an RFIC chip, whether it is fabricated in CMOS, BiCMOS or III-V technology (see ***Figure 1a***). The main advantages of this solution lie in the absence of any RF interconnect and the co-integration of all RF and baseband functions on a single module a few square millimeters in size. However, for silicon-based AoCs, the high permittivity (ε_r = 11.7 to 11.9) and low resistivity ($\rho \sim 10\ \Omega\cdot$cm) of the substrate severely degrade the matching bandwidth and radiation efficiency. Still, the properties of AoC antennas can be improved by locally modifying the properties of the substrate. This can be done, for example, by etching an air cavity below the radiating element or by realizing a suspended membrane. The presence of an air layer in both cases minimizes the dielectric loss and lowers the effective permittivity. Other innovative solutions include the local modification of the silicon substrate resistivity using an ion-implantation process or the above-IC integration of coupled radiating elements.

In an antenna-in-package (AiP) integration approach, the antenna is realized on a separate substrate, independent of the RFIC chip (see ***Figure 1b***). This substrate can either be specifically dedicated to the radiating element and its feeding lines or play the role of a package for transceiver assembly and heterogeneous integration. For this reason, AiP designs play a key role in a 3D integration scenario for mmWave transceivers, while giving an additional degree of freedom with the choice of low permittivity and/or high resistivity substrates. Moreover, the area allowed for the antenna stage can be greater than what is allowed by AoCs. Consequently, a valid base of comparison of integrated antenna performance should take into account the allocated area, and we can define a new figure of merit normalizing the realized gain (in linear scale) per unit area. ***Figure 2*** plots a literature survey of 60 GHz integrated antennas,

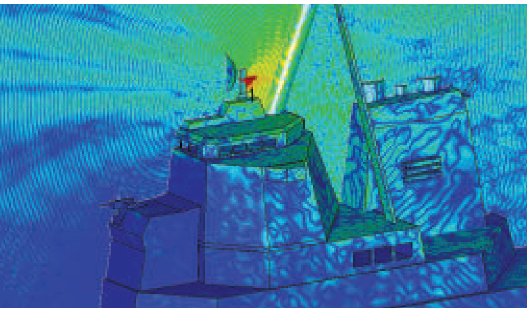

TABLE 1

QUALITATIVE COMPARISON OF SILICON AND GLASS INTERPOSER TECHNOLOGIES

Material	Pros	Cons
Silicon	• Line/Space < ~1 µm • Manufacturability • Thermal Management	• TSV Extra Cost • Post-Thinning Warpage • Need for HR Substrates • Isolator (SiO_2) Barrier for Via
Glass	• Very Low Loss Substrates • Low Cost Materials • High Volume Panel Manufacturing • Roll-to-Roll Processing • Hermetic Assembly	• Thermal Management • Supply Chain • Via Drilling and Filling • Warpage Management (Large Panels)

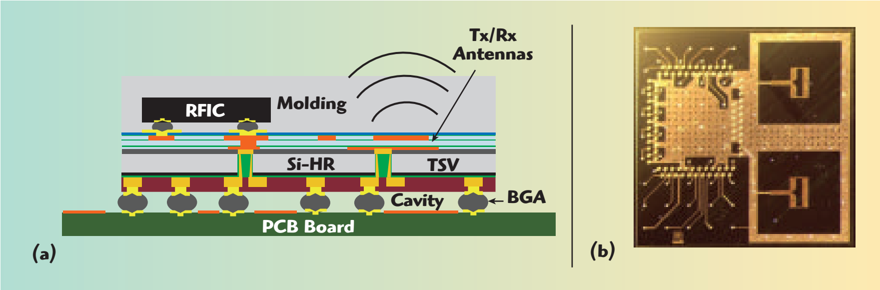

▲ *Fig. 3 Schematic cross section of the 60 GHz module (a) and microphotograph of the silicon interposer chip (b).*

showing that the gain of AiPs is two to four times higher than AoCs, due to the use of low loss substrates instead of CMOS-grade silicon.

MAINSTREAM mmWAVE PACKAGING

The selection of a given technology for the integration of wireless transceivers is a trade-off between several constraints: electrical performance, thermo-mechanical reliability, compactness, manufacturability and cost. Inherited from the well established and mature PCB technology, today's high density interconnect (HDI) design rules allow lines and gaps below 40 µm and micro-via formation with diameters under 100 µm, which are compatible with the requirements of mmWave integration. Moreover, the new generation of multi-layer organic (MLO) packages uses high quality dielectrics in both thin and thick film configurations. As a result, standard FR-4 cores and redistribution-layer laminates are progressively being replaced with low loss dielectrics such as the RO family and liquid crystal polymers (LCP). As one example, STMicroelectronics developed a 60 GHz, HDI, organic package using a technology based on a symmetric stack-up with an RO4003C core.[3]

In the same context, ceramic packages were introduced about two decades ago to meet the needs of critical systems, thanks to their properties of chemical stability, mechanical reliability and hermetic assembly. Ceramic processing allows the creation of a variety of via and cavity structures as well as the assembly of external capacitors and inductors. The vertical resolution for standard multilayer ceramic packages is around 50 µm. The two main multilayer ceramic processes currently used are low temperature co-fired ceramic (LTCC) and high temperature co-fired ceramic (HTCC), with respective maximal co-firing temperatures of about 900°C and 1600°C. While the HTCC process provides a great physical stability to the package, only high melting point metals such as tungsten (T_f = 3422°C) and molybdenum (T_f = 2623°C) can be used for routing in the internal layers. Unfortunately, these metals exhibit relatively low conductivity (8.9×10^6 and 18.7×10^6 S/m, respectively) compared to LTCC's copper, titanium/gold alloy or

silver metallization, which have lower conductive losses at high frequencies. Several convincing contributions from the industry can be found in the literature, such as IBM's 60 GHz LTCC module along with an MLO package (RO4000 and LCP).[4,5]

One of the fastest growing packaging technologies, embedded wafer-level ball grid array (eWLB) is a wafer-level packaging approach that combines advanced redistribution layer processing with a wafer-to-molding transfer technique. The molding polymer plays a double role in protecting the ICs and supporting fan-out routing. The eWLB processes (including under-bump metallization) are inherited from silicon micro-fabrication lines. Thanks to the use of low stress molding polymers, eWLB packages can be suitable for large packages featuring antenna arrays, while ensuring a line/space critical dimension around 15 µm. Several demonstrations of mmWave packages with integrated antennas can be found in the literature, with an emphasis on radar applications as demonstrated by Linz University and DICE GmbH.[6,7] This recent technology offers promising perspectives for 3D integration thanks to package-on-package (PoP) assembly possibilities using through-package interconnects.

Today's silicon back-end lines provide a large panel of micro-fabrication techniques to realize systems-in-package (SiP), such as micromachining, photolithography, ion and laser etching as well as a large panel of deposition and lamination techniques. Standard silicon processes can easily achieve micron resolutions and meet the requirements of mmWave and even sub-THz systems. In the last five years, organic and silicon interposer packages have been popularized by ASIC and memory applications, but recent trends in heterogeneous integration show more demonstrations of RF functionality as well as the introduction of glass as a potential candidate for high frequency applications.

SILICON VS. GLASS INTERPOSERS

As stated before, silicon microfabrication is particularly suitable for mmWave applications thanks to the unequaled resolutions with mature and standard back-end processes. Silicon packages provide excellent thermal conductivity ($\sigma \sim 150$ W·m^{-1}·K^{-1} at 25°C) compared to ceramics ($\sigma <$ 20 W·m^{-1}·K^{-1}) and PCB materials ($\sigma <$ 1 W·m^{-1}·K^{-1}), important in a typical scenario where an external power amplifier is assembled with the transceiver chip.

Recent years have produced increasing interest for 2.5D and 3D glass interposers and the new integration opportunities they offer. Glass substrates are known to have excellent dielectric properties with a low dielectric constant ($\varepsilon_r \sim 4$ to 6, depending on the composition and process) and a low loss tangent, which make them good candidates for RF packaging and passives integration. ***Table 1*** compares glass and silicon interposers. The replacement of wafers with large panels favors mass production, while significant advances have been made in through-glass-via (TGV) drilling and filling as well as redistribution layer (RDL) processing. Today's glass interposer task force is driven by manufacturers and suppliers such as Asahi, Corning Glass and 3D Glass Solutions as well as academic research organizations such as Georgia Tech, which leads an international interposer consortium. However, the supply chain for glass panels and processing equipment is not as well defined as for silicon, organic, ceramic and eWLB technologies. 2.5D/3D glass interposer technology is more likely to reach full maturity with the next generation of 3D integrated devices; currently, it is adequate for niche applications such as high performance computing and datacenters, where there are less concerns about cost.[8]

The first fully functional interposer package developed at CEA-Leti is based on a high resistivity ($\rho > 1$ kΩ·cm), 120 µm thick silicon substrate with two front-side and one back-side copper redistribution layers. Each side of the interposer carries an under-bump metallization used, respectively, for RFIC flip-chip (using copper pillars or micro-bumps) and package assembly on the main PCB board using ball grid array (BGA) solder balls.[9] The two sides of the interposer chip are interfaced using copper-filled through-silicon-via (TSV) interconnects with 60 µm diameter (an aspect ratio of 2:1). The total area

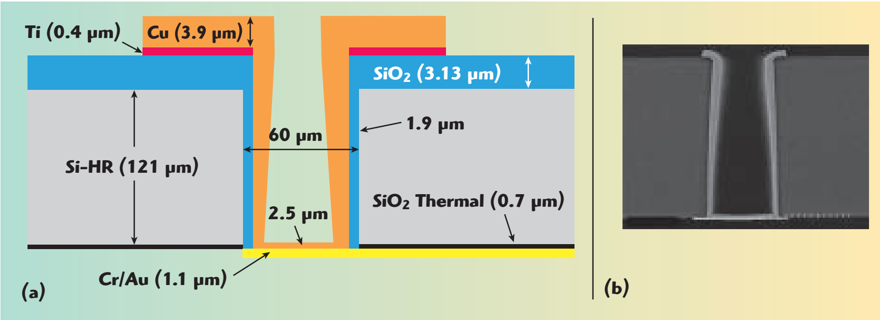

▲ *Fig. 4 Schematic cross section (a) and SEM view (b) of a TSV-Last.*

of the interposer is 6.5 mm × 6.5 mm, making it the most compact 60 GHz transceiver with integrated antennas reported to date. ***Figure 3a*** shows an unscaled cross section of the module with the interposer, RFIC chip and the molding polymer used to ensure the integrity of the assembly. The 60 GHz RFIC transceiver is fabricated using 65 nm CMOS technology.[10] Two folded dipole antennas (for transmit and receive) are hosted on the upper front-side RDL level. A guard ring made of a copper strip and an array of TSVs is used to mitigate surface wave coupling between the two cavity-backed antennas (see ***Figure 3b***).

This module is a typical demonstration of a 2.5D integration scheme, where the RFIC is assembled on top of the interposer and placed with an offset from the antennas. The vertical interconnects are realized using Leti's custom TSV Via-Last process. ***Figure 4*** shows a cross section and SEM image of a TSV. While the main function of TSV interconnects in the transceiver is to drive low frequency and baseband signals, the test vehicle included additional test features to investigate their suitability for mmWave through-package routing and back-side antenna feeding. The TSV electrical performance has been investigated using RF

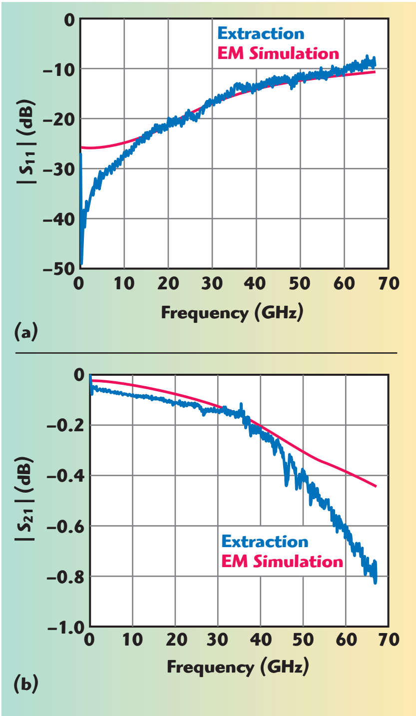

▲ *Fig. 5 Reflection (a) and transmission (b) of a 50 Ω terminated TSV transition in the GSG configuration.*

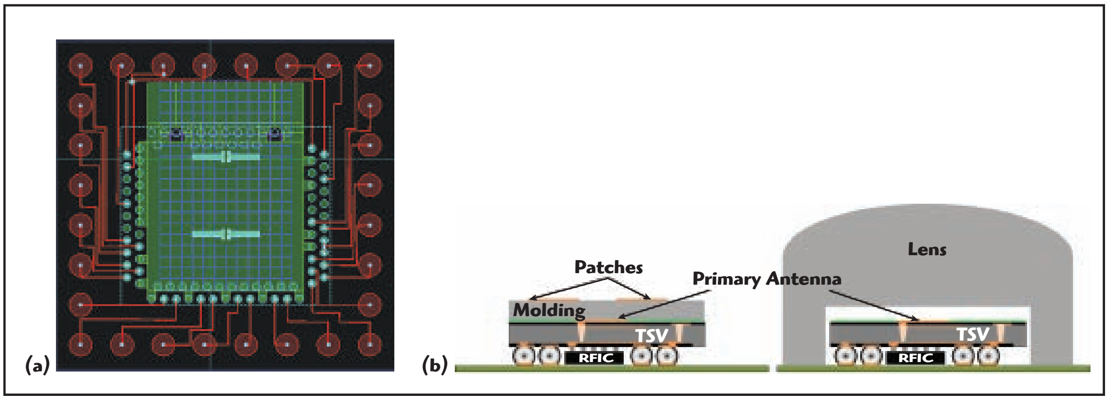

◀ *Fig. 6 Simplified layout of the 3D interposer, courtesy of A. Moknache (a) and new 3D integration schemes with HIS-based antennas (b).*

probe measurement and proper de-embedding techniques to extract the broadband response of a single GSG transition across DC to 67 GHz.[11] The transitions demonstrated about 0.6 dB insertion loss at 60 GHz, with the impedance mismatch to the 50 Ω terminations as a major contributor, i.e., 0.46 dB (see ***Figure 5***). In addition to broadband characterization, baseband signal integrity has been investigated using an inverse Fourier transform of the frequency domain response. The transient eye diagram analysis with a 5 Gbps pseudo-random binary sequence (PRBS) demonstrated an eye opening of 96 percent.

ONGOING DEVELOPMENT

The ongoing research at Leti aims to create a new generation of mmWave interposer packages with enhanced electrical and mechanical properties and reasonable cost and manufacturability, compared to other competing technologies. The new module, currently undergoing layout and prefabrication analysis, keeps the same overall thickness as the first demonstrator; however, the total area is reduced by about 33 percent (from 6.5 mm × 6.5 mm to 5.3 mm × 5.3 mm) thanks to an integrated high impedance surface (HIS) reflector design (see ***Figure 6a***).[12] Two evolutions are being evaluated to enhance antenna performance, as shown in ***Figure 6b***. The first involves laminating a molding polymer on top of the interposer and processing metal parasitic patches to enhance the bandwidth. The second aims to provide mid-range communication capabilities (around 10 m) with an external dielectric lens. In this case, the targeted gain at 60 GHz is 15 dBi. The proposed lens designs are based on hemispherical and parabolic geometries using PA6-class machined plastics (ε_r = 4.3). Two of the four designs, with 6

mm and 1 cm diameter hemispherical lenses, have been experimentally validated. The first measurement used an open WR15 waveguide feed and demonstrated gains of 12 to 16 dBi across 57 to 66 GHz. Following a system-level validation workflow, the lenses have been co-integrated with a 60 GHz QFN transceiver module[13] and demonstrated a range improvement by factors of four for one transmit lens and 7.5 for transmit and receive lenses. ■

ACKNOWLEDGMENT

This work is partially supported by the French Ministry of Defense, DGA (Direction Générale de l'Armement) and the Carnot Institut program under the "RF INTERPOSER" project.

References

1. L. Dussopt, Y. Lamy, J. Lantéri, H. Sibuet, B. Reig, C. Dehos, P. Vincent, S. Joblot, P. Bar and J.F. Carpentier, "Silicon Interposer with Integrated Antenna Array for mmW Short Range Communications," *IEEE International Microwave Symposium*, Montreal, Canada, 2012.
2. Research and Markets, "Millimeter Wave Market — By Technology, Components, Products and Applications," www.researchandmarkets.com.
3. R. Pilard, D. Titz, F. Gianesello, P. Calascibetta, J. Riviere, J. Lopez, R. Coffy, E. Saugier, A. Poulain, F. Ferrero, C. Luxey, P. Brachat, G. Jacquemod and D. Gloria, "HDI Organic Technology Integrating Built-In Antennas Dedicated to 60 GHz SiP Solution," *IEEE Antennas and Propagation Society International Symposium (APSURSI)*, Chicago, Ill., 2012.
4. D.G. Kam, D. Liu, A. Natarajan, S.K. Reynolds and B.A. Floyd, "Organic Packages with Embedded Phased-Array Antennas for 60 GHz Wireless Chipsets," *IEEE Transactions on Components, Packaging and Manufacturing Technology*, Vol. 1, No. 11, p. 1806, 2011.
5. D.G. Kam, D. Liu, A. Natarajan, S. Reynolds and B. Floyd, "Low-Cost Antenna-in-Package Solutions for 60 GHz Phased-Array Systems," *IEEE 19th Conference on Electrical Performance of Electronic Packaging and Systems (EPEPS)*, Austin, Texas, 2010.
6. A. Fischer, Z. Tong, A. Hamidipour, L. Maurer and A. Stelzer, "A 77 GHz Antenna in Package," *41st European Microwave Conference (EuMC)*, 2011.
7. M. Wojnowski, C. Wagner, R. Lachner, J. Böck, G. Sommer and K. Pressel, "A 77 GHz SiGe Single-Chip Four-Channel Transceiver Module with Integrated Antennas in Embedded Wafer-Level BGA Package," *62nd ECTC*, San Diego, Calif., 2012.
8. 3DInCites, "Glass vs. Silicon Interposers for 2.5D and 3D IC Applications," www.3dincites.com.
9. C. Ferrandon, A. Jouve, S. Joblot, Y. Lamy, A. Schreiner, P. Montmeat, M. Pellat, M. Argoud, F. Fournel, G. Simon and S. Cheramy, "Innovative Wafer-Level Encapsulation & Underfill Material for Silicon Interposer Application," *IEEE Electronic Components and Technology Conference (ECTC)*, Las Vegas, Nev., 2013.
10. A. Siligaris et al., "A 65-nm CMOS Fully Integrated Transceiver Module for 60 GHz Wireless HD Applications," *IEEE Journal of Solid-State Circuits*, Vol. 46, No. 12, pp. 3005–3017, 2011.
11. T. Lacrevaz, C. Bermond, O. El Bouayadi, G. Houzet, P. Artillan, Y. Lamy, K. Dieng and B. Flechet, "Electrical Broadband Characterization Method of Dielectric Molding in 3-D IC and Results," *IEEE Transactions on Components, Packaging and Manufacturing Technology*, Vol. 4, No. 9, pp. 1515–1522, 2014.
12. O. El Bouayadi, Y. Lamy and D. Laurent, "A High-Impedance Surface Antenna On Silicon Interposer for 3D Integrated mmW Transceivers," *European Microwave Week*, Rome, Italy, 2014.
13. J. Zevallos Luna, L. Dussopt and A. Siligaris, "Packaged Transceiver with On-Chip Integrated Antenna and Planar Discrete Lens for UWB Millimeter-Wave Communications," *IEEE International Conference on Ultra-Wideband*, Paris, France, 2014.

Most Valuable **Product**

Scan page using layar app

A Lab Oscilloscope in a Handheld Package

Rohde & Schwarz
Munich, Germany

Field applications are gaining in complexity, and even machinery on the production floor is employing increasingly elaborate electronics. Such environments call for a portable instrument able to adapt and capable of testing relevant functionality. Designed specifically to address such complexities, the R&S Scope Rider is a handheld oscilloscope with the functionality, touch and feel of a state-of-the-art lab oscilloscope.

Combining five instruments in a compact format, the instrument is based on a high performance oscilloscope featuring a precise digital trigger system, 33 automatic measurement functions, XY diagram mode (see ***Figure 1***) and mask test mode (see ***Figure 2***). It also functions as a logic analyzer with eight additional digital channels, as a protocol analyzer with trigger and decoding capability, as a data logger and as a

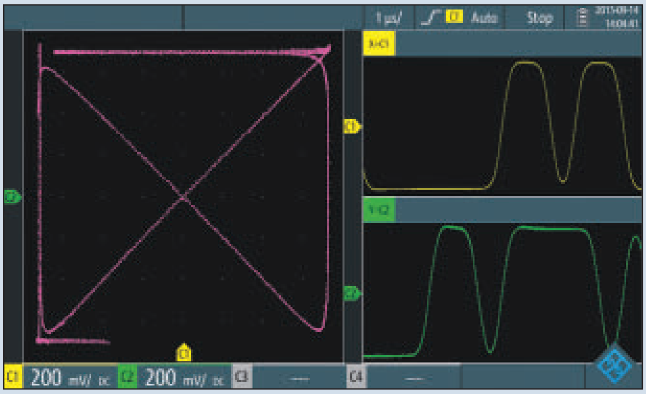

▲ *Fig. 1 Relative phases between two signals can be easily measured with the dedicated XY mode that also shows the individual time signals.*

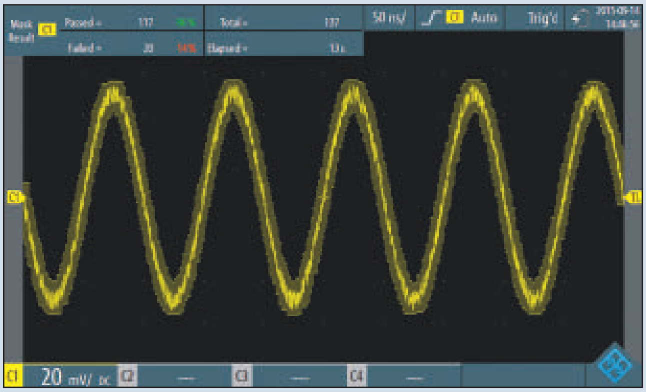

▲ *Fig. 2 The mask test mode shows pass and fail statistics, making it easy to set up masks based on test signals.*

RF-LAMBDA
THE POWER BEYOND EXPECTATIONS
ITAR & ISO9000
Registered Manufacture
Made in USA
ITAR
LEADER OF RF
BROADBAND SOLUTION
ULTRA BROADBAND
LOW NOISE AMPLIFIER
R50G69GSC
(50-69GHZ LNA)
RLNA00M50GA
(0.01-50GHZ LNA)
ULTRA BROADBAND
POWER AMPLIFIER
RFLUPA01G22GA
(1-22GHZ 8W)
RFLUPA0618GC
(6-18GHZ 25W)
RFLUPA32G38GB
(32-38GHZ 10W)
RFLUPA0706GF
(0.7-6.0GHZ 35W)
BROADBAND RF
SYSTEM AC AMPLIFIER
RAMP27G34GA
(27-34GHZ 10W)
RAMP02G06GB
(2-6GHZ 50W)
www.rflambda.com
sales@rflambda.com
1-888-976-8880
1-972-767-5998
Plano, TX, US
San Diego, CA, US
Ottawa, ONT, Canada

digital multimeter. The following outlines the implementation of these functions:

Logic analyzer: The digital logic probe (MSO) of the new oscilloscope features eight additional digital inputs for analyzing control signals, time correlated to the analog channel signals. With 250 MHz bandwidth, 1.25 GSPS sampling rate and configurable thresholds, it adapts to almost any digital interface.

Protocol analyzer: Protocols such as I2C or SPI are frequently used for transferring control messages between integrated circuits. The R&S Scope Rider has a trigger and decoding capability for in-depth troubleshooting. Triggering on protocol events or data enables selective acquisition of relevant events, data and signals.

Data logger: Sporadic sensor signal faults or rare glitches in a power supply can cause complex system failures without any obvious indication of the root cause. The long-term data logger makes it possible to monitor up to four key measurements at a speed of 1, 2 or 5 measurements per second to uncover such rare failures. The large memory of 2 million samples per channel allows more than 23 days of log duration. The statistics display provides information about minimum and maximum values with exact times.

Digital multimeter: The two channel variant features a dedicated, isolated digital multimeter with 10,000 count resolution. Measurement functions include AC, DC, AC + DC voltage, resistance, continuity and capacitance as well as current or temperature with suitable shunts. The four channel variant features a digital voltmeter on each input channel. Statistics information shows minimum, average and maximum values with corresponding time stamps.

EASE OF USE

The handheld oscilloscope is equipped with a large format, high resolution capacitive color touch screen, allowing it to be operated as intuitively as a tablet PC. Oscilloscope settings can easily be adjusted on the screen while dedicated keys provide quick access to important oscilloscope functions. A central multifunction wheel allows adjustment of settings, such as the trigger level or the vertical position of each channel. Fully controllable via the keypad, the oscilloscope can also be used with gloves when required for safety or weather conditions.

Easy-to-understand diagrams explain important settings such as the trigger mode, the automatic measurement functions or the channel settings. The Scope Rider has an acquisition rate of 50,000 waveforms per second (see ***Figure 3***), a 10-bit A/D converter and a maximum bandwidth of 500 MHz for analog input channels.

In addition to a microSD card, the instrument features USB and Ethernet ports for uncomplicated storage and transfer of measurement data. Measurement documentation is simplified with documentation project directories on the microSD card or USB flash drive. Screenshots, measurement results and settings files are saved with a single button press in the selected project directory. Data can easily be accessed and downloaded using the web browser interface.

The R&S Scope Rider also has an integrated WLAN interface. This can be

MORION US

80 YEARS OF STABILITY

Ultra-Low Phase Noise OCXOs 10 & 100 MHz

MV317

- Frequency range: 80-120 MHz
- Aging ±1E-7 per Year
- Package: 25.4 x 25.4 x 10.3 mm

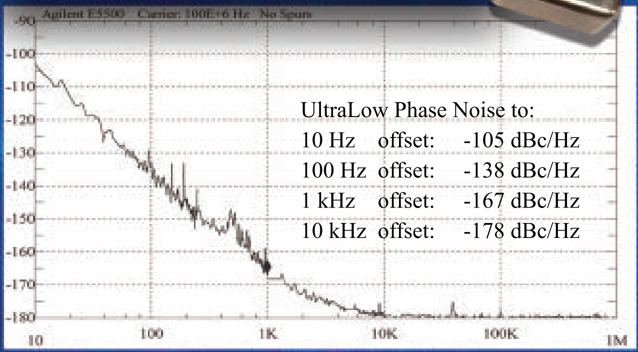

MV269

New

- Frequency range: 60-120 MHz
- Aging: ±1E-7 per Year
- Package: 20.3x12.7x9.5 mm (DIL14)

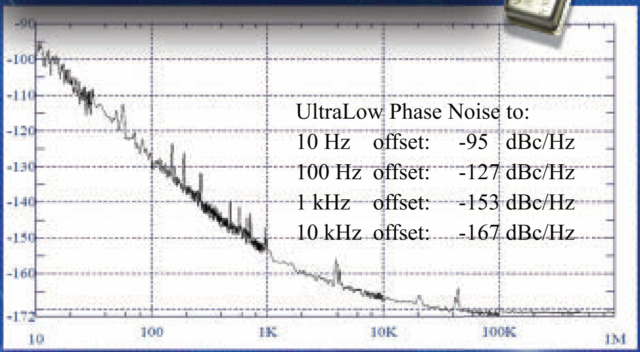

MV341

- Standard Frequency: 10 MHz
- Allan Deviation: <2E-13 per Sec.
- Package: 50.8 x 50.9 x 16.0 mm

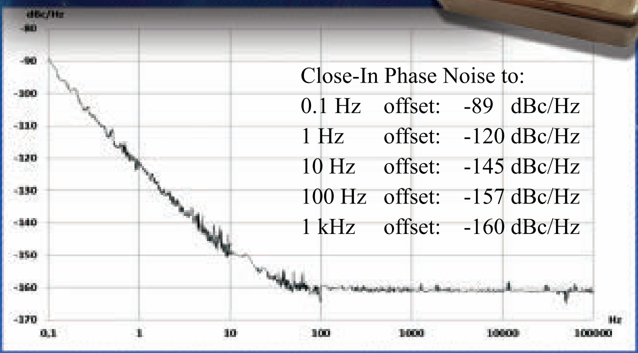

MV272M Low G Sensitivity

New

- Standard Frequency: 10 MHz
- Allan Deviation: <5E-12 per Sec.
- Package: 36.7 x 27.0 x 16.0 mm (SMD)

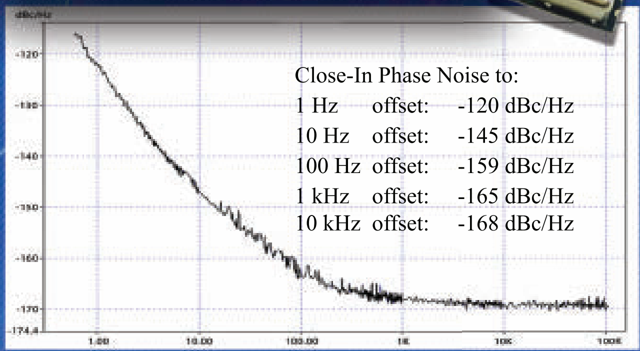

Located in California's Silicon Valley, Morion US supplies customers with high performance, high reliability crystal oscillator and crystal filter products for telecommunications, navigation and test & measurement applications.

Morion US is a company for which quality and reliability of products supplied are uncompromised. This is the essence of Morion US, LLC.

Our technologies are based on more than 80 years experience in precision quartz products, including those for Military and Space. We have a highly skilled workforce, excelent manufacturing and R&D capabilities.

Morion US, LLC
1750 Meridian Ave. #5128
San Jose, CA 95150
+1 408 329-8108
sales@morion-us.com
www.morion-us.com

Fig. 3 The high speed acquisition system of the R&S Scope Rider captures up to 50,000 waveforms each second and uncovers rare and unexpected signal anomalies.

configured as a hotspot to allow the instrument to be remotely controlled via a smartphone, tablet PC or laptop. A simple web browser on the mobile device is all that is required, with no need for additional software or apps. All settings can be adjusted on the PC and image compression ensures that the screen image is rapidly updated.

In history mode, the instrument automatically stores up to 5000 waveforms in a separate history buffer. At any point in time, acquisition can be stopped and any waveform in the buffer analyzed using full oscilloscope functionality.

With more than four hours of battery runtime, the 2.4 kg oscilloscope offers users a high degree of flexibility during installation, maintenance and in emergency situations, going beyond traditional electrical engineering to serve a broad range of industries. Technicians and specialists can use it to gain a clear understanding of the condition of electrical installations, systems and components – everything from measurement data acquisition in industrial and manufacturing settings to repairing shipboard electrical drives and carrying out vehicle test drive analyses.

Well prepared for harsh environments, the handheld oscilloscope's IP51 certified housing offers protection from environmental hazards such as dust and dripping water and has passed all mechanical load tests in line with military standards. The fully isolated instrument offers maximum safety and meets measurement category requirements defined in IEC 61010-1 for CAT IV up to 600 V and for CAT III up to 1000 V.

The R&S Scope Rider is available as a four channel or two channel instrument, the latter with a digital multimeter, with bandwidths of 60, 100, 200, 350 and 500 MHz. There are also trigger and decoding options available for I2C, SPI, UART, RS-232, RS-422 and RS-485.

VENDORVIEW

Rohde & Schwarz
Munich, Germany
+49 89 4129 12345
www.rohde-schwarz.com

INVITED PAPER

Wireless Infrastructure Market View: Waiting for China to Come Back

Earl Lum
EJL Wireless Research, Salem, N.H.

Wireless base station equipment shipments at the end of 2014 were supposed to accelerate to an even higher amount in 2015. However by the fourth quarter of 2014, demand was softening in China against all logic. Demand was supposed to increase due to China Mobile's continued deployment of its TDD-LTE network while China Unicom and China Telecom were to ramp deployment of their FDD-LTE networks.

By last year's Mobile World Congress (2015), EJL Wireless Research was seeing signs of a major anomaly within the industry, one that was not obvious. End market demand was completely uncorrelated to wireless industry financial conditions. Lead times were no longer stretched to the max, no bookings were doubled or tripled and no more orders were expedited. In some cases, orders were pushed out one quarter; in other cases, orders were cancelled. The party in China was over. We believe that a perfect storm of events occurred in China, beginning in the fourth quarter of 2014, that ultimately led to the widescale corruption and grafting probe by the Chinese government, one that impacted demand in the telecom market (see ***Figure 1***).

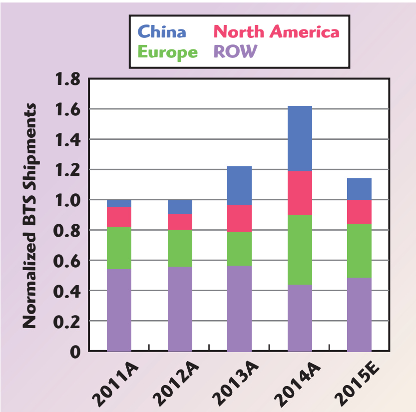

▲ *Fig. 1 Trend in base station shipments by region, normalized to 2011. 2015 shipments are estimated. Source: EJL Wireless.*

This demand has not disappeared; it has merely been pushed out by one year. Our expectations are for wireless equipment demand in 2016 to pick up, with China leading the way. India may still support demand for TDD- and FDD-LTE, as operators continue deployment of their networks. Europe is in a holding pattern waiting for LTE demand to increase to a level where current coverage at 800 MHz (Band 20) is near capacity and the next overlay for capacity at 2600 MHz (Band 7) is required.

The strength that North America has supported from 2012 to 2014 is no longer there. North America is facing a new reality of wireless capital expenditures. The FCC's auction 97 for AWS-3 spectrum (G, H, I and J blocks of paired spectrum and A1 and B1 blocks of unpaired spectrum in the 2100 MHz frequency band) essentially broke the bank of North American carriers. Gross bids of $44.9 billion forced tier-one operators such as AT&T and Verizon to find alternative ways to fund their spectrum purchases. With LTE coverage deployments at 700 MHz (Bands 13 and 17) es-

We'll help you do the math.
TRM Quality
TRM Resources
+ TRM Experience
YOUR Success
Air
Sea
Land
Space
Dividers
Couplers
TR Switches
Beamformers
Quads & Hybrids
Harmonic Filters
TRM
MICROWAVE
COMPLETING YOUR IDEAS®
Custom Passive RF Components Since 1970.
info@TRMMicrowave.com
A Woman-Owned Small Business
Apps Engineering Support Line 888.677.6877

sentially completed, focus in 2014 had shifted to adding capacity using the higher frequency bands, such as 1900 MHz (Bands 2 and 25) and 2100 MHz (Band 4), along with the introduction of 3GPP release 10 LTE-A features such as carrier aggregation.

IT'S THE SPECTRUM, STUPID

The wireless game is driven by spectrum. That is the bottom line. Nothing else matters to the mobile operator. There can never be too much spectrum. However, acquiring new spectrum for mobile operators results in a substantial financial impact at the initial stages of the acquisition: a government sponsored auction, then the implementation and deployment of new equipment for the new spectrum.

Germany recently auctioned a subset of 1500 MHz spectrum (Band 32) for supplemental downlink (SDL) with the U.K. slated to follow in 2016. Latin America and Asia Pacific are in the midst of auctioning APT 700 MHz (Band 28) "digital dividend" spectrum. In Europe, there is the potential for a digital dividend II (703 to 733 MHz and 758 to 788 MHz), which is a subset of Band 28. (Band 20 at 800 MHz was deemed the original digital dividend spectrum for Europe.) The repurposing of legacy WiMAX spectrum (3.4 to 3.7 GHz) to TDD-LTE technology allows for more wireless equipment to be sold. The promise of 5G is set to be the millimeter wave industry's ultimate fantasy and dream come true.

How does new spectrum impact the wireless equipment ecosystem? Without new spectrum becoming available, the wireless equipment industry would stagnate and stall. There would not be any growth at all. Given these regional and spectrum constraints, how will the various segments of the wireless infrastructure market fare?

BTS ANTENNAS

Five major events could trigger a mobile operator to upgrade their antenna mast systems:

- New technology (e.g., LTE)
- New spectrum
- Updating radio transceiver MIMO capability to two transmit and two receive (2T2R), 2T4R, 4T4R, 4T8R or 8T8R
- Site acquisition issues
- Migration to semi-active or active beam forming antennas.

Each of these causes potentially complex issues to be resolved by the mobile operator, and each macrocell site may have a different issue. As an example, in North America the current frequency bands for LTE are

- 700 MHz (Bands 12, 13 and 17)
- 800 and 850 MHz (Bands 5 and 26)
- 1900 MHz (Bands 2 and 25)
- 2100 MHz (Band 4).

The eventual deployment of AWS-3 spectrum will force mobile operators to replace existing AWS-1 remote radio units (RRU) with updated ones that may support 2T4R or 4T4R configurations, as well as the expansion of the frequency band to support the AWS-3 spectrum. We believe that the majority of Band 4 RRUs will be upgraded from 2T2R to 2T4R, requiring two additional ports on the antenna.

The potential impact of the upcoming 600 MHz auction in 2016 will again force mobile operators to deploy a separate antenna panel to support this specific band, due to the size of the dipole columns needed at this lower frequency range.

For a worst case scenario, where each band (700, 850, 1900 and 2100 MHz) supports a 2T4R configuration without diplexing low or high bands together and not counting for different electrical tilts for different types of wireless services, a single sector panel antenna would need 16 ports and potentially eight dipole columns using a cross polarization (xpol) type of dipole array. One simple issue relating to the realities of panel antennas is that weight and wind load play a significant factor in their deployments. The width of the panel antenna is typically kept to

▲ *Fig. 2 Multi-band antenna faceplate, showing four low band (red outline) and eight high band (blue outline) ports integrated into a single housing. Source: Commscope.*

a maximum of 400 mm to minimize wind loading. It is very difficult to get approval to mount a door on a tower; however, we have seen instances of very wide antennas being deployed on rooftops where the wind load is offset by supporting structures.

We estimate that BTS macrocell antenna shipments increased 37 percent year-over-year in 2014, and 2015 shipments will show a decline of 30 percent in unit volume due to the weakness in China and North America. The market for TDD-LTE antennas (e.g., 8+1 ports) was approximately 24 percent of overall shipments in 2014. We also estimate that FDD-LTE four-port antennas were the largest product segment, followed by two-port and six-port antennas. The semi-active/active antenna segment was only 2 percent in 2014.

We believe that there are two major trends over the next several years for macrocell antennas: higher and higher port count to 8, 10, 12 and 14 (see ***Figure 2***) and migration to 4.3/10 mini-DIN connector ports. While there may be some specific requirements for semi-active antennas (e.g., passive antennas with RRUs), we believe that these may be due to site acquisition issues and not necessarily because of performance improvements.

OUTDOOR SMALL CELLS

The North American market has seen a complete shift in strategy towards small cells, as AT&T Wireless

▲ *Fig. 3 Ericsson microcells for Bands 2 and 4, deployed on a streetlight in San Francisco, Calif. Source: EJL Wireless.*

shifted its position from deploying 40,000 small cells to no longer focusing on them. Conversely, Verizon Wireless has stated it will spend $500 million on small cells in certain markets (see ***Figure 3***).

With Verizon, the advent of outdoor small cell deployments is finally seeing some larger scale demand. There is currently a 400+ "small cell" deployment ongoing in San Francisco, Calif.; however, this questions the definition of a small cell. We believe that stand-alone small cells have the baseband processing modem integrated with the radio transceiver, with either a direct Iub connection to the core network or an Iuh connection to a gateway controller. Otherwise, we classify "small cells" deployed with a fiber fronthaul link as an outdoor distributed antenna system (oDAS) remote radio node — not a small cell. We believe that the San Francisco deployment is a hybrid of both traditional small cells and oDAS radio nodes.

In Europe, announcements from Vodafone U.K. and advertising giant JCDecaux are paving the way for outdoor small cell deployments. Unlike the North American market, we believe that mobile operators in Europe will not share infrastructure and will deploy single operator small cell solutions, not oDAS radio nodes. The acquisition of sites and street furniture for small cells has been one of the largest impediments for deploying outdoor small cells, with backhaul also being a large issue. With the ability to use JCDecaux street furniture across Europe, the site acquisition issue may have been solved for mobile operators.

IN-BUILDING WIRELESS

The term in-building wireless (IBW) encompasses many different solutions and technologies and is confusing for the wireless industry. We classify the following solutions as in-building wireless:

- BTS OEM picocells
- Passive distributed antenna systems (p-DAS)
- Active analog distributed antenna systems (aa-DAS)
- Active digital distributed antenna systems (ad-DAS)
- BTS OEM solutions such as Ericsson's Radio Dot (shown in ***Figure 4***) or Huawei's LampSite
- Third party small cells with controller gateways (e.g., SpiderCloud or equipment from CommScope).

The North American market has historically led the global IBW industry, given the large sporting venues, airports and convention centers located within the U.S., with aa-DAS the predominant technology used. However, we see other regions such as Asia Pacific and Europe adopting single operator solutions offered by BTS OEMs and third party small cells, since the neutral host model in these regions is not as defined as it is in North America.

Wi-Fi LAA/LTE-U

The use of unlicensed spectrum at 5.8 GHz through the license assisted access (LAA) specifications in 3GPP release 13 will allow mobile operators to leverage an 80 MHz chunk of


Innovation
That Deceives.
To protect our platforms and warfighters, next-generation electronic and radar-directed attack solutions require deep domain expertise in analog, digital, and mixed-signal technologies. Mercury is a leader in the development of software-defined subsystems leveraging open architecture RF and Microwave building blocks that are designed and made in America, to detect, intercept and defeat signals of interest on land, at sea and in the air.
MERCURY
SYSTEMS™
INNOVATION THAT MATTERS™
MADE IN AMERICA
Visit mrcy.com/EW to download the whitepaper:
Introducing a Better Alternative for Advanced Electronic Warfare Solutions
Copyright © 2015 Mercury Systems and Innovation That Matters are trademarks of Mercury Systems, Inc. - 3143

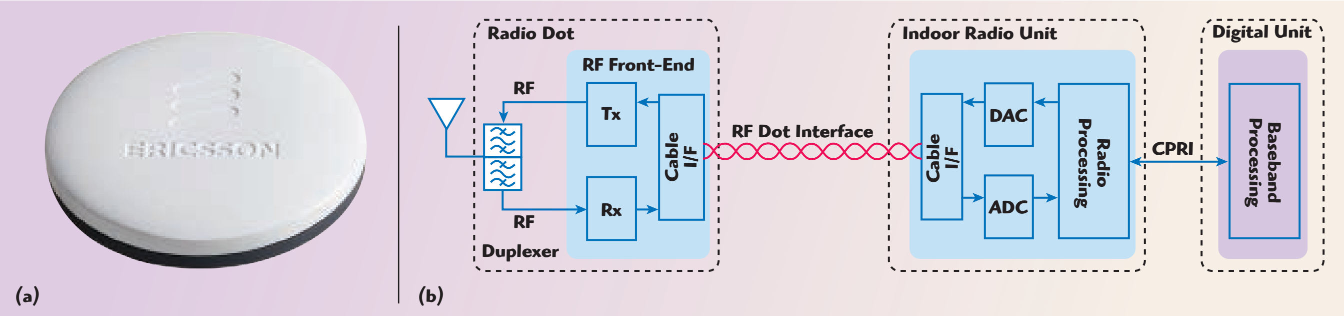

Fig. 4 Ericsson's indoor small cell solution connects multiple RF front-ends (a) to an indoor radio unit (IRU), with multiple IRUs connected to a single digital unit for baseband processing (b). Source: Ericsson.

spectrum, essentially for free. This is the equivalent of offering mobile operators billions of dollars of free spectrum. Using licensed LTE spectrum for signaling, the unlicensed 5.8 GHz spectrum may be used to transmit and receive LTE signals from user equipment (UE). Incumbent Wi-Fi proponents argue that LAA technology will essentially block their Wi-Fi signals. We do not believe that this will be the case, as the LTE transmissions will be subject to the same restrictions as any other Wi-Fi access point deployed within the same area. We believe that LAA will be deployed in both in building and outdoor use cases globally, beginning in 2016.

2016 OUTLOOK

Data usage and spectrum drive the wireless industry. Auctions for spectrum worldwide will continue to fuel the industry while LTE/LTE-A adoption and usage continue to increase globally.

The demand for LTE in China will be the key barometer for the industry. The partnership agreement between China Telecom and China Unicom following swirling rumors of operator consolidation may dampen the outlook and shift the industry's focus to India. We expect global base station demand to be flat to up if China comes back or flat to down if China fails to meet expectations.

Wi-Fi calling and LAA/LTE-U will be a hot topic for 2016 as mobile operators attempt to offload voice and data traffic from LTE and W-CDMA networks to the unlicensed band at 5.8 GHz. Mobile operator carrier grade Wi-Fi deployments will likely drive demand worldwide should operators quickly adopt LTE-A to access these features. ■

5G Opportunities and Challenges for the Microwave Industry

Thomas Cameron
Analog Devices Inc., Norwood, Mass.

As we embark on the road to 5G, the next generation wireless communications system, there are countless challenges and opportunities emerging for the engineering community. 5G represents both an evolution and a revolution of mobile technologies, to reach the various high-level goals that have been published to date by various members of the wireless ecosystem. 5G is widely seen as the generation of wireless that will enable cellular to expand into a completely new set of use cases and vertical markets. While 5G is generally seen as the technology to deliver ultra-broadband services, including HD and ultra-HD video streaming, 5G technology will also enable cellular to enter the world of machines, contributing to autonomous vehicles, as well as connecting millions of industrial sensors and a multitude of wearable consumer devices.

The evolutionary path to 5G consists of incremental enhancements of 4G in the conventional cellular bands and extending up in frequency to emerging bands in the 3 to 6 GHz range. Massive MIMO has industry momentum and will evolve from first systems based on LTE to adopt new waveforms designed to improve throughput, latency and cell efficiency. Spectrum is seen as the lifeblood of the cellular industry, and the spectrum in the legacy cellular bands (sub 6 GHz) just cannot support the exponentially growing demand in upcoming years. As such, the bands above 6 GHz are currently under study, to test the viability of deploying wireless access in those frequency allocations. While the collective global spectrum available below 6 GHz is on the order of hundreds of MHz, the amount of potential spectrum above 20 GHz is in the tens of GHz. The taming of this spectrum is considered essential to achieving the 5G vision of a truly connected world. As a result, a segment of 5G is likely to operate on much higher frequencies (possibly up to millimeter waves) and adopt new air interface technologies that are not backward compatible to LTE. The frequency bands discussed among key industry players include higher frequency bands such as 10, 28, 32, 43, 46 to 50, 56 to 76 and 81 to 86 GHz. However,

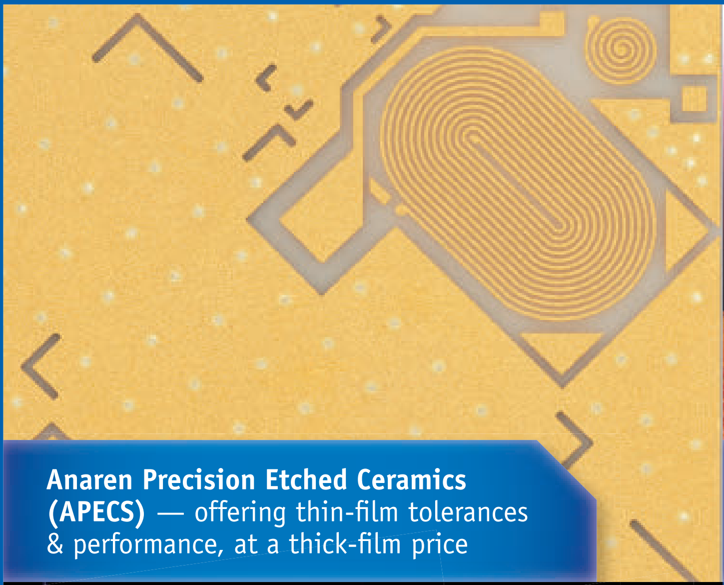

Anaren Precision Etched Ceramics (APECS) — offering thin-film tolerances & performance, at a thick-film price

Space/Mil-grade Xinger® couplers — proven in Mars missions & ready for tough terrestrial settings, too

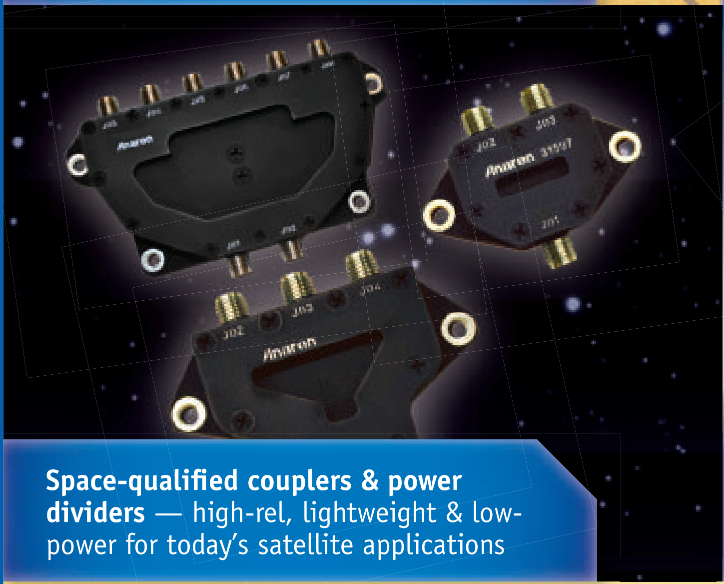

Space-qualified couplers & power dividers — high-rel, lightweight & low-power for today's satellite applications

RF solutions for next-gen AESAs — including manifolds, T/R modules & beam-formers for air, sea, and land platforms

Isn't it time to put Anaren innovations like these to work for *you*?

Fast-approaching our 50th anniversary — and this year celebrating our 1 billionth Xinger®-brand coupler sold! — today's Anaren continues to drive innovative, best-in-class RF technology for the world's most demanding space, defense, wireless, and consumer electronics customers.

> **Our Space & Defense Group** offers a fast-growing range of passive and active solutions, including multichip modules, IMAs, and custom solutions for today's digital radars. Exciting, new PCB and ceramic substrates and multilayer packaging techniques. And a growing line-up of space-grade components and high-temperature modules.

> **Our Wireless Group** continues to reinvent the passive components category. From new, Femto-sized and mil-grade Xinger®-brand SMTs. To subminiature baluns and couplers for consumer products. To our growing family of Anaren Integrated Radio (AIR) modules and other solutions for the wireless IoT.

To learn more about how today's Anaren can make you more competitive tomorrow — visit **www.anaren.com** or email us at **sales@anaren.com** today!

Anaren®

What'll we think of next?®

800-411-6596 > www.anaren.com

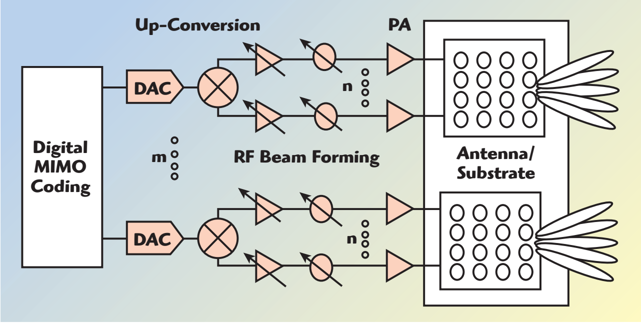

▲ *Fig. 1 MIMO transmitter functional block diagram.*

these bands are currently in the proposal stages and much work remains to be completed in channel modeling prior to the radio system definition and standards deliberations. The ITU recently published a plan for 5G standardization, with a target to publish the first generation of IMT-2020 specifications around year 2020.

Given that 5G is still in its infancy, work also remains relative to channel modeling, radio architecture definition and chipset development before the first commercial systems will be deployed. However, there are certain trends and requirements already agreed upon and problems to be solved that will lead to final 5G systems. Let's consider 5G access systems at microwave and millimeter wave frequencies. One of the major hurdles in implementing radio access at microwave frequencies is overcoming the unfavorable propagation characteristics. Radio propagation at these frequencies is highly affected by atmospheric attenuation, rain, blockage (buildings, people, foliage, etc.) and reflections. Microwave point-to-point links have been deployed for many years, but these are generally line-of-sight systems. The fact that they are stationary makes the link manageable, and systems have been developed in recent years that support very high throughput using high order modulation schemes. This technology continues to evolve, and we will leverage the microwave link technologies into 5G access.

Early in the cycle, it has been acknowledged that adaptive beam forming will be required to overcome the propagation challenges for access systems. Unlike point-to-point systems, beam forming will need to adapt to users and the environment to deliver the payload to the user. It is generally agreed in the industry that hybrid MIMO systems will be used in the microwave and low millimeter wave bands, while in V- and E-Bands, where bandwidth is plentiful, the systems will likely only employ beam forming to reach the required throughput goals.

Figure 1 shows a high-level block diagram of a hybrid beam forming transmitter. The receiver can be envisioned as the reverse. The MIMO coding is performed in the digital section, along with the typical digital radio processing. There may be a multitude of MIMO paths processed in the digital section from the various data streams feeding the antenna system. For each data stream, the D/A converter converts the signal into analog


38GHz
60GHz
24GHz
79GHz

at either a baseband or IF frequency, depending on the selected architecture. The signal is up-converted and split into the constituent RF paths to feed individual antennae. In each RF path, the signal is processed to set the gain and phase to form the beam out of the antenna. While the block diagram is simplistic, the system challenges and trade-offs are complex. In this short treatment of the topic, only a few issues will be discussed, but let's focus on the architecture and radio challenges. It is critical to design this system with power, size and cost in mind from the start to bring these systems to reality.

While such radios can and are being built today for prototype 5G systems using discrete (mainly GaAs) devices from Analog Devices (ADI) and our peers, we need to bring the same high levels of integration to bear in the microwave space as what has been implemented in cellular radios. High integration and high performance make a tough problem for the industry to solve. But integration alone is not the solution to this problem facing the industry. It requires smart integration. When we think of integration, we need to first consider architecture and partition to leverage the benefits of integration. In this case, mechanical and thermal design also need to be considered as the circuit layout and substrate are interrelated. First of all, an architecture conducive to integration needs to be defined. If we consider the examples of highly integrated transceiver ICs for cellular base stations, many use a zero IF (ZIF) architecture to either eliminate or minimize the filtering in the signal path. Particularly at microwave frequencies, one must minimize the loss in the RF filters, as RF power is expensive to generate. While ZIF will reduce the filter issue, the trade-off is LO suppression, shifting the problem from physical structures to signal processing and algorithms. Here we can leverage Moore's Law, whereby passive microwave structures do not follow the same scaling dynamics. It is necessary to take advantage of the ability to optimize analog and digital simultaneously to reach our goals. There are many algorithms and circuit techniques that have been employed at cellular frequencies that may benefit the microwave space.

Next, consider the semiconductor technology requirements. As mentioned above, state-of-the-art microwave systems are generally implemented with GaAs components. GaAs has been the mainstay of the microwave industry for many years, but SiGe processes are overcoming the barriers of high frequency operation to rival GaAs in many of the signal path functions. High performance microwave SiGe BiCMOS processes enable a high level of integration required for these beam forming systems, encompassing much of the signal chain as well as auxiliary control functions. GaAs PAs may be required, depending on the output power required at each antenna. However, even GaAs PAs are inefficient at microwave frequencies, as they are generally biased in the linear region. Linearization of microwave

PAs is an area ripe for exploration in the 5G era, more than ever before. What about CMOS? Is it also a contender? It is well documented that CMOS is well suited for high volume scaling and is being proven in WiGig systems at 60 GHz. Given the early stage of development and uncertainty of use cases, it is difficult to say at this point if or when CMOS will be a technology choice for 5G radios. Much work needs to be done first in the area of channel modeling and use cases, to form a conclusion on radio specifications and where microwave CMOS may fit in future systems.

The final consideration of 5G systems is the interdependency of the mechanical design and RFIC partitioning. Given the challenges to minimize losses, the IC needs to be designed with the antenna and substrate in mind to optimize the partition. Below 50 GHz, the antenna will be part of the substrate, and it is expected that the routing and some passive structures may be embedded in the substrate. There is a body of research ongoing in the area of substrate integrated waveguides (SIW) that looks promising for such integrated structures. In such a structure it will be possible to mount much of the RF circuitry on one side of the multi-layer laminate and route to the antennae on the front face. The RFICs may be mounted in die form on this laminate or in surface-mount packages. There are good examples in industry literature of such structures for other applications. The antenna elements and spacing become small enough above 50 GHz to possibly integrate the antenna structure in or on the package. Again, this is an area of ongoing research that may push 5G systems forward. In either case, the RFIC and mechanical structure must be co-designed to ensure symmetry in routing and minimize losses. None of this work will be possible without powerful 3D modeling tools for the extensive simulations required for these designs.

While this is a brief perspective on the challenges 5G brings to the microwave industry, there will be boundless opportunities to bring forth RF innovations in the coming years. A rigorous systems engineering approach will yield the optimum solution by leveraging the best technologies throughout the signal chain, developing processes and materials, creating design techniques and modeling, and defining high frequency test and manufacturing. All disciplines will play a role in reaching 5G goals. Analog Devices brings a strong contribution to the 5G microwave effort with its unique "bits to microwave" capability. ADI's broad technology portfolio and continued RF technology advances combined with its rich history in radio systems engineering puts the company in a position to pioneer new solutions for designers at microwave and millimeter wave frequencies for emerging 5G systems.

It is an exciting time to be an RF engineer in the wireless industry. 5G is just starting and there is much work ahead to realize commercial 5G radio networks by 2020. ■

Scan page
using layar app

DefenseNews

Cliff Drubin, Associate Technical Editor

Military Robots Market Global Forecast to 2020

VIEW VIDEO

The global military robots market is expected to grow from an estimated $13.55 billion in 2015 to $21.11 billion by 2020, at a CAGR of 9.27 percent from 2015 to 2020 according to a recent ABI Research report. The market for military robots is driven by critical factors, such as increasing demand for the effectiveness and efficiency of operations for automation, rising need for better cross border surveillance and minimization of casualties.

The key applications considered are warfield robots, firefighting robots, pick n' place robots, metal detector robotic vehicle and voice controlled robotic vehicles. The firefighting robots market is estimated to grow at the highest CAGR during the forecast period, among all applications. They are increasingly being used to tackle fire situations, in order to avoid casualties. Firefighting robots were first used by the U.S. Navy and are named Shipboard Autonomous Firefighting Robots (SAFFiR). These are human-sized autonomous robots, which can successfully find and suppress shipboard fires. They can detect fire, implement a broad range of fire suppressing techniques, withstand higher temperatures for long periods and respond to any enemy movements simultaneously.

The North American region dominated the global military robot market in 2014, and is expected to continue its dominance during the forecast period. The U.S. is considered to be the largest developer, operator and exporter of military robots, globally, thereby resulting in the large share of the North American region in the global military robots market. The main functions of these robots include ISR (Intelligence, Surveillance, and Reconnaissance), ensuring border security and minimizing the risks of terrorism on the domestic assets and population.

The market in Europe is projected to grow at the highest CAGR during the forecast period. This rapid growth can be attributed to the fact that nearly 26 nations in Europe currently have active UAV and robotic programs, including the U.K., Russia and Germany, among others. With the rapid advancements and adoption of military technologies in the region, the military robot market in Europe is projected to grow significantly during the forecast period. Other key factors driving the growth of the European market are the increasing investments and development of advanced ground robots for transportation, surveillance and combat applications.

U.S. Navy photo.

The major companies profiled in the report include Northrop Grumman (U.S.), Lockheed Martin (U.S.), AeroVironment (U.S.), Israel Aerospace Industries (Israel), iRobot (U.S.) and Boston Dynamics (U.S.), among others.

DARPA Awards NGC Third Phase of Tern Unmanned Systems Program

The Defense Advanced Research Projects Agency (DARPA) and the Office of Naval Research have awarded Northrop Grumman Corp. the third phase of the Tern unmanned systems program. Phase three plans to include final design, fabrication and a full-scale, at-sea demonstration of the system.

Tern seeks to develop an autonomous, unmanned, long-range, global, persistent intelligence, surveillance, reconnaissance (ISR) and strike system intended to safely and dependably deploy and recover from small-deck naval vessels with minimal ship modifications. Designed to operate in harsh maritime environments, Tern aims to enable greater mission capability and flexibility for surface combat vessels without the need for establishing fixed land bases or requiring scarce aircraft carrier resources.

"We intend to highly leverage our Unmanned Systems Center of Excellence to develop and demonstrate this type of demanding unmanned systems capability to advance the Navy's mission," said Chris Hernandez, VP of research, technology and advanced design, Northrop Grumman Aerospace Systems. "We believe our unique ship-based unmanned systems experience, expertise, and lessons learned from programs including our MQ-8B/C Fire Scout, MQ-4C Triton, X-47A Pegasus and X-47B UCAS, is critical to the success of the Tern."

> "Our full-scale demonstrator system is highly traceable to our operational concept..."

The Northrop Grumman Tern team includes its wholly owned subsidiary Scaled Composites, as well as General Electric (GE) Aviation, AVX Aircraft Co. and Moog. Northrop Grumman's Tern solution seeks to provide an innovative system that integrates mature and advanced technologies, including a distinctive propulsion solution designed to help expand global persistent ISR/strike capabilities for small-deck naval surface vessels.

"Using an innovative design that integrates vertical takeoff and landing transitioning to an efficient flying-wing for cruise, our team is creating a system that we believe

For More Information Visit mwjournal.com for more defense news would achieve Tern's revolutionary performance objectives in support of our combatant commanders," said Ralph Starace, director, advanced design, Northrop Grumman Aerospace Systems. "Our full-scale demonstrator system is highly traceable to our operational concept to burn down risk, resulting in a compelling step forward for this game-changing, multi-mission capability," said Bob August, Tern program manager, Northrop Grumman Aerospace Systems.

Illustration of Tern (courtesy Northrop Grumman).

BAE to Develop EW Suite for USAF C-130J Fleet

BAE Systems has been selected by the U.S. Special Operations Command (USSOCOM) to develop a new electronic warfare system for the fleet of C-130J aircraft. The contract, worth more than $20 million, is the first phase of a multi-phase program to upgrade aircraft system survivability and the capability to detect, identify, locate, deny, degrade, disrupt and defeat threat systems in operational significant environments. The life cycle value of the contract is expected to exceed $400 million.

The Radio Frequency Countermeasure (RFCM) system offers fully integrated, precision geo-location, and radio frequency countermeasure capabilities. The advanced system will significantly enhance the electronic threat protection capability of the C-130J, increasing the aircraft's ability to detect and defeat both surface and airborne threats in signal-dense and highly contested environments.

Designed to be integrated into both the MC-130J Commando II and the AC-130J Ghostrider aircraft, the RFCM system will support the varied and critical missions of Special Operation Forces. These missions include the use of C-130Js for armed over-watch and refueling of helicopters in denied territories, and for close air support and interdiction missions in the most sensitive and hostile of territories.

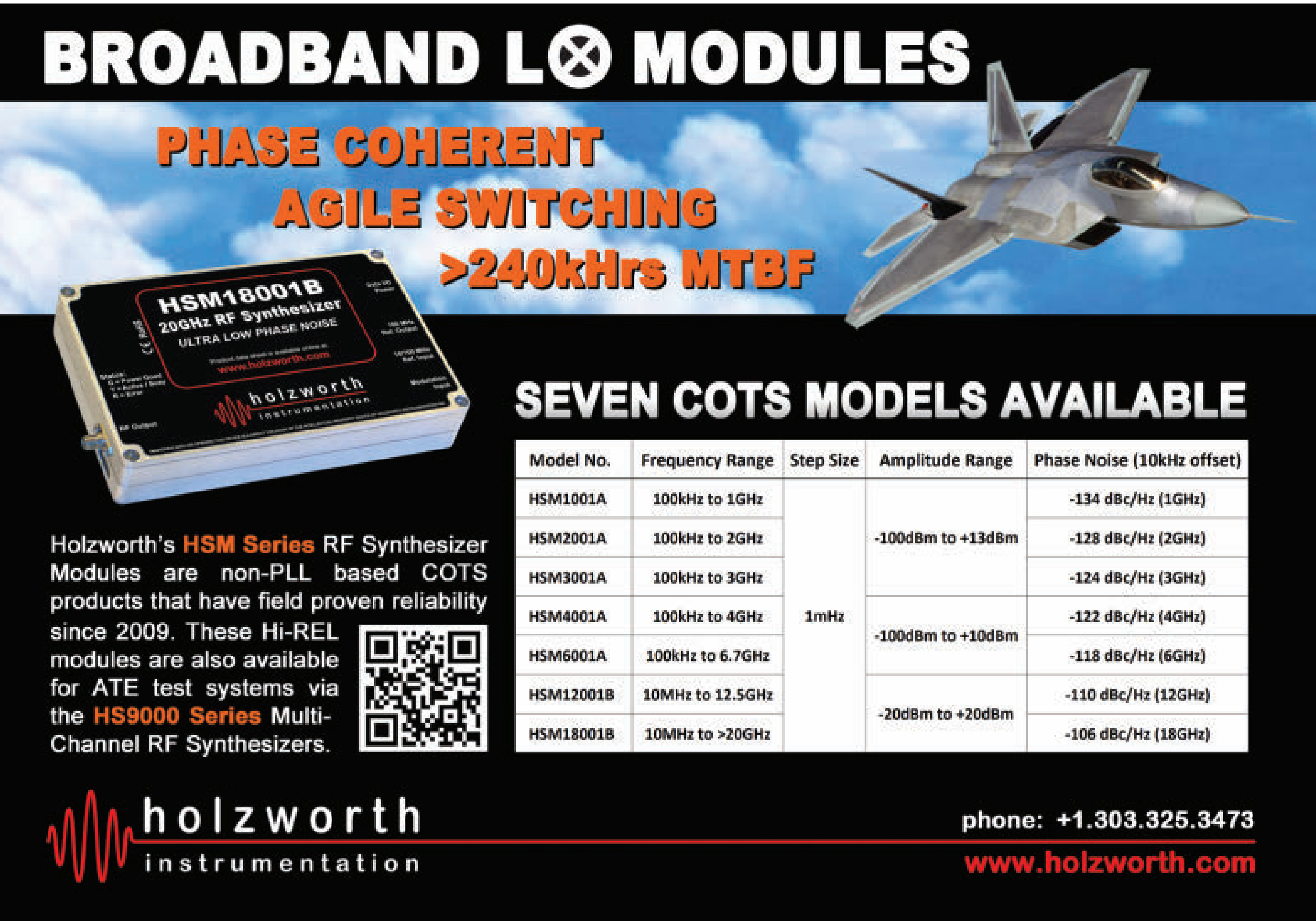

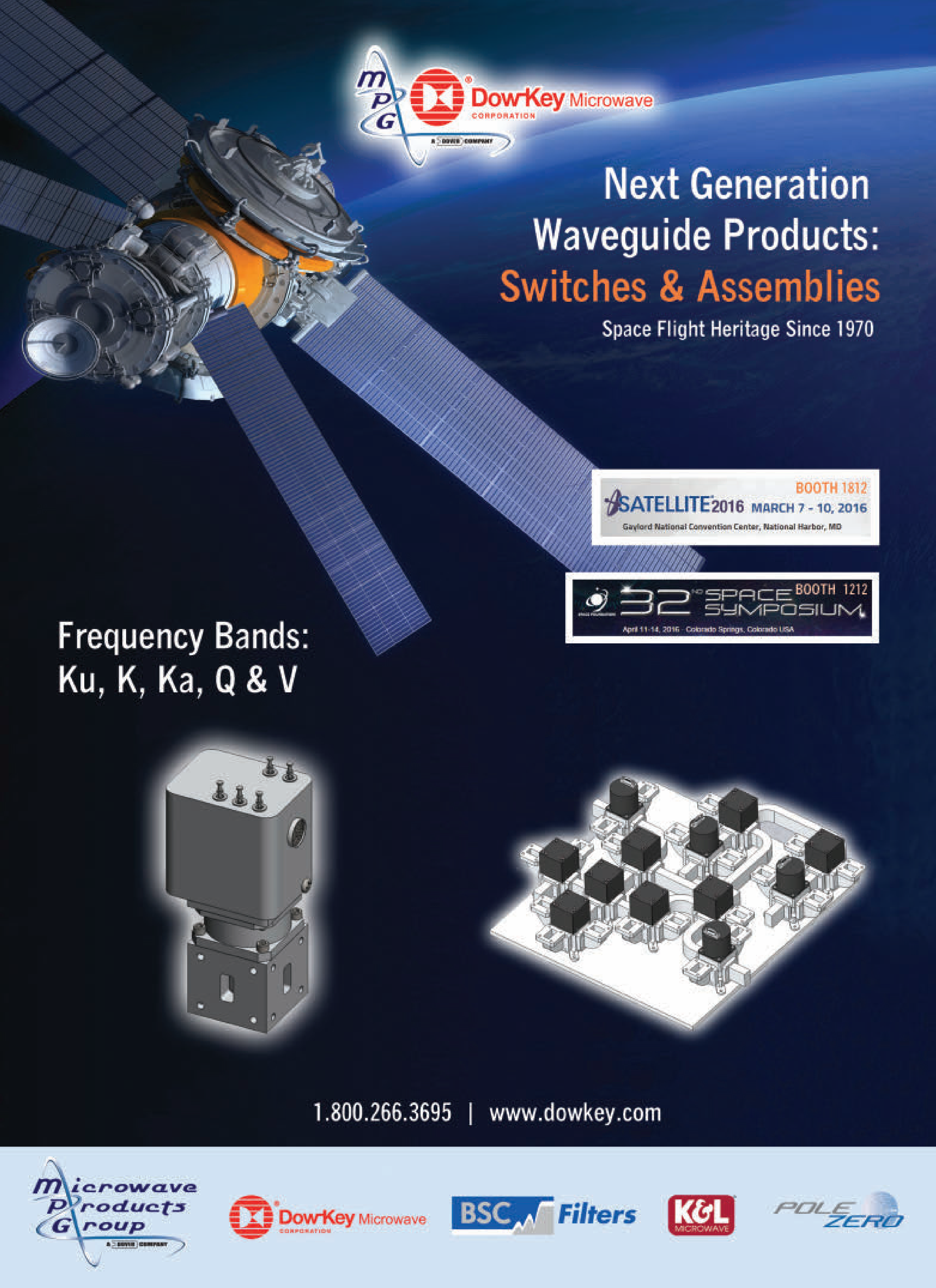

MPG
Dow-Key Microwave
CORPORATION
A DOVER COMPANY
Next Generation
Waveguide Products:
Switches & Assemblies
Space Flight Heritage Since 1970
BOOTH 1812
SATELLITE 2016 MARCH 7 - 10, 2016
Gaylord National Convention Center, National Harbor, MD
32ND SPACE SYMPOSIUM BOOTH 1212
April 11-14, 2016 · Colorado Springs, Colorado USA
Frequency Bands:
Ku, K, Ka, Q & V
1.800.266.3695 | www.dowkey.com
Microwave Products Group
A DOVER COMPANY
Dow-Key Microwave
CORPORATION
BSC Filters
K&L MICROWAVE
POLE ZERO

World's Smallest Temperature Sensor Powered By Radio Waves

Researchers at the University of Eindhoven (TU/e), The Netherlands, have developed a wireless temperature sensor, which measures 2 mm^2 and weighs 1.6 mg that is powered by radio waves that are part of the sensor's wireless network. This means that the sensor does not need a single wire, nor a battery that would have to be replaced.

The current version of the sensor, which is based on 65 nm CMOS technology, has a range of 2.5 cm; the researchers expect to extend this to 1 m within a year, and ultimately to 5 m. The sensor has a specially developed router, with an antenna that sends radio waves to the sensors to power them. Since this energy transfer is accurately targeted at the sensor, the router consumes very little electricity.

The sensors are constructed in such a way that their energy consumption is extremely low. The sensor contains an antenna that captures the energy from the router. The sensor stores that energy and, once there is enough, the sensor switches on, measures the temperature and sends a signal to the router. This signal has a distinctive frequency, depending on the temperature measured and the router can deduce the temperature from this frequency.

TU/e researcher Hao Gao was awarded his Ph.D. for his thesis entitled, "Fully Integrated Ultra-Low Power mmWave Wireless Sensor Design Methods," in which he developed the sensor. The project, called PREMISS, received funding from the STW technology foundation. The integrated circuits research was done in the Mixed-Signal Microelectronics group and also involved the TU/e group's Electromagnetics and Signal Processing Systems as well as the Centre of Wireless Technology.

The same technology enables other wireless sensors to be made, for example to measure movement, light and humidity. The application areas are significant, ranging from payment systems and wireless identification to smart buildings and industrial production systems. Also, it is expected that mass production will keep the cost of a sensor down to around 20 cents.

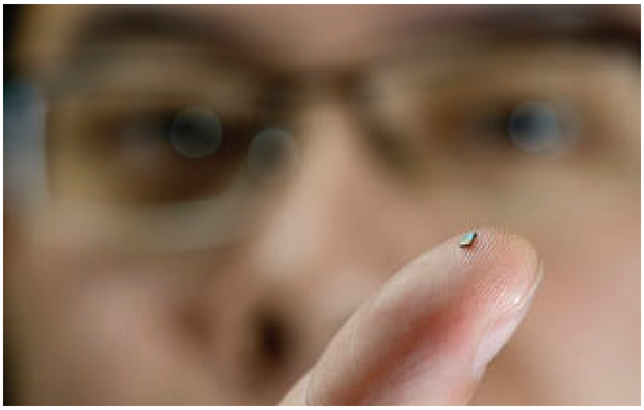

Photo Courtesy: Bart van Overbeeke

EU-China Collaboration Calls for Research and Innovation Proposals

The Chinese Ministry of Science and Technology (MOST) has published its first call for proposals under the EU-China Co-Funding Mechanism (CFM) for Research and Innovation.

The CFM is designed to support mainland China-based research and innovation organisations participating in Horizon 2020 (H2020) projects.

The first call covers a variety of areas including information and communication technology, space, aviation, energy, transportation, advanced manufacturing and new materials to name just a few, together with the exchange of young scientists. Two deadlines are planned for 2016 – 31 March and 31 July 2016, depending on the field of activity.

The EU-China CFM is the last of a series of support schemes put in place by EU international partner countries to enable a stronger and more balanced collaboration between their universities, research institutes and enterprises with European ones under Horizon 2020. The Horizon 2020 work programme for 2016-2017 includes a number of topics which specifically encourage cooperation with China.

> ..stronger and more balanced collaboration...

Under the CFM, up to RMB200 million, or €28 million, will be made available annually by the Chinese Ministry of Science and Technology on the Chinese side for the benefit of China-based entities that will participate in joint projects with European partners under Horizon 2020. Similarly, the European Commission expects to continue spending €100 million per year for the benefit of Europe-based entities in joint projects under H2020 with Chinese participants.

EU Researchers Develop Efficient Nanowire Analysis Technique

Researchers working through the EU-funded NANOWIRING project have developed a new cost-effective and time-efficient technique for determining the individual polarity of semiconducting nanowires. This is a vital step in the fabrication of nanomaterials, since the polarity — whether nanowires are positively or negatively charged — defines the properties of any device made from these cutting edge structures.

Semiconducting nanowires are the smallest dimensional structures that allow optical guiding and electrical contacting simultaneously. Their large surface to volume ratio also enhances their interaction with the environment, turning them into optimal chemical and biological sensors.

The new technique developed by NANOWIRING uses an atomic-strength microscope and a Kelvin probe to

For More Information Visit mwjournal.com for more international news

> ...achieving scalable and low cost nanowire production.

detect minuscule forces, and measure the electrical characteristics of the sample's surface. When combined with advanced data analysis, these measurements reveal the polarities of hundreds of nanowires at the same time.

This development has been a key result of the NANOWIRING project, the overall objective of which has been to create a European network of experts to provide assistance to early stage researchers. The scope of this project, which has now been officially completed, has also been driven by industrial needs, such as achieving scalable and low cost nanowire production. Industrial partners have been involved throughout in order to ensure that research and results are as market-focused and applicable as possible. Furthermore, interaction with associated industrial partners will enhance the employability of researchers through exposure to the private sector.

Ericsson and Verizon to Take IoT Development to Next Level

Ericsson and Verizon have announced joint activities to further the development and deployment of cellular low-power wide-area (LPWA) networking for a diverse range of IoT applications. The two companies have been engaged in IoT trials since 2014 to demonstrate the range of IoT use cases – both consumer and industrial applications – that today's mobile networks can support.

Adam Koeppe, vice president, Network Technology and Planning, Verizon, said, "Verizon's nationwide LTE network provides an ideal platform for the acceleration of IoT applications that benefit consumers, industry and cities. We're committed to simplifying IoT and have introduced a developer platform – ThingSpace – and new network advancements that do just that. Ericsson's new software will enable us to expand our coverage of low-cost IoT devices while supporting years of battery life."

> "...IoT applications will drive 5G development..."

LTE is already especially well-suited to support high-capacity, low-latency applications. Ericsson's LPWA solution will scale Verizon's LTE network to connect a wider variety of IoT use cases by supporting the connectivity requirements of lower power, lower cost and reduced complexity.

Arun Bansal, senior vice president and head of Business Unit Radio, Ericsson, said, "Verizon has been a great partner in the advancement of cellular technologies to address IoT networking requirements. IoT applications will drive 5G development so it is essential for us to work with leading operators like Verizon to proactively spearhead the industry and ecosystem."

Cliff Drubin, Associate Technical Editor

Consumer Robotics Market to Hit $17B in 2025

VIEW VIDEO

The consumer robotics market is set to close out 2015 at 33 million shipments with total revenues of $3.5 billion. By 2025, both shipments and revenues are expected to dramatically increase, with ABI Research forecasting total shipments to increase to 165 million and total revenue to more than quadruple, reaching $17 billion.

"In 2015, robotic toys accounted for more than half of the year's total shipments, but consumer UAVs is proving to be the fastest growing segment over the next decade," says Phil Solis, research director at ABI Research. "We anticipate consumer UAVs including toy UAVs to surpass robotic toys in terms of shipment share in a few years and account for more than half of consumer robotics product shipments by 2021."

Additionally, data findings suggest that, throughout the 10-year forecast, the homecare segment will remain the most powerful in terms of revenue generation. In 2020, consumer UAVs will surpass robotic toys to take second place. By 2025, personal robots will also surpass robotic toys to take third place in revenue generation among segments.

> Homecare stays on top as personal robotics starts to make substantial headway.

"Right now, the personal robots coming to market are stationary, embodied products that can successfully interface with users and leverage information and services in the cloud," continues Solis. "As these products advance in their technological capabilities and grow from stationary to mobile and add manipulation, average product prices will rise at times. So, though unit volumes will be relatively small in comparison to other market segments, the personal robotics segment will generate a generous amount of revenue and increase its revenue share."

The consumer robotics market, as a whole, covers a wide range of companies that lead in different segments. These include iRobot, Samsung, LG, Hasbro, WowWee, Parrot, DJI, 3D Robotics, Jibo, Blue Frog and hundreds of others.

Bluetooth Enabled Device Shipments to Reach 19 Billion by 2020

ABI Research anticipates annual Bluetooth enabled device shipments to increase from 2.8 billion units in 2015 to more than 4.6 billion in 2020, with a total of 19 billion devices to be equipped with Bluetooth technology over the next five years. Smartphones will continue to represent the bulk of the Bluetooth product market, accounting for more than 45 percent of shipments in 2020. However, the shares of emerging market segments, including beacons, smart lighting, home automation and consumer robotics devices, will increase significantly within the next five years to collectively represent more than 20 percent of the total market by 2020.

"The Bluetooth Special Interest Group (SIG), which added more than 2,800 new members this year alone, made significant enhancements to Bluetooth specifications in order to increase its viability for IoT applications," says Andrew Zignani, research analyst at ABI Research. "The recently announced Bluetooth Developer Studio (BDS) will also help Bluetooth technology gain more traction among the developer community and accelerate innovation time to market, most notably in nascent IoT applications."

This is set to continue in 2016, as Bluetooth evolves toward becoming a key enabler of larger scale networks consisting of increasingly heterogeneous devices. Significant upcoming Bluetooth technological enhancements include a quadrupling of range capacity and doubling of throughput. The range increase will better suit Bluetooth for full-home coverage and outdoor applications, which will enhance robustness and reliability. The increase in throughput from 1 to 2 Mbps will not only reduce latency and increase responsiveness, but it will also provide Bluetooth with a very compelling performance to power consumption ratio when compared with competing technologies, such as 802.15.4 (limited to 250 Kbps) or Wi-Fi (higher power consumption).

> Bluetooth is evolving toward becoming a key enabler of larger scale networks consisting of increasingly heterogeneous devices.

The ubiquity of smartphone devices will also play a factor, allowing Bluetooth to take advantage of unique use cases and opportunities when compared with competing low-power technologies not present in this space. Bluetooth is also working toward adopting mesh networking within the standard, providing the scalability and range required for wireless sensor network applications. However, it remains to be seen how fast Bluetooth mesh will hit the market and which use cases will take advantage of the technology in the short to medium term.

Yet, according to the report, there will be considerable challenges in terms of security, provisioning and interoperability that suppliers will need to target over the next few years. Chipset suppliers, such as Nordic Semiconductor, are working toward integrating IPv6 over Bluetooth Smart, which will help provide the foundation for IP-based application layer level interoperability between different types of devices operating on different transport layers, such as 802.15.4 and Wi-Fi.

"As the IoT incorporates a more diverse range of device types, the adoption of a common language across various con-

For More Information
Visit mwjournal.com for more commercial market news

nectivity types will become increasingly critical in ensuring interoperability and helping to grow the overall market," concludes Zignani. "In addition, the development of Bluetooth and NFC combo ICs can assist with the secure provisioning of headless devices, such as smart light bulbs, sensors and other IoT devices, simplifying the installation process while strengthening the overall security of the network."

Smart Meter Rollouts from Water Utilities Gain Momentum

Smart electricity meters will constitute the largest share, occupying more than 72 percent of the overall installed base of smart meters, but research suggests water meters are on track to witness the most overall growth.

"The global smart meter market for electricity and gas is reaching a degree of maturity, as utilities in most regions are either in advanced stages of rollouts or have laid out plans for phased deployment," says Adarsh Krishnan, senior analyst at ABI Research. "The focus is starting to shift toward modernizing the aging water distribution network, offering substantial market opportunity for OEMs, utilities and end-users."

Itron, Landis+Gyr, Kamstrup, Diehl, Sensus and ARAD, among others, offer end-to-end solutions and continue to dominate the vendor landscape. Data findings suggest, however, that there is growing concern among water utilities, especially those in cities, as they attempt to efficiently manage limited fresh water resources while keeping up with the increasing demand due to rapid urbanization.

"Smart water meters and data analytics are more critical components for water utilities," continues Krishnan. "They can help improve distribution efficiency by reducing leakages and also serve to implement and monitor the effectiveness of water conservation programs. The lack of regulatory framework or a government mandate in the water sector has resulted in a lack of shared vision to modernize the water network."

As smart water meters are battery powered devices, choosing the right connectivity solution poses another unique challenge. Long battery life of more than 10 years and signal propagation to reach meters that are often underground in pavements or driveways are critical to connect meters.

Wireless mesh networking and Low Power-WAN (LPWAN) technologies are popular connectivity technology choices for smart water meters, with the latter gaining momentum. Cellular and non-cellular LPWAN technologies that operate in either the licensed or un-licensed portions of the spectrum band, such as LTE-M, NB-LTE, Sigfox, LoRa, Ingenu and FlexNet, are strong contenders to meet connectivity requirements.

Around the **Circuit**

Barbara Walsh, Multimedia Staff Editor

MERGERS & ACQUISITIONS

M/A-COM Technology Solutions Holdings Inc. announced it has successfully completed its previously announced acquisition of **FiBest Ltd.**, a Japan-based merchant market component supplier of optical sub assemblies, in an all-cash transaction valued at approximately $60 million. MACOM funded the purchase price of the FiBest acquisition with cash on hand.

Comtech Telecommunications Corp. announced that the applicable waiting period under the Hart-Scott-Rodino Antitrust Improvements Act of 1976 (HSR) with respect to the previously announced tender offer by its direct wholly owned subsidiary, Typhoon Acquisition Corp., for all outstanding shares of common stock of **TeleCommunication Systems Inc.** at a price of $5.00 per share, net to the seller in cash, without interest and less required withholding taxes and subsequent merger of Typhoon Acquisition Corp. with TCS terminated on December 18, 2015. The termination of the HSR waiting period satisfies one of the conditions to the closing of the pending acquisition, which remains subject to other customary closing conditions.

Mercury Systems Inc. announced that it has acquired **Lewis Innovative Technologies Inc.** (LIT). A privately-held company based in Decatur, Ala., LIT is at the forefront of technology development necessary to protecting systems critical to national security while meeting strict DoD Program Protection Requirements. These technologies have proven application to a broad range of secure processing needs for several critical military missions. Terms of the transaction were not disclosed. The company intends to maintain LIT's presence in the Huntsville, Ala. tech corridor.

JADAK LLC, a supplier of HF RFID, optical data collection and machine vision technologies to original equipment manufacturers (OEM) in medical, security, gaming and kiosk industries, announced it has acquired the assets of **SkyeTek**, a Denver, Colo.-based provider of embedded and stand-alone UHF RFID solutions for OEM equipment suppliers. SkyeTek specializes in high performing UHF RFID technologies that maximize efficiency and visibility for OEMs serving the medical and pharmaceutical, government, hospitality and manufacturing industries.

COLLABORATIONS

Anritsu Corp. and **Verkotan Oy** are working together to enable support for the Over-The-Air (OTA) performance testing of wireless devices such as wearables and smart phones. Verkotan Inc. is a CTIA accredited OTA test house specializing in testing and analyzing the performance of wireless devices, which is helping to mitigate problems with accurate testing during the product development phase. Based in Finland, Verkotan is the only accredited test house in the world with its own in-house developed test software.

NEC Corp. and **Intel Corp.** will collaborate to jointly develop the Cloud-Radio Access Network (Cloud-RAN) solution for virtualizing the functions of mobile base stations. Both companies will start a joint proof of concept trial from early 2016 to verify the capabilities of the Cloud-RAN solution. Mobile base stations are comprised of a Digital Unit (DU) that handles data processing and a Radio Unit (RU) that sends and receives radio waves. The Cloud-RAN solution separates the DU functions from mobile base stations, and enables the functions to be run on general-purpose servers equipped with Intel's multi-core processors.

Rohde & Schwarz and **EMITE** have announced that the new R&S CMWflexx wideband radio communication tester setup has been successfully used in combination with the EMITE E500 reverberation chamber and a channel emulator to test up to 4CC LTE-A FDD CA with 2×2 MIMO on each carrier and more realistic isotropic urban-macro (UMA) fading profiles. The tests were performed for a leading U.S. carrier. The R&S CMWflexx is specially designed for testing LTE-A with a high number of component carriers. It is the latest addition to the R&S CMW500 wideband communication tester family.

NEW STARTS

Custom MMIC has launched a new website. The site features over 80 products from their catalog and over a dozen recently released high performance, GaAs and GaN low noise amplifiers, distributed amplifiers, power amplifiers, driver amplifiers, attenuators, mixers, multipliers, phase shifters and switches. In addition to several industry-leading performance characteristics driven by customer demand, this new suite of standard MMICs also includes solutions to signal chain design challenges.

ACHIEVEMENTS

Keysight Technologies Inc. is the first test and measurement company to achieve the silver status SC21 award for its hardware and support services. SC21 is a U.K.-based change program designed to accelerate the competitiveness of the aerospace & defense industry by raising the performance of its supply chains. Keysight has consistently achieved above 95 percent on quality and delivery performance metrics. Keysight also has the highest manufacturing and business excellence scores amongst the 300 companies who have been recognized for an SC21 award since 2006. Keysight's recently acquired Electroservices, also received a silver status award.

Radio Frequency Systems (RFS) was recently awarded with a Supplier Innovations Award from **SPIE Sud-Eston** at a ceremony in Lyon, France. The award was bestowed on RFS to recognize the new Transparent Antenna line as a major breakthrough in the telecommunications industry. The Transparent Antennas blend seamlessly into any landscape, reducing visual impact on its surroundings. SPIE Sud-Eston noted that this new type of antenna could be erected in new locations, including urban areas, business districts and transport environments (such as airports) without looking like an eyesore. The nearly-invisible nature

For More Information

For up-to-date news briefs, visit mwjournal.com

Exceptional
Phase Noise Performance
Dielectric Resonator Oscillator

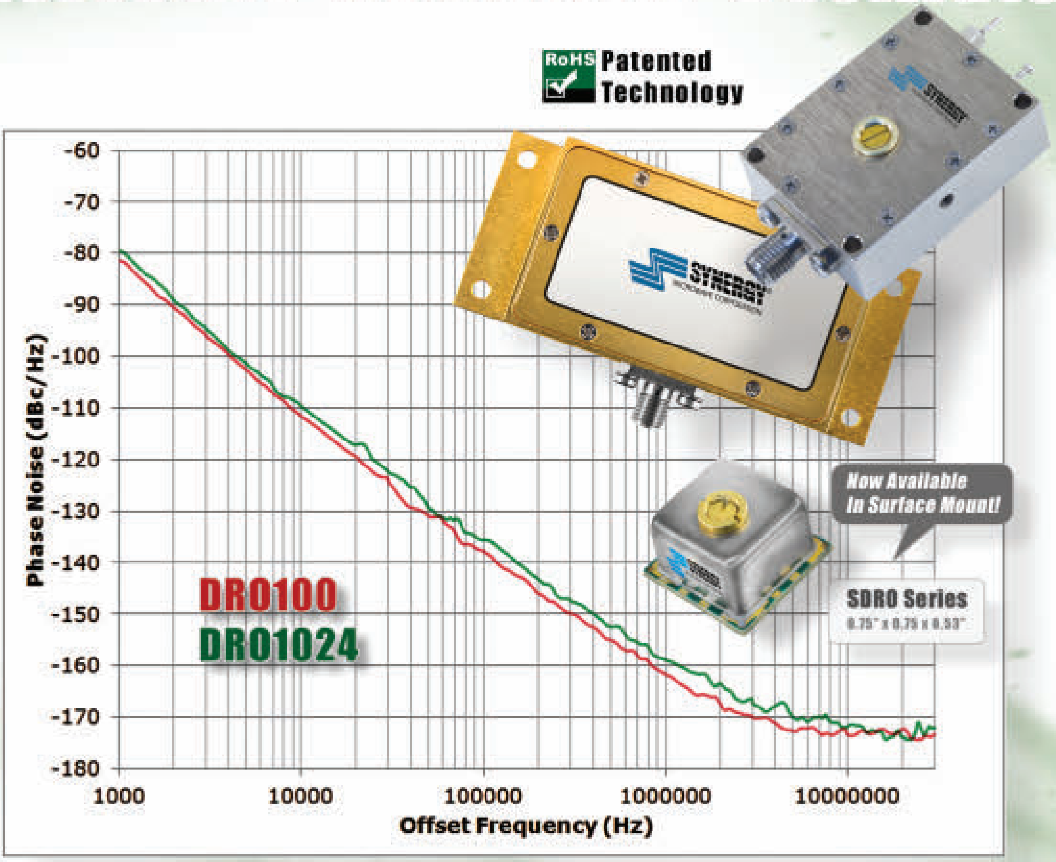

Model	Frequency (GHz)	Tuning Voltage (VDC)	DC Bias (VDC)	Typical Phase Noise @10kHz (dBc/Hz)
Surface Mount Models				
SDRO1000-8	10	1 - 15	+8 @ 25 mA	-107
SDRO1024-8	10.24	1 - 15	+8 @ 25 mA	-111
Connectorized Models				
DRO100	10	1 - 15	+7 - 10 @ 70 mA	-111
DRO1024	10	1 - 15	+7 - 10 @ 70 mA	-109

Model	Center Frequency (GHz)	Mechanical Tuning (MHz)	Supply Voltage (VDC / Current)	Typical Phase Noise @10kHz (dBc/Hz)
Mechanical Tuning Connectorized Model				
KDRO145-15-411M	14.5	±10 MHz	15 V / 130 mA (Max.)	-88

Talk To Us About Your Custom Requirements.

SYNERGY®
MICROWAVE CORPORATION

Phone: (973) 881-8800 | Fax: (973) 881-8361
E-mail: sales@synergymwave.com
Web: WWW.SYNERGYMWAVE.COM
Mail: 201 McLean Boulevard, Paterson, NJ 07504

of these Transparent Antennas also makes site approvals and lease renewals easier. The RFS Transparent Antennas will soon be available in a version that can be incorporated in to existing indoor signage.

PsiKick is a start-up that is working towards creating self-powered sensing solutions. Their systems-on-chips operate at up to 1,000× lower power than existing state-of-the-art "low power" solutions. They have recently announced a $16.5 million series B financing round, led by Osage University Partners and joined by existing investors New Enterprise Associates (NEA), the University of Michigan Investment in New Technologies Fund (MINTS) as well as individual angels. This brings total funding raised by the company to over $22 million. Prior to this funding round, PsiKick created a platform of fundamental technologies for wireless devices that are entirely self-powered.

CONTRACTS

Lockheed Martin has received a $302.2 million contract from the **U.S. Air Force** for continued production of the Joint Air-to-Surface Standoff Missile (JASSM®) and its Extended Range (ER) version. The Lot 14 contract includes 146 baseline JASSMs for U.S. and international partners, 140 JASSM-ER missiles for the U.S., as well as data, tooling and test equipment. The award brings the total number of missiles under contract to more than 2,600. The contract represents the sixth production order for JASSM-ER, which received full-rate production approval in 2014.

Gilat Satellite Networks Ltd. reported a new award by Peru's **Fitel** (Fondo de Inversion en Telecomunicaciones/Telecommunications Investment Fund) of a regional telecommunications infrastructure project for $108 million, in the region of Cusco. This new project is in addition to the projects previously awarded to Gilat by Fitel in the regions of Huancavelica, Ayacucho and Apurimac which are currently underway.

The Space and Naval Warfare Systems Command in San Diego, Calif. has awarded **Raytheon Space and Airborne Systems** a $103 million contract — which could be worth up to $467 million if all options are exercised — to develop, test and deliver Navy Multiband Terminals, which will provide protected transmission of tactical data, imagery, video, maps and targeting information. The terminal, which the Navy refers to as NMT, is the fourth generation of the Navy's extremely high frequency terminals. According to a Navy fact sheet, NMT will deliver about a fourfold increase over current terminals and will include wideband options for communicating with other military satellite systems, including the Defense Satellite Communications System and the Wideband Global Satellite.

Harris Corp. has received $66 million in orders to provide a Middle East nation with Falcon III® wideband tactical radios and accessories as part of an overall communications modernization effort. Harris will provide several configurations of its Falcon III radios including the RF-7800H, a wideband HF tactical radio that delivers expanded data

capabilities for long-range, beyond-line-of-sight environments; the RF-7850M, for wideband, mobile ad-hoc networking; the RF-7800V, for expanded narrowband data capabilities; and the RF-5800H, a narrowband HF tactical radio that delivers data and voice capabilities for long-range, beyond-line-of-sight environments. The company also will supply vehicular systems, accessories and training services.

Cobham recently received two awards totaling $20.5 million to provide actuators for the Mars 2020 mission. **NASA** has again selected Cobham's actuators to drive the rover wheels and provide steering motion, move the high-gain antenna and perform remote sensing mast deployment. Cobham's actuators were also selected by **Malin Space Science Systems** for two of the mission's cameras. Work under the contracts will be performed by Cobham Integrated Electronic Solutions, a business unit of the Cobham Advanced Electronic Solutions sector, at the Hauppauge, N.Y. site which specializes in high reliability motion control solutions.

BAE Systems has received a $16.5 million contract from the **U.S. Navy** to perform overhaul and maintenance services for the USNS Washington Chambers (T-AKE 11), a Lewis and Clark-class dry cargo ammunition ship. The work, which will take place at the company's shipyard in San Francisco, Calif., is scheduled to conclude in April. The scope of work under the competitively awarded contract includes dry docking the 689-foot-long ship, overhauling its main engines, performing maintenance work on its bow thruster and propeller systems, clearing and preserving internal tanks and voids, working on its heating, ventilating, and air conditioning systems, and conducting underwater hull cleaning and painting.

GE Aviation received a contract for the research and development of silicon carbide-based power electronics supporting the high-voltage next generation ground vehicle electrical power architecture for the **U.S. Army**. The $3.4 million contract consists of an 18 month development program that will demonstrate the benefits of GE's Silicon Carbide MOSFET technology in two critical systems: a 35 kW main engine cooling fan controller and a 3 kW coolant pump controller. The hardware will be more efficient than present day silicon based systems and will allow better management of the vehicle's available on-board power, increasing mission capability.

Airbus Defence and Space has been awarded the contract by the French defence procurement agency (DGA) for one of two military satellites for the COMSAT NG secure telecommunications programme. Airbus Defence and Space will also be co-responsible, together with **Thales Alenia Space** (lead contractor), for the entire space programme, which includes two satellites, their launch, the ground control segment, Ka-Band anchor stations, options for additional satellites, as well as the studies and operational maintenance of the system. Designed to replace the Syracuse III system, COMSAT NG is scheduled to go into operation from 2021, and will provide high-throughput capacity in the Ka Military Band in addition to those in the Syracuse III X-Band.

Around the **Circuit**

CACI International Inc. announced it has been awarded a multi-million dollar task order contract to continue its Command, Control, Communications and Prototyping Operations (C3PO) support for the **U.S. Army Intelligence and Information Warfare Directorate (I2WD)**. This multi-year contract, awarded under the Rapid Response - Third Generation contract vehicle, represents continuing work for CACI in its Intelligence Systems and Support market area. I2WD is the Army's center for research and development of advanced cyber operations, electronic warfare, signals intelligence technologies, radar, and intelligence analysis, exploitation, and dissemination capabilities. Under the C3PO award, CACI will provide software and hardware engineering support to help I2WD secure air and ground platforms against electronic warfare (EW) attack and assist in developing EW countermeasures.

COM DEV International Ltd. received an order to start work on the third satellite of a multiple-satellite contract that was awarded to the firm in October 2013. The contract is valued in excess of CA$12 million. Each of the satellites built under this contract will deliver high throughput commercial communications services. COM DEV has completed delivery on the equipment built for the first satellite and commenced work on the second in April 2015.

MacDonald, Dettwiler and Associates Ltd. has signed a contract valued in excess of CA$10 million with **Orbital ATK** to provide a communication antenna subsystem for the HYLAS 4 telecommunication satellite. HYLAS 4 is expected to launch in 2017.

PEOPLE

▲ ***Simon Mao and Chris Noade***

Knowles Capacitors has restructured its sales and product management teams. **Simon Mao**, previously Asia marketing manager, is now product manager of MLCs. By staffing the position in China, Mao will be best positioned to work closely alongside the Suzhou factory operations team where Knowles commercial MLC products are made. **Chris Noade**, previously product manager of MLCs, has accepted the position of European sales manager with responsibility for the full product portfolio. In this role he will focus on key account development and relationship management.

▲ ***Lauren Tully***

Microwave Journal welcomes **Lauren Tully** as digital content production specialist. Tully will manage day-to-day digital campaigns and maintain a comprehensive schedule of electronic products including newsletters, white papers, webinars, videos, digital and mobile edition ads, blogs and social media. She brings more than 20 years of experience to the position, having worked on retail CSM channels, web content administration and media content production in her prior roles. She can be reached at ltully@mwjournal.com.

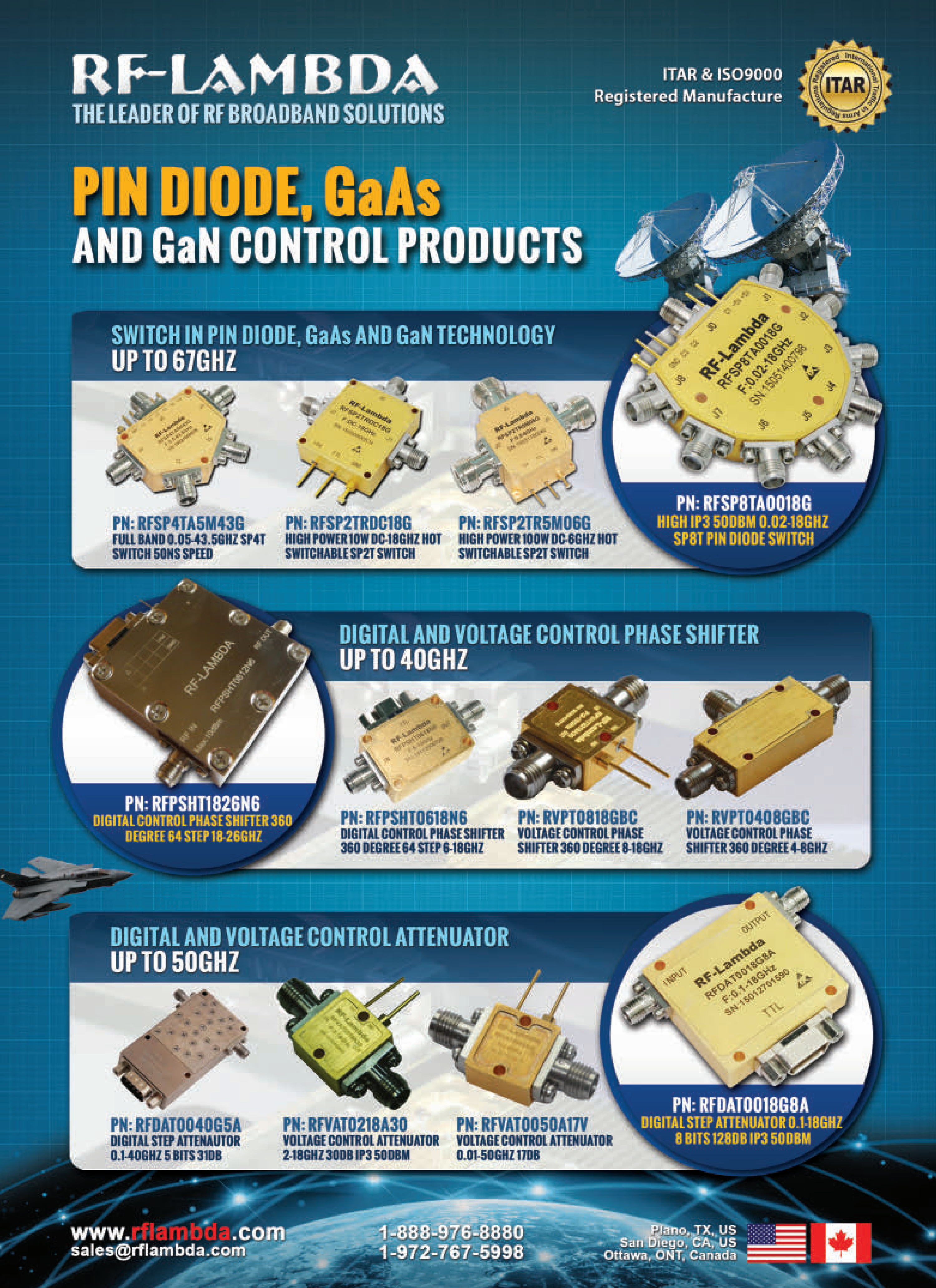
RF-LAMBDA
THE LEADER OF RF BROADBAND SOLUTIONS
ITAR & ISO9000
Registered Manufacture
ITAR
PIN DIODE, GaAs
AND GaN CONTROL PRODUCTS
SWITCH IN PIN DIODE, GaAs AND GaN TECHNOLOGY
UP TO 67GHZ
PN: RFSP4TA5M43G
FULL BAND 0.05-43.5GHZ SP4T SWITCH 50NS SPEED
PN: RFSP2TRDC18G
HIGH POWER 10W DC-18GHZ HOT SWITCHABLE SP2T SWITCH
PN: RFSP2TR5M06G
HIGH POWER 100W DC-6GHZ HOT SWITCHABLE SP2T SWITCH
RF-Lambda
RFSP8TA0018G
F:0.02-18GHz
SN:1505140798
PN: RFSP8TA0018G
HIGH IP3 50DBM 0.02-18GHZ
SP8T PIN DIODE SWITCH
RF-LAMBDA
DIGITAL AND VOLTAGE CONTROL PHASE SHIFTER
UP TO 40GHZ
PN: RFPSHT1826N6
DIGITAL CONTROL PHASE SHIFTER 360 DEGREE 64 STEP 18-26GHZ
PN: RFPSHT0618N6
DIGITAL CONTROL PHASE SHIFTER 360 DEGREE 64 STEP 6-18GHZ
PN: RVPT0818GBC
VOLTAGE CONTROL PHASE SHIFTER 360 DEGREE 8-18GHZ
PN: RVPT0408GBC
VOLTAGE CONTROL PHASE SHIFTER 360 DEGREE 4-8GHZ
DIGITAL AND VOLTAGE CONTROL ATTENUATOR
UP TO 50GHZ
PN: RFDAT0040G5A
DIGITAL STEP ATTENAUTOR 0.1-40GHZ 5 BITS 31DB
PN: RFVAT0218A30
VOLTAGE CONTROL ATTENUATOR 2-18GHZ 30DB IP3 50DBM
PN: RFVAT0050A17V
VOLTAGE CONTROL ATTENUATOR 0.01-50GHZ 17DB
OUTPUT
INPUT
RF-Lambda
RFDAT0018G8A
F:0.1-18GHz
SN:1501270590
TTL
PN: RFDAT0018G8A
DIGITAL STEP ATTENUATOR 0.1-18GHZ
8 BITS 128DB IP3 50DBM
www.rflambda.com
sales@rflambda.com
1-888-976-8880
1-972-767-5998
Plano, TX, US
San Diego, CA, US
Ottawa, ONT, Canada

Around the **Circuit**

REP APPOINTMENTS

Astrodyne TDI, a designer and manufacturer of EMI and RFI power line filters, has recently partnered with Geneva, Ill.-based **Richardson RFPD**, an Arrow Co., to offer its line of filter products worldwide. With 35 locations across the globe, Richardson RFPD is a specialized electronic component distributor providing design engineers with technical expertise and localized global design support for the latest products on the market from the world's leading suppliers of RF, wireless, energy and power technologies.

RFMW Ltd. and **Southwest Antennas** of San Diego, Calif., have announced a distribution agreement effective immediately. Southwest Antennas manufactures over 600 RF and microwave antennas and accessories operating in frequencies up to 8.5 GHz, with capabilities beyond 20 GHz. Under the agreement, RFMW is franchised worldwide for Southwest Antennas' full range of antenna related products which includes accessories such as antenna mounting solutions, block down-converters, low noise amplifiers and filter modules.

PLACES

Altair Semiconductor, a provider of LTE chipsets, announced the opening of a research and development (R&D) center in Taiwan to support the company's technical advancement in the major Asian growth-center. Headquartered in Israel, Altair Semiconductor has six worldwide offices, including four in Asia: China, Taiwan, Japan and India. R&D teams, spread throughout the company's corporate network, work to develop next-generation LTE chipsets for the IoT/M2M and broadband markets.

COMSOL announced the expansion of its office in Shanghai, China. A larger facility enables continued expansion and recruitment of technical and sales staff to keep pace with the growing COMSOL® software user base in China and increasing demand for COMSOL Multiphysics® and COMSOL Server™ products. Services in Shanghai include sales, technical support, training sessions, on-site workshops and customer visits.

GeoSync Microwave's president Arthur Faverio announced the purchase of a 20,000 square foot building at 320 Oser Avenue in the Hauppauge Industrial Park within a half a mile of GeoSync's current facilities in Hauppauge, N.Y. The new building significantly increases GeoSync's manufacturing space which will be immediately used to increase production capacity of its RF Satcom products and provides for additional engineering offices and labs. Renovations will be completed by the end of the first quarter and transitioning from the current offices will be completed in early April.

Programmable ATTENUATORS

0 to 120 dB   0.25 dB Step   1 to 8000 MHz†*   from $395

FEATURES
- 0 – 30, 60, 63, 90, 110, and 120 dB
- USB, Ethernet & RS232 control options
- User-friendly GUI and DLLs included
- Sweeping and hopping capability
- Available from stock!

Perfect for…
- Fading simulators
- Handover system evaluation
- Automated test equipment
- And MORE!

***Visit minicircuits.com** for detailed model specs, application notes, and more!*
Place your order today and have them on your test bench as soon as tomorrow!

* Model RCDAT-3000-63W2+ specified step size 1 dB
† Model RCDAT-3000-63W2+ specified from 50 – 3000 MHz; 120 dB models specified from 1 – 4000 MHz
†† No drivers required. DLL objects for 32/64 bit Windows® environments using ActiveX® and .NET® frameworks.

Mini-Circuits®

www.minicircuits.com   P.O. Box 350166, Brooklyn, NY 11235-0003   (718) 934-4500   sales@minicircuits.com

523 RevG

INVITED PAPER

Editor's Note: This is the second of a two-part series on antenna anechoic chamber design. Part one, published in the January 2016 issue, discussed absorber requirements for rectangular, far field ranges. Part two discusses compact ranges and near field measurements.

Basic Rules for Anechoic Chamber Design, Part Two: Compact Ranges and Near Field Measurements

Vince Rodriguez
MI Technologies, Suwanee, Ga.

The task of adequately specifying performance for an indoor anechoic chamber without driving unnecessary costs or specifying contradictory requirements calls for insight that is not always available to the author of the specification. Although there are some articles and books[1-3] that address anechoic chamber design, a concise compendium of reference information and rules of thumb on the subject would be useful. This second part of the series intends to do that, concentrating on the sizing of compact ranges and chambers for near field systems. As was done in part one, simple approximations are used for absorber performance to generate a series of equations that help specify performance and size of facilities.

Part one of this series identified limitations in using far field chambers, mainly related to the electrical size of antennas that can be tested. As was shown, an 18" dish used by a popular satellite TV service will be almost impossible to test in a far field chamber. The satellite service operates at 18.55 GHz, the dish antenna is 28.29 wavelengths (λ) in size, so the far field is at approximately 1600 λ or 25.9 m (84.8 ft). Clearly for such an electrically large antenna, far field illumination indoors is not economically feasible. For this antenna, a compact range or near field measurement is more suitable.

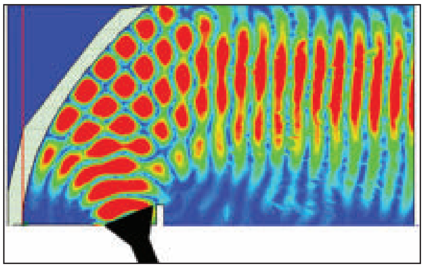

▲ *Fig. 1 Simulated results of a parabolic reflector, showing plane wave behavior on the right.*

COMPACT RANGES

Although barely mentioned in the IEEE standard test procedure for antennas,[4] the compact range (CR) has become an important tool for measuring electrically large antennas. The CR uses a parabolic reflector to create a plane wave illumination at the location of the antenna under test (AUT). This plane wave simulates the field distribution that the antenna experiences in the far field. ***Figure 1*** shows a parabolic reflector illuminated by a source located at the focal point of the parabola. The plane wave behavior can be seen a short distance from the reflector. The reflector system is the controlling factor when sizing the range. The reflector must be large enough to provide a plane wave that illuminates the entire antenna being tested, and the reflector should be properly terminated. The

TABLE 1

COMMERCIALLY AVAILABLE COMPACT RANGE REFLECTORS

QZ Size (Length and Diameter) (cm)	Overall Reflector Size (Including Serrations) (cm)	Length of Serrations (cm)	Frequency of Operation (GHz)	Focal Length f_l (cm)
61	216 × 188	38	4 to 200	182
122	432 × 335	76	2 to 200	366
182	488 × 416	76	2 to 200	366
244	864 × 670	152	1 to 200	732
366	975 × 833	152	1 to 200	732

purpose of the termination is to reduce the effects of the terminated paraboloid on the illumination. The two most common ways of terminating a reflector are serrations and rolled edges.[6] In the case of serrated edge reflectors, serrations can be between 3 λ and 5 λ at the lowest frequency of operation. ***Table 1*** provides a typical list of reflectors, showing their overall size and frequency ranges. Note that as frequency increases, the reflector becomes more efficient. While some reflectors can operate well into the millimeter wave range, extra care should be taken during manufacturing and surface finishing, as surface imperfections will affect the performance.

Reflector size is the determining factor when sizing the width and height of the chamber. The length of the chamber will be affected by the focal length of the reflector. The distance from the vertex of the reflector to the quiet zone (QZ) is given by the following rule:

$$r = \frac{5}{3} f_l \qquad (1)$$

where f_l is the focal length of the reflector. Referring to the satellite TV antenna, requiring a far field distance of 25 m to test, one might expect long chambers and large distances for CR testing. However, Table 1 with Equation 1 indicates the test distance for a 61 cm QZ is 3 m. This is sufficient to test the satellite TV antenna.

As a rule, the length of a CR chamber is given by the following equation:

$$L = R_{clr} + \frac{5}{3} f_l + \frac{1}{2} QZ + (2 + t)\lambda \qquad (2)$$

where R_{clr} is the reflector clearance. This includes the mechanical structure to support the reflector, which ranges from 60 cm to 2 m, depending on the overall reflector size. In general, the wall behind the reflector has a small absorber, usually λ/2 in thickness, and only covers the perimeter of the wall. The parameter t is the thickness of the end wall absorber. For a CR, this is the most critical wall and should have the lowest reflectivity; it is recommended the value of t be no less than 3 to 4.

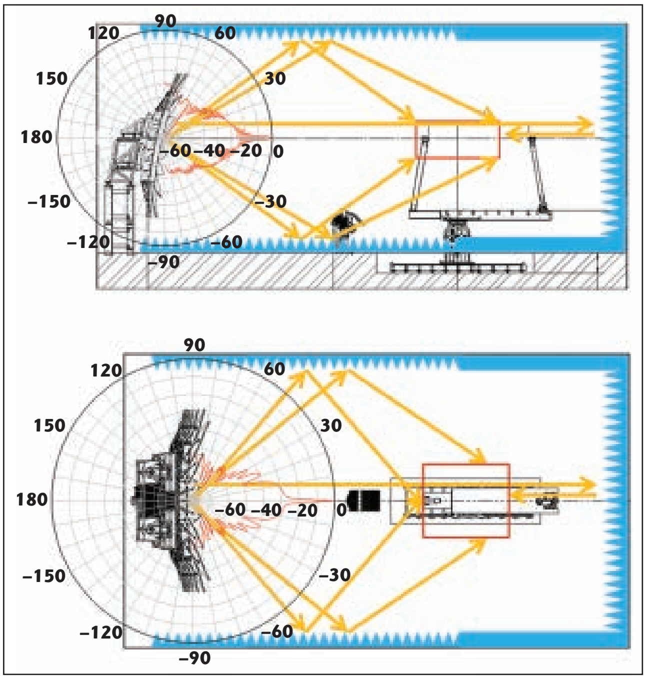

▲ *Fig. 2 A typical compact range layout showing the reflector pattern, side (a) and top (b) views. At 2 GHz, the energy incident on the side walls, floor and ceiling is more than 40 dB down.*

Top 10 Tips for GaN Success

High-performance gallium nitride on silicon carbide (GaN on SiC) semiconductor technology is making inroads in infrastructure, aerospace, defense, and commercial products. Qorvo® – a pioneer of GaN for high-power RF devices, power amplifiers, transistors, oscillators, switches, and more – strives to deliver high-performance, reliable devices to solve the RF challenges for the world's leading companies. What are the hallmarks of a quality GaN supplier? Read on to learn what to look for.

1 PROVEN DESIGN TOOLS

Nonlinear models, electromagnetic finite element modeling, and stability and loop stability analyses aid in designing best-in-class power and efficiency in high-power MMICs. Qorvo's robust design methodology leads to more first-pass successes and reliable designs.

2 ROBUST POPULATION TESTING

Industry standards allow testing of small samples of GaN products. Although this is usually adequate, Qorvo has fully characterized product failure modes by testing large populations at temperatures of interest over extended times.

3 HIGH MEDIAN TIME TO FAILURE (MTTF)

MTTF estimates a device's lifetime. Suppliers should measure device reliability at a minimum of three temperatures because higher temperatures lead to shorter device life. All Qorvo GaN products have an MTTF at 200°C extrapolated to over 10^7 hours.

4 NO PRECONDITIONING

Some suppliers add time and cost by requiring a preconditioning or burn-in step before delivery. Qorvo's GaN solutions have maturity in performance, reliability and manufacturing yield data that enables products to ship without preconditioning, confident in delivering high-quality performance every time.

5 JUNCTION TEMPERATURE CHARACTERIZATION

Low-resolution techniques like infrared microscopy underestimate product life expectancies and peak junction temperatures. Qorvo's thermal models and finite element analyses are verified with micro-Raman measurement, permitting more accurate temperature and device-life prediction.

6 ACCURATE FAILURE CRITERIA

One common parametric failure criteria is a current drop of 20% of I_{max}. Qorvo sets its I_{max} parametric failure at a 10% drop, ensuring less than 1dB of power degradation over the life of the part.

7 LOW FALLOUT RATES

Reliability is also measured by rates of catastrophic failure or fallout. Less than 0.002% of Qorvo's GaN devices fallout per 1 million hours at 200°C. Also check the expected operating life, T1, T5, and T10, at which 1%, 5%, and 10% of devices, respectively, will have failed based on a large population of devices.

8 PROVEN FIELD PERFORMANCE

Do your GaN supplier's products have a demonstrated track record of reliability in the field? Qorvo's fielded GaN power amplifiers have accumulated more than 65,800,000 device-hours with a field failure rate of less than 0.013% failures per million device-hours.

9 HIGH TOLERANCE FOR ENVIRONMENTAL STRESS

Check for devices that stand up to the highly accelerated stress test (HAST), which measures device performance after 96 hours at 130°C, 85% relative humidity, and atmospheric pressure up to 4 atm. THB compliance is also a critical measurement.

10 MANUFACTURING READINESS LEVEL

MRL is the Department of Defense's measurement of a supplier's ability to transition a product successfully from the factory to the field with operational maturity, technology development; and quality and manufacturing management. Qorvo was the first GaN supplier to achieve MRL 9.

www.qorvo.com

qorvo®
all around you

STRENGTH IN NUMBERS

Qorvo® GaN technology enables the systems all around you

#1

GaN Supplier In **DEFENSE**

Industry leader of GaN on Silicon Carbide

9 MRL

Only supplier to achieve MRL 9 using USAF MRA tool

More than 2,608,000 GaN devices shipped since 2008

GaN

Demonstrated MTTF reliability with 200°C / 10^7 hrs.

Top supplier of DOCSIS® 3.1 GaN components

125 new products in 18 months

0.013% per million device hour report failures

65,800,000 device hours on 16,920 GaN PAs

qorvo® all around you

For more information text **Qorvo** to **82257** or visit Qorvo.com/GaN

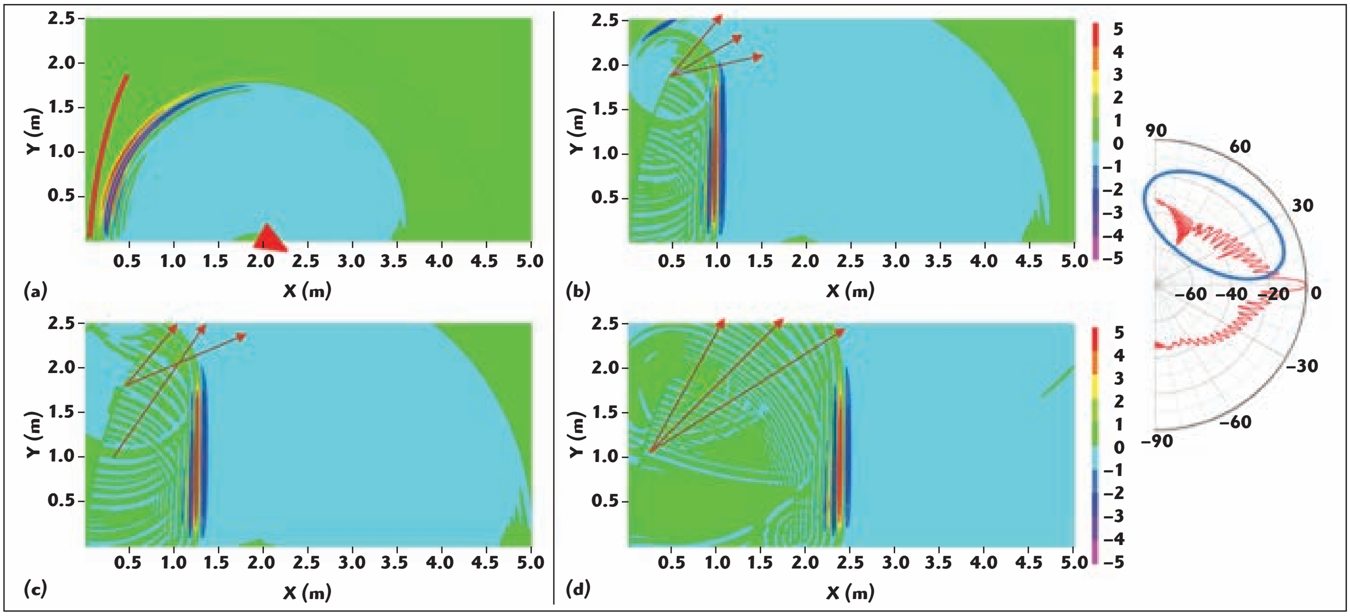

Fig. 3 Wave propagation from the source horn vs. time – 6.6 ns (a) 10.4 ns (b) 11.3 ns (c) 15.1 ns (d) – compared to the far field pattern.

The width of the chamber is calculated using:

$$W = CR_w + (4 + 2t)\lambda \tag{3}$$

where CR_w is the overall width of the reflector. There is an additional 2 λ from the tips of the serrations to the absorber tips on each side of the reflector, although in some cases the spacing can be as small as one wavelength on each side. The final item determining the width of the range is the thickness of the absorber.

While for far field ranges the absorber on the ceiling, floor and side walls should be thick enough to provide good bistatic reflectivity at oblique angles, in the CR the side wall absorber does not need to be as thick. ***Figure 2*** shows a typical CR chamber. The radiation pattern of the CR reflector has been superimposed over the chamber drawing. The reflector in the figure provides a 3.66 m × 1.82 m elliptical QZ. The depth of the QZ is 3.66 m. The important aspect of the CR is that it has a very directive pattern, with directivities in excess of 25 dBi. As Figure 2 shows, the energy incident on the absorber on the side walls is already 40 dB below the direct path. A 1λ thick absorber will provide 10 dB of absorption at over 60 degrees of incidence (see Figure 4 in part one, published in January 2016). Combining the reflectivity with the difference in magnitude between the direct ray and the reflected ray, results in a reflected energy level of approximately -50 dB. The reflector is being used in the near field while the radiation pattern of the reflector is a far field concept. However, this is an acceptable approximation, as it provides a method for estimating the level of energy that radiates from the reflector in the direction of the walls. As ***Figure 3*** shows, the reflector will send some energy towards the side walls, estimated from the far field pattern of the reflector.

The height of the chamber has a similar equation for calculating the size:

$$H = CR_h + (2 + K + 2t)\lambda \tag{4}$$

where CR_h is the overall height of the reflector. The spacing between the tips of the reflector and the tips of the ceiling absorber is 2 λ. The parameter K provides a factor for the spacing between the floor and the reflector. For the floor absorber, we want a larger separation between the edge of the reflector and the tips of the floor absorber. This reduces the angle of incidence at the specular point between the reflector feed and the reflector to minimize the impact of the floor reflection on the reflector illumination (see ***Figure 4***). Equation 4 includes K wavelengths of space between the tips of the floor absorber and the serration tips. K should be large enough to provide sufficient space for the feed positioner supporting the feed antenna that illuminates the reflector. As was the case with the side walls, the absorber on the floor and the ceiling can be 1λ thick. Special consideration must be given to the floor absorber between the feed and the reflector, which may be 2λ thick. In general, the absorber electrical thickness at the lowest frequency can be t ≤ 1.2 and

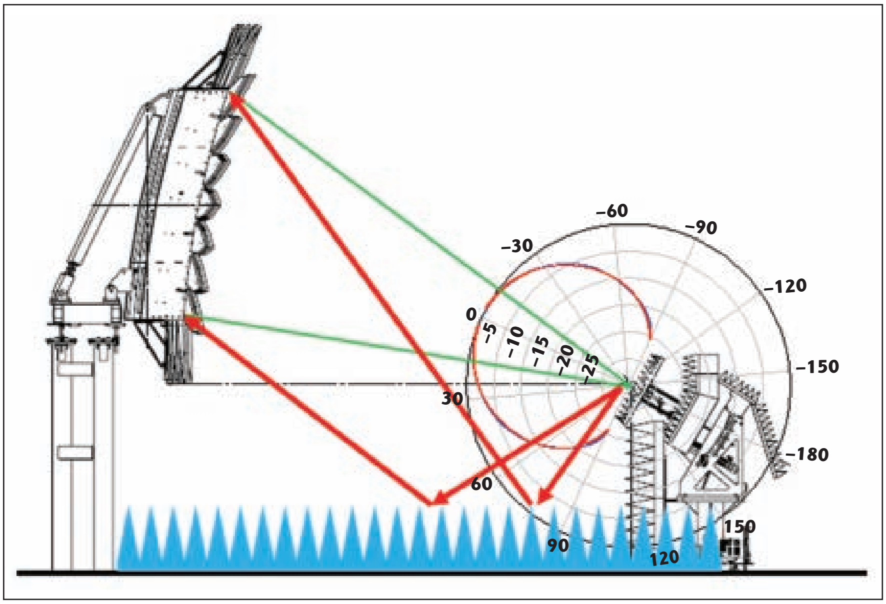

▲ *Fig. 4 Absorber on the floor between the feed positioner and the reflector is critical to reduce the reflected energy from illuminating the reflector.*

$t \geq 0.75$ for the side wall and ceiling treatments, respectively.

NEAR FIELD RANGES

Different techniques are used for performing near field measurements; they align with the type of antenna being measured. With all approaches, the field (amplitude and phase) radiated from the AUT is measured on a surface, and the far field behavior is derived mathematically from this measurement. Three different near field techniques — planar (PNF), cylindrical (CNF) and spherical (SNF) — represent the surface where the data is measured.[7-9] The most basic near field measurement approach is planar scanning, where the field radiated from the antenna is scanned on a single plane. This is a good technique for high gain antennas, as there is a very small amount of energy radiating to the back of the antenna. Cylindrical scanning is where the field is measured on the surface of a cylinder excluding the top and bottom surfaces. This is ideal for long antennas that are omnidirectional or have a wide beam on one of the principal planes but a narrow beam in the perpendicular plane. Spherical scanning is a more general measurement approach. Here the field is measured on a sphere that contains the entire antenna. In general, the test distance for PNF measurements is between 3λ and 10λ. For SNF, the probe can be further away.

The same equations developed for far field chambers can be used for SNF with the exception of the test distance. In general, the equation is given by:

$$L = d_{pp} + \left(n + 6 + 2t_e\right)\lambda \quad (5)$$

where d_{pp} is the depth of the probe (measuring antenna) and its positioner. The variable n is the diameter in wavelengths of the minimum sphere that contains the AUT. The absorber on the two end walls will have a thickness of $t_e\lambda$, where t_e is the thickness, in wavelengths, of the end wall absorber. As is customary, 2λ is added between the minimum sphere and the absorber tips. Finally, 4λ is estimated to be the distance between the probe and the sphere containing the antenna.

The width of the SNF chamber is given by:

$$W = \left(n + 4 + 2t_s\right)\lambda \quad (6)$$

In this case, t_s is the thickness, in wavelengths, of the side wall absorber. This is a rough approximation. For both Equations 5 and 6, a minimum of 1 meter should be added to prevent the positioning equipment from hitting the probe as it rotates the antenna being measured. The chamber also should provide room for people to work inside to set up the measurement. This is more critical for higher frequencies (above 2 GHz), where the

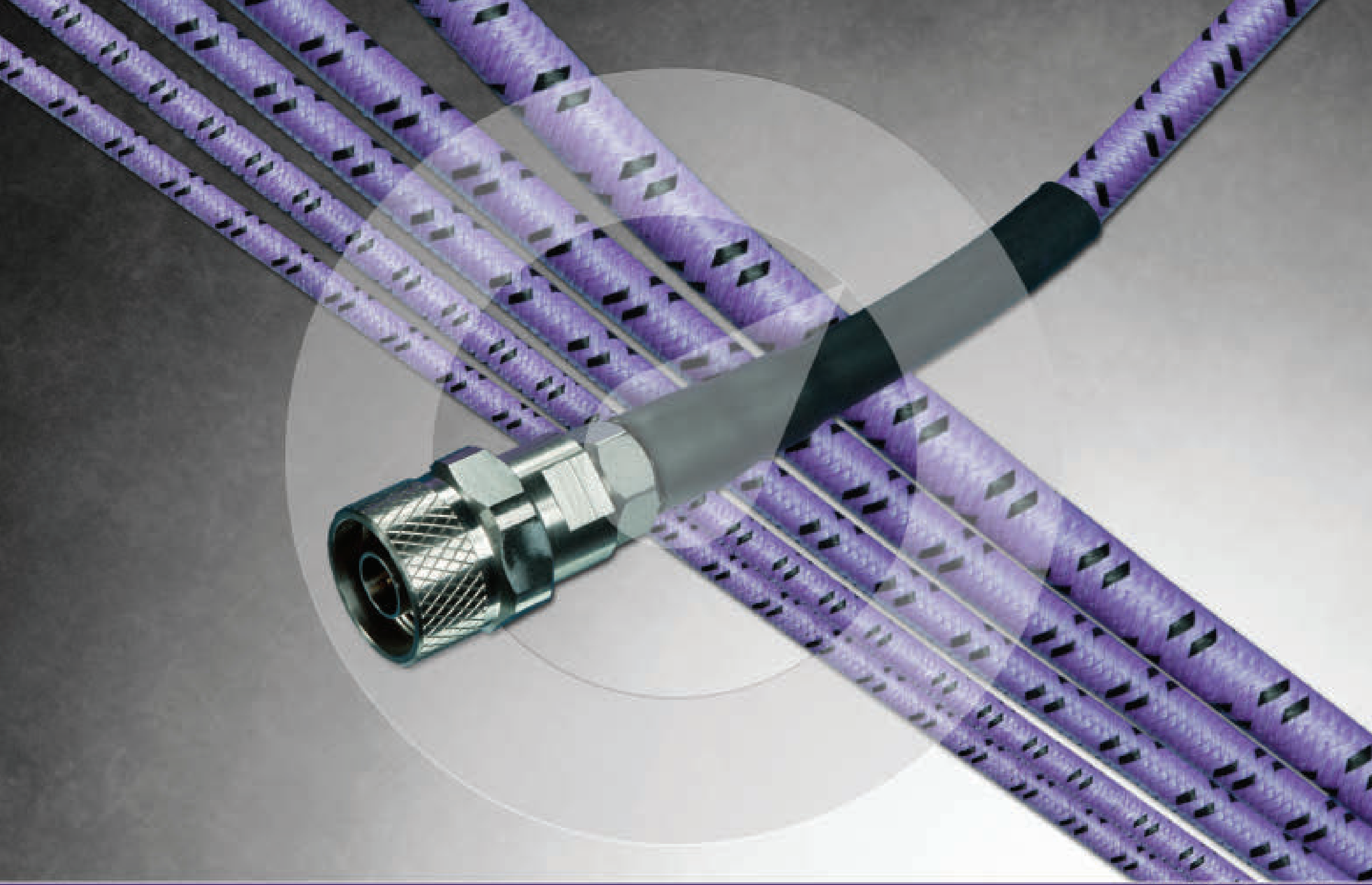

4λ separation may not be enough for the positioner to clear the probe.

The angle of incidence onto the side absorber is:

$$\theta = \arctan\left(\frac{4n+16}{2n+16}\right) \qquad (7)$$

Taking the limit as $n \to \infty$, $\theta < 63.4$ degrees. Using the absorber approximations presented in part one of this series, we can estimate that $t_s \approx 2t_e$. To do this, we check the reflectivity of the end wall absorber at normal incidence and select the thickness of the absorber that will provide similar reflectivity for the 63.4 degree incident angle. The ceiling and the floor will have the same absorber as the side walls.

The chamber height can be estimated using the following equation:

$$H = h_p + \left(n + 4 + t_s\right)\lambda \qquad (8)$$

where the variable h_p accounts for the height of the positioning equipment. In a typical roll-over azimuth positioner used in SNF measurements, h_p should include the height of the floor slide, the azimuth positioner and the offset slide. The positioning equipment in the far field chamber equations or the CR equations (except for the feed positioning) is not an issue because other dimensions are so dominant in these ranges (i.e., the far field test distance or the reflector size).

PNF systems use a planar scanner to measure highly directive antennas (i.e., gain > 20 dB). The high gain of the AUT benefits the design of the range, as some regions of the range do not need to be treated with absorber, such as those behind the AUT. The test distance, as stated above, is between 3λ and 10λ. The dominant factor for sizing a PNF range is the scanner, where the scan size is given by:

$$L_x = \left(n + 2k\tan\left(\theta_s\right)\right)\lambda \qquad (9)$$

θ_s is the maximum angle for accurate far field and $n\lambda$ is the electrical size of the antenna being tested (see ***Figure 5***). The variable k is the test distance in wavelengths; hence, $3 < k < 10$. The physical scanner will usually be slightly larger than the scan plane. Typically, 2λ is the separation to the absorber tips.

The width of the range becomes:

$$W = \left(n + 2k\tan\left(\theta_s\right) + 4 + 2t_s\right)\lambda + \Delta_{scn} \qquad (10)$$

which can be written as:

$$W = L_x + \left(4 + 2t_s\right)\lambda + \Delta_{scn} \qquad (11)$$

where Δ_{scn} is the additional space required for the scanner structure, and t_s is the thickness of the absorber.

The length of the range is given by the following equation:

$$L = S_{clr} + A_d + \left(4 + k + t\right)\lambda \qquad (12)$$

Where S_{clr} is the scanner depth, which should include the spacing to the absorber, if any (the scanner can be placed very close to the tips), and the probe length. A_d is the depth of the AUT and the support structure for aligning that antenna with the scanner. The 4λ in Equation 12 is the space between the back of the AUT and the range wall. For very high gain antennas, this wall does not need absorber treatment. If absorber is desired, the thickness of absorber for this wall can be as small as $\lambda/4$. The thickness of the absorber on the wall behind the scanner takes advantage of the directivity of the probe used to scan the plane. Thus, $t \geq 2$.

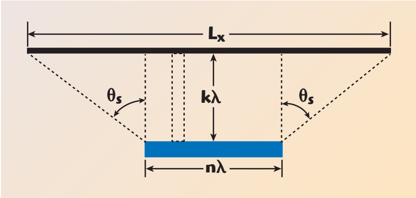

Fig. 5 Geometry of a planar near field measurement.

The remaining value to be defined is the absorber on the side walls. This is dependent on the angle θ_s and the factor k. The width is approximated as:

$$W \approx \left(n + 2k\tan\left(\theta_s\right) + 4 + 2t_s\right)\lambda \qquad (13)$$

Using the approximation that

$$\left(n + 2k\tan\left(\theta_s\right) + 4 + 2t_s\right)\lambda > \Delta_{scn} \qquad (14)$$

it follows that the angle of incidence onto the side walls is:

$$\theta = \arctan\left(\frac{k}{kn + k\tan\left(\theta_s\right) + 4}\right) \qquad (15)$$

Planar Monolithics Industries, Inc.

State of the Art High Isolation & Broadband Switches, 0.1 to 50 GHz

- Amplifiers
- Attenuators - Variable
- DLVA & ERDLVA & SDLVA's
- DTO's & Frequency Synthesizers
- Filters
- Form, Fit & Function Products
- IFM's & Frequency Discriminators
- Integrated MIC/MMIC Modules
- I/Q Vector Modulators
- Limiters & Detectors
- Log Amplifiers
- Pulse & Bi-Phase Modulators
- Phase Shifters
- Rack & Chassis Mount Products
- Receiver Front Ends & Transceivers
- Single Sideband Modulators
- SMT & QFN Products
- Solid-State Switches
- Switch Matrices
- Switch Filter Banks
- Threshold Detectors
- USB Products

PMI offers a full line of RF and Microwave, Solid-State Switches that range from DC to 50 GHz. Wide range of standard models with various options are available that include:

- SPST to SP8T Configurations.
- Hermetic Sealing is available.
- Military or Stringent Screening is available.
- High Reliability to MIL-STD-883.
- Small Quantity Requirements accepted.
- Specialized Testing & Custom designs welcome!

New designs operate from 0.1 to 50.0 GHz and feature low insertion loss and high resolution in a slimline package with 2.4mm female connectors. These modules incorporate a TTL compatible driver for ease of system integration.

Model P2T-100M50G-100-T

Absorptive, SP2T PIN Diode Switch

Frequency Range	Insertion Loss (Measured)	VSWR ON/OFF (Typ)	Isolation (Measured)
0.1 to 1.0 GHz	1.5 dB	1.76:1	103.7 dB
1 to 18 GHz	3.0 dB	1.85:1	107.8 dB
18 to 40 GHz	5.2 dB	1.96:1	90.8 dB
40 to 50 GHz	9.1 dB	2.54:1	95.9 dB

- Package Size: 1.0"x0.75"x0.40"
- DC Voltage: +/-5 V @ 100 mA
- Switching Speed: 50 ns Max

Model P4T-100M50G-100-T-RD

Absorptive, SP4T PIN Diode Switch

Frequency Range	Insertion Loss (Measured)	VSWR ON/OFF (Typ)	Isolation (Measured)
0.1 to 1.0 GHz	1.7 dB	1.70:1	109.9 dB
1 to 18 GHz	3.5 dB	1.96:1	112.0 dB
18 to 40 GHz	6.7 dB	2.24:1	98.2 dB
40 to 50 GHz	11.4 dB	2.67:1	82.1 dB

- Package Size: 1.25"x1.25"x0.40"
- DC Voltage: +/-5 V @ 200 mA
- Switching Speed: 50 ns Max

West Coast Operation:
4921 Robert J. Mathews Pkwy, Suite 1
El Dorado Hills, CA 95762 USA
Tel: 916-542-1401
Fax: 916-265-2597

East Coast Operation:
7311-F Grove Road
Frederick, MD 21704 USA
Tel: 301-662-5019
Fax: 301-662-1731

sales@pmi-rf.com • www.pmi-rf.com

ISO9001-2008 REGISTERED

Notice that the angle of incidence is only dependent on the size of the AUT, the maximum angle for accurate far field and the test distance in wavelengths. ***Figure 6*** shows that even at 10λ for a test distance, the largest angle of incidence is close to 20 degrees. From the absorber approximations presented in part one, the reflectivity of a given piece of absorber of certain electrical thickness does not deteriorate much within that range of angles of incidence. If the AUT is a simple passive antenna, the high gain can be a benefit. Since the antenna will not radiate much energy to the side walls, a smaller absorber ($t < 1$) may be used. However, if the AUT is a complex antenna with beam steering, then the side walls should have more thickness ($t \geq 2$).

The height of the chamber should be calculated in the same way as the width. In some cases, the scan distance is different between vertical and horizontal; it is not rare for the chamber to have a non-square cross section. The equation for the height is:

$$H = L_y + y_o + (2 + t_s)\lambda \qquad (16)$$

Where y_o is the minimum height of the probe, i.e., the location of the probe at the bottom of the vertical motion. This includes the rails on which the scanner moves in the horizontal axis and should also be large enough to include the floor absorber; at a minimum, $y_o > t_s\lambda$.

The above rules for SNF and PNF ranges can be combined to arrive at a range size for a CNF system.

CONCLUSION

Part two of this series provided an overview of the rules and physics that guide the selection and sizing of indoor anechoic chambers for compact ranges and for near field scanning measurements. All the equations are approximations. The length, in most cases, is a minimum; more space may be required for the loading and unloading of the AUT, changing feeds and range antennas and connecting additional equipment. Both parts of this series provide a general overview and equations for sizing anechoic rooms for the most common antenna measurement methods currently being used. ■

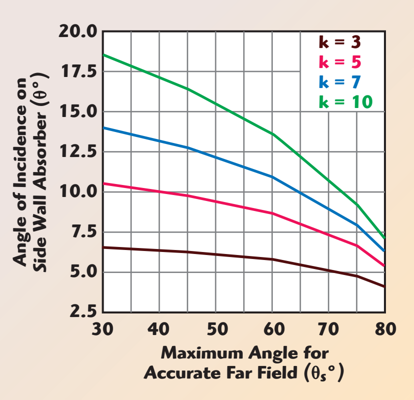

▲ *Fig. 6 Angle of incidence on the side wall absorber vs. maximum angle for accurate far field patterns, plotted for several test distances. The antenna aperture is 20λ.*

References

1. L. Hemming, "Electromagnetic Anechoic Chambers: A Fundamental Design and Specification Guide," IEEE Press/Wiley Interscience: Piscataway, N.J., 2002.
2. G. Sanchez and P. Connor, "How Much is a dB Worth?," *23rd Annual Symposium of the Antenna Measurement Techniques Association (AMTA)*, Denver, Colo., October 2001.
3. J. Hansen and V. Rodriguez,"Evaluate Antenna Measurement Methods," *Microwaves and RF*, October 2010, pp. 62–67.
4. ANSI/IEEE STD 149-1979 149-1979 - *IEEE Standard Test Procedures for Antennas*, 1979, reaffirmed 2008.
5. J.R.J. Gau, D. Burnside and M. Gilreath "Chebyshev Multilevel Absorber Design Concept," *IEEE Transactions On Antennas Propagat.*, Vol. 45, No. 8, pp. 1286–1293, 1997.
6. T.H. Lee and W. Burnside, "Performance Trade-Off Between Serrated Edge and Blended Rolled Edge Compact Range Reflectors," *IEEE Transactions on Antennas and Propagation*, Vol. 44, No. 1, January 1996, pp. 87–96.
7. D. Hess, "Near-Field Measurement Experience at Scientific Atlanta," White Paper, www.mitechnologies.com/papers/91/Near-Field%20Measurement%20Experience%20at%20Scientific-Atlanta.pdf.
8. Yaghjian, "An Overview of Near-Field Antenna Measurements," *IEEE Transactions on Antennas and Propagation*, Vol. AP-34, No. 1, January 1986, pp. 30–45.
9. J. E. Hansen ed., "Spherical Near-Field Antenna Measurements," IEEE Peter Peregrinus Ltd.: London, UK, 1988.

Vince Rodriguez *is a senior applications engineer with MI Technologies in Suwanee, Ga., where he brings his expertise in numerical modeling, RF absorber and anechoic range design to the design of antenna, radar cross section and radome testing facilities. His full biography appeared in part one of this series, published in the January 2016 issue.*

Leading Global Communications

PP10-10/-11 0.1µm Power pHEMT

- 0.1µm high performance power / low noise process
- 50µm and 100µm thickness are standard
- Useable gain to 110GHz
- 4V operation - Psat > 800mW/mm, > 50% PAE, and 13dB Gain at 29GHz

PP10 Transfer Curve

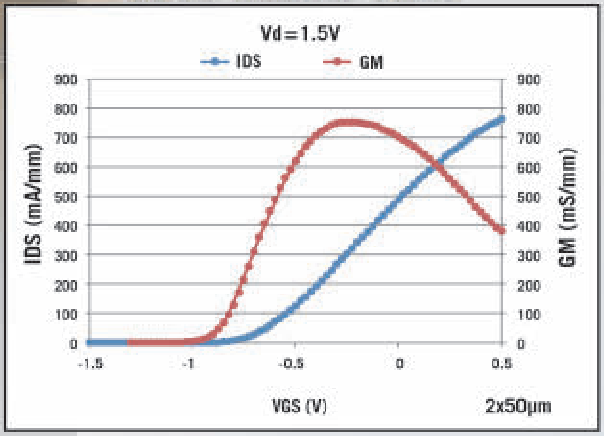

PP10 I-V Curves

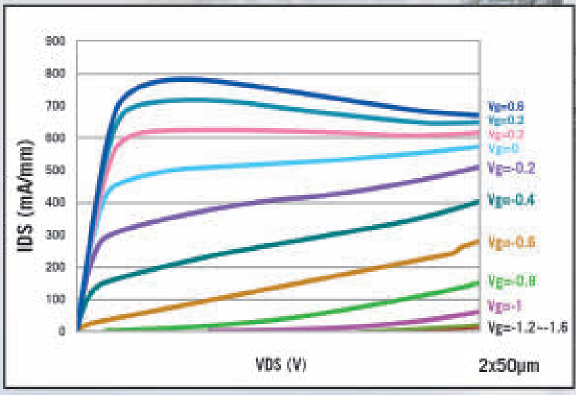

PP10 Load Pull Data

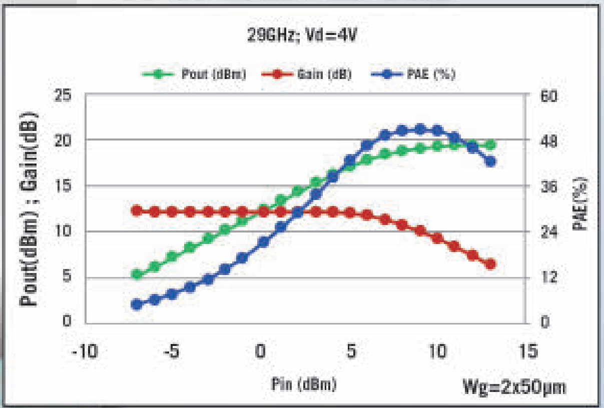

PP10 Max Gain

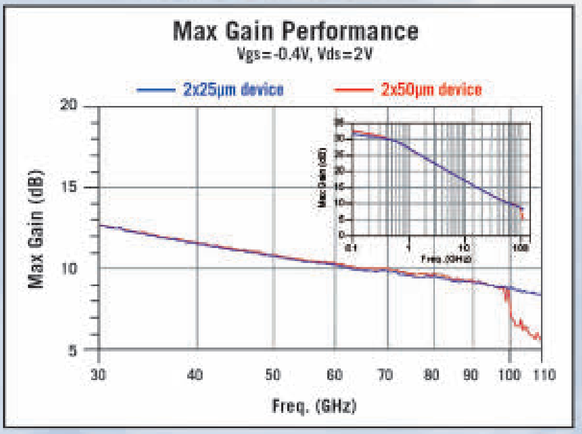

WIN SEMICONDUCTORS CORP. Tel:+886-3-397-5999 Fax:+886-3-397-5069 http://www.winfoundry.com

High Efficiency Continuous Inverse Class F Power Amplifier with Harmonic Impedance Control

Liang Ma, Jianyi Zhou and Weichen Huang
Southeast University, Nanjing, China

This article presents a new set of expressions for current and voltage in the continuous Class F^{-1} mode to produce a variable third harmonic impedance. The harmonic matching network (MN) in the conventional Class F^{-1} is adopted and placed in front of the fundamental MN to control the second and third harmonic impedances as well. The simplified real frequency technique (SRFT) algorithm is utilized to match the fundamental impedance over a wide band. A 10 W GaN HEMT device is used to design a continuous Class F^{-1} power amplifier. Greater than 71 percent drain efficiency is achieved from 2.1 to 2.4 GHz with a maximum efficiency of 84.3 percent at 2.3 GHz. The power amplifier can provide 39.7 to 40.8 dBm output power with greater than 10 dB saturated gain. For a 20 MHz OFDM signal with a peak-to-average power ratio (PAPR) of 8.4 dB, the adjacent channel leakage power ratio (ACLR) is below -50 dBc by employing digital predistortion (DPD), with an average output power of 31.2 dBm and 29.5 percent efficiency. For a 100 MHz, five carrier OFDM signal with a PAPR of 7 dB and an average output power of 32.8 dBm, an ACLR below -45 dBc can be achieved with the help of DPD; in this case, the efficiency is 39 percent. The continuous Class F^{-1} power amplifier has good linearity and is suitable for use in modern communication systems.

The power amplifier (PA) is a key element in wireless communication systems. Higher efficiency is always an important goal for PA designers, as high efficiency means less cost for cooling, system stability and energy conservation. Harmonically-tuned PAs such as Class F and inverse Class F (Class F^{-1}),[1,2] can offer high efficiency via non-overlapping voltage and current waveforms. For example, the Class F PA can offer high efficiency by controlling the first three harmonic impedances.[3] Due to bandwidth limitations, however, they can hardly satisfy the wide band requirements of modern communication networks such as LTE-Advanced, which needs up to 100 MHz signal bandwidth.[4]

To address the narrow bandwidth of the Class F and Class F^{-1} modes, continuous Class F and continuous Class F^{-1} modes have been proposed.[5,6] These continuous modes exhibit broadband characteristics while offering the same power and efficiency as conventional Class F and Class F^{-1}. For continuous modes, the fundamental and second harmonic impedances are extended over wide ranges, providing a wider design space. Initially, the continuous

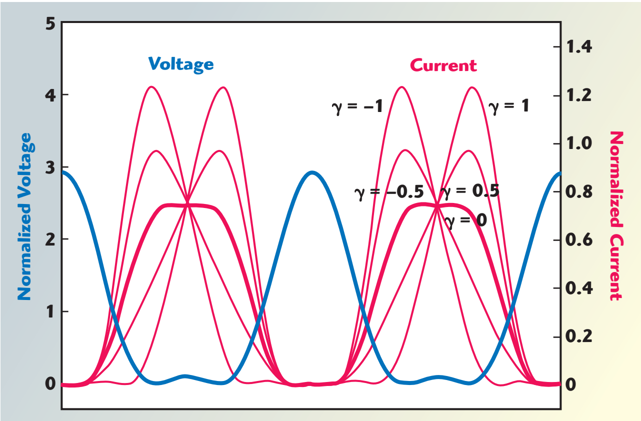

▲ *Fig. 1 Voltage (normalized to V_{dc}) and current (normalized to I_{max}) waveforms of the continuous Class F^{-1} mode.*

mode was validated experimentally using the active load-pull measurement system developed at Cardiff University. In recent years, many physical continuous mode PAs have been realized and reported.[7-11] All show high efficiency over a wide band; however, the harmonic impedances were not as well controlled as the theory showed.

Neither the continuous Class F nor the continuous Class F^{-1} theoretically relieves the third harmonic impedance condition, which cannot be realized in practical design. In this article, the expressions for voltage and current of the continuous Class F^{-1} mode are modifed to extend the range of the third harmonic and a method for matching with harmonic control is described. Both continuous wave and modulated signals are used to test PA performance.

CONVENTIONAL CONTINUOUS INVERSE CLASS F PA

To solve the narrowband problem for Class F and Class F^{-1} PAs, the continuous mode has been presented and researched in recent years.[5,6,12] The continuous Class F^{-1} is one example. Its voltage and current waveforms are described by[11]

$$v(\theta) = V_{dc}\left(1 + \sqrt{2}\cos\theta + \frac{1}{2}\cos 2\theta\right) \quad (1)$$

$$i(\theta) = I_{max}\left(i_{dc} - i_1\cos\theta + i_3\cos 3\theta\right)(1 - \gamma\sin\theta) \quad (2)$$

where V_{dc} is the drain operating voltage, I_{max} is the saturation current of the device, $i_{dc} = 0.37$, $i_1 = 0.43$, and $i_3 = 0.06$, with $-1 \le \gamma \le 1$. ***Figure 1*** shows the voltage and current waveforms.

The load impedance is[11]

$$Z_n = -\frac{V_n}{I_n} \quad (3)$$

where the subscript n is the order of the harmonic component. We define Y_{opt} in terms of the knee voltage V_{knee} and the quiescent bias current I_q as

$$Y_{opt} = \frac{\frac{I_{max} - I_q}{2}}{V_{dc} - V_{knee}} \quad (4)$$

So, the admittances of the continuous Class F^{-1} mode can be expressed as

$$Y_1 = \left(\sqrt{2}i_1 + j\sqrt{2}i_{dc}\gamma\right)Y_{opt}$$
$$Y_2 = -j2(i_1 + i_3)\gamma Y_{opt}$$
$$Y_3 = \infty \quad (5)$$

Figure 2 shows these admittances on a Smith Chart.

MODIFIED CONTINUOUS INVERSE CLASS F PA

As shown in Figure 2, the continuous mode theoretically eliminates the restriction of impedance being a single point, expanding it over a wide range

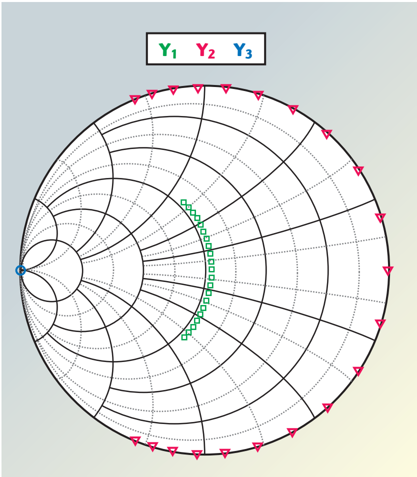

▲ *Fig. 2 Admittances of the continuous Class F^{-1} mode.*

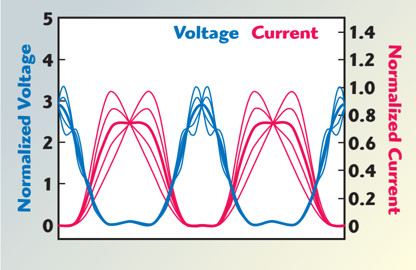

▲ *Fig. 3 Modified voltage (normalized to V_{dc}) and current (normalized to I_{max}) waveforms of the continuous Class F^{-1} mode.*

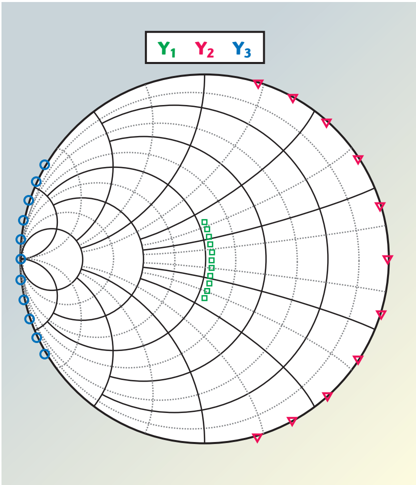

▲ *Fig. 4 Admittances of the modified continuous Class F^{-1} mode.*

on the Smith Chart. This makes designing wideband PAs more feasible. However, there are two drawbacks. First, with variation of γ, the current will exceed the maximum current of the device and current clipping will occur.[13] Second, the third admittance of the continuous Class F^{-1} is just a single point.

Carrubba, et al.,[14] proposed a set of voltage and current waveform formulations that allow reactive excursions of the third harmonic impedance of the continuous Class F PA. Similarly, new voltage and current waveforms of the continuous Class F^{-1} mode, are expressed as

$$v(\theta) - V_{dc}\left(1+\sqrt{2}\cos\theta+\frac{1}{2}\cos 2\theta\right)\left(1+\frac{\gamma}{5}\sin 5\theta\right) \quad (6)$$

$$i(\theta) = I_{max}\left(i_{dc} - i_1\cos\theta + i_3\cos 3\theta\right)(1-\gamma\sin\theta) \quad (7)$$

In order to eliminate current clipping, the current waveform should be modified so as not to exceed the maximum current, I_{max} The modified current from Equation 7 is

$$i(\theta) = I_{max}\left(i_{dc} - i_1\cos\theta + i_3\cos 3\theta\right)\left(1-\frac{\gamma}{2}\sin\theta\right) \quad (8)$$

the new current stays below I_{max} with $-1 \le \gamma \le 1$ as shown in ***Figure 3***. Using Equations 3, 6 and 8, the first three harmonic admittances are

$$Y_1 = \left(\sqrt{2}i_1 + j\frac{\gamma}{\sqrt{2}}i_{dc}\right)Y_{opt}$$

$$Y_2 = -j(i_1 + i_3)\gamma Y_{opt}$$

$$Y_3 = j\frac{40 i_3}{\gamma} \quad (9)$$

Figure 4 shows the impedance condition for the modified continuous Class F^{-1} mode, which has a more flexible third harmonic impedance range compared to the conventional one.

DESIGN OF THE MODIFIED CONTINUOUS CLASS F^{-1} PA

The continuous Class F^{-1} mode theoretically provides high efficiency over a wide bandwidth, but it is difficult to control the fundamental, the second and the third harmonic impedances simultaneously. Some avoid this by matching the fundamental impedance first and then optimizing the matching network to keep away from the low efficiency regions of the second and the third harmonic impedances.[7,8] In these designs, the harmonic impedances are not located in their theoretical regions — the harmonic impedances are matched before the fundamental impedance is matched.

GaN devices, having high breakdown voltages, are suitable for designing continuous Class F^{-1} PAs. The design implemented in this article uses a 10 W CGH40010F GaN HEMT, a packaged device from Cree. The entire output match is shown in ***Figure 5***; the device package[11] is also included.

In order to control the harmonic impedances effectively, the harmonic MN is placed prior to the fundamental MN. The structure of the harmonic MN is illustrated in ***Figure 6***.[15] All of the transmission lines have the same characteristic impedance of 50 Ω.

The transmission line TL_2 is a quarter-wave short-circuited stub, providing a short circuit condition

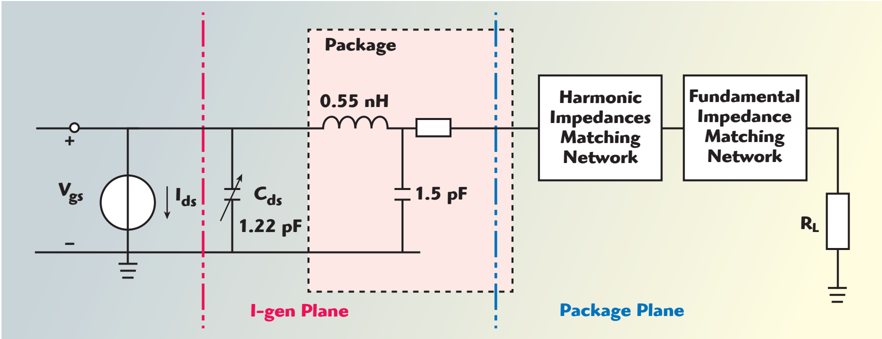

Fig. 5 Output match of the continuous Class F^{-1} PA with approximated equivalent network of device output parasitics.

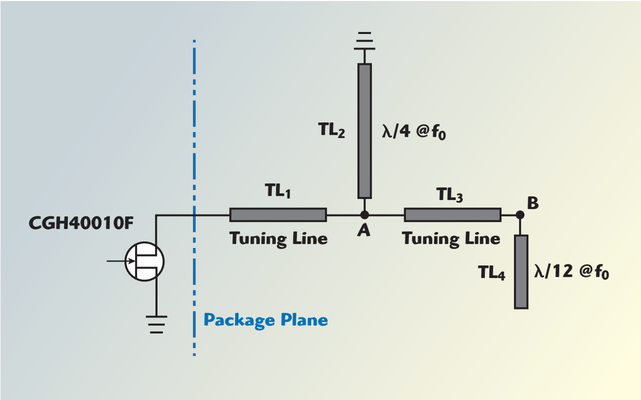

Fig. 6 Harmonic matching network.

to the second harmonic at point A. The effect from posterior circuits to the second harmonic impedance is eliminated. TL_1 is a tuning line that transfers the short-circuit condition at point A to the open-circuit condition at the I-gen plane, together with the device output parasitics. At the

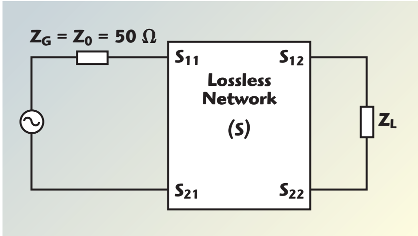

Fig. 7 SRFT matching network.

third harmonic, TL_4 provides a short-circuit condition at point B, while TL_2 provides an open-circuit condition at point A. In this case, the transmission lines TL_1 and TL_3 together with the device parasitics present a short at the I-gen plane. Although the second and third harmonic impedances move from the open-circuit point and the short-circuit point, respectively, with the operational frequency deviating from the center frequency, f_0, the excursion is acceptable in the modified continuous Class F^{-1} mode.

To accomplish broadband matching, the SRFT algorithm is a good method for its simplicity, and it has been widely used in broadband PA design.[8,16] This algorithm was first introduced by Yarman[17] for solving the double-matching problem. In this work, it can be simplified by making the source impedance 50 Ω as shown in ***Figure 7***, where Z_L is frequency dependent complex impedance.

The S-parameters of the lossless network are

$$S_{11}(s) = \frac{h(s)}{g(s)}$$

$$S_{21}(s) = S_{12}(s) = \pm\frac{sk}{g(s)}$$

$$S_{22}(s) = -(-1)^k\frac{h(-s)}{g(s)} \tag{10}$$

where k is the order of the zero of transmission at s = ∞, h(s) and g(s) are n order polynomials, with g(s) a strictly Hurwitz polynomial. h(s) and g(s) can be expressed as

$$h(s) = h_0 + h_1 s + \cdots + h_n s^n$$

$$g(s) = g_0 + g_1 s + \cdots + g_n s^n \tag{11}$$

where n is the number of elements in the lossless network. These two polynomials meet the requirement

$$g(s)g(-s) = h(s)h(-s) + (-1)^k s^{2k} \tag{12}$$

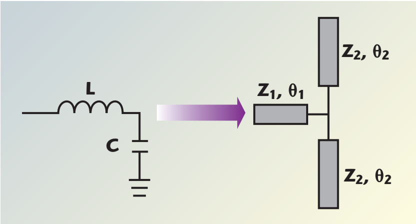

▲ *Fig. 8 Conversion from LC to transmission line network.*

Usually, an LC ladder network consisting of series inductors and shunt capacitors is used as a matching network. In this case, k is 0 and s = jω. The transducer power gain (TPG) can be expressed as

$$\mathrm{TPG}(\omega) = \frac{|l_{21}|^2}{|g(j\omega) + S_L h(-j\omega)|^2} \qquad (13)$$

where $S_L = (Z_l - Z_0)/(Z_L + Z_0)$ and $|l_{21}|^2 = 1 - |S_L|^2$

The nearer TPG approaches 1, the better the matching effectiveness.

Equations 12 and 13 show that the TPG function depends only on the coefficients of h(s). Optimization algorithms can be used to determine these optimal coefficients, and the polynomial is calculated using Equation 12. The normalized driving-point impedance is calculated with

$$\tilde{Z} = \frac{1 + S_{11}}{1 - S_{11}} = \frac{g(s) + h(s)}{g(s) - h(s)} \qquad (14)$$

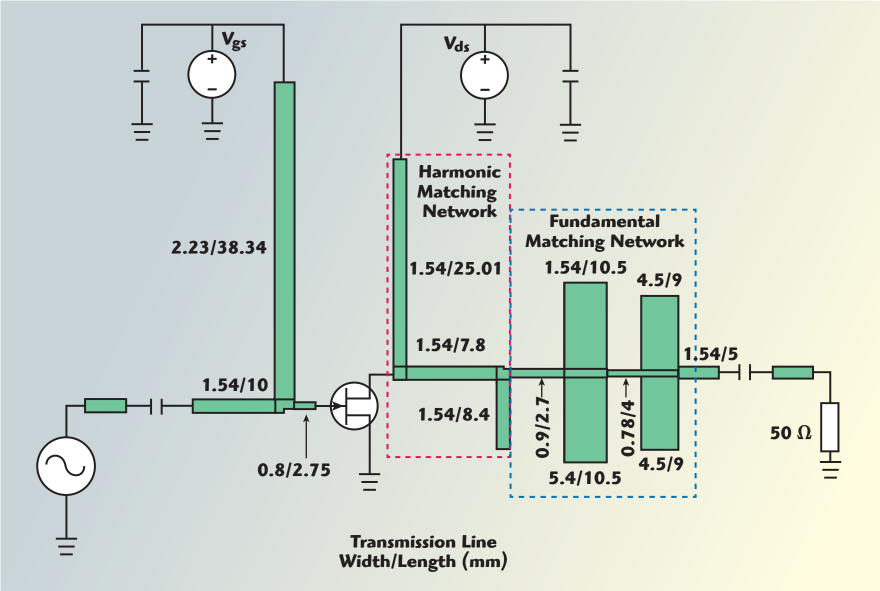

▲ *Fig. 9 Schematic of the continuous Class F⁻¹ PA.*

then the Darlington procedure[18] is used to produce the LC ladder network.

The resulting LC network must be converted to transmission lines in the practical PA design. The series inductor is replaced by a shorted transmission line with a high characteristic impedance,[19] while the shunt capacitor is replaced by two shunt open-circuited stubs, as shown in ***Figure 8***, where

$$\omega L = Z_1 \tan\theta_1$$
$$\omega \frac{c}{2} = \frac{\tan\theta_2}{Z_2} \qquad (15)$$

This design, initially chooses Z_1 as 75 Ω and Z_2 as 25 Ω.

After designing the harmonic MN, the device model and the harmonic MN are used as a whole to perform load-pull in order to determine the

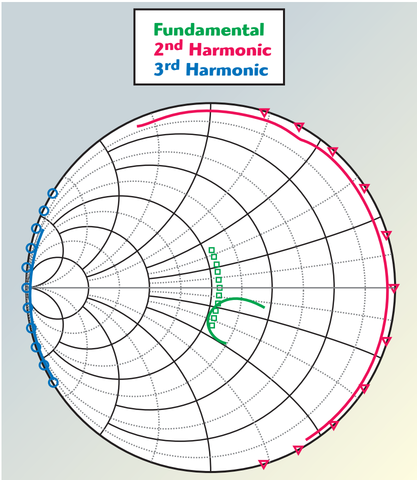

▲ *Fig. 10 Admittances at the I-gen plane.*

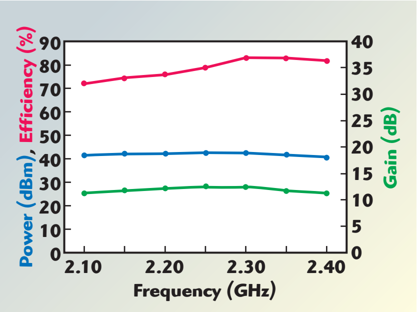

▲ *Fig. 11 Simulated performance of the continuous Class F^{-1} PA.*

optimal fundamental impedance. This is done in the AWR Design Environment using harmonic balance simulation. Then, SRFT is employed to design the fundamental MN. In this design, there are four elements in the LC ladder network.

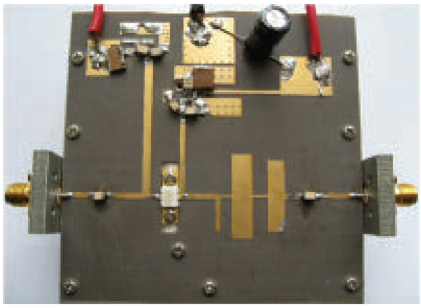

▲ *Fig. 12 Fabricated power amplifier.*

The input match network is designed for high gain, adopting a simple form of a series high impedance transmission line and a short-circuited stub. After the input and output MNs are designed, optimization of the transmission line dimensions is necessary to achieve the best possible

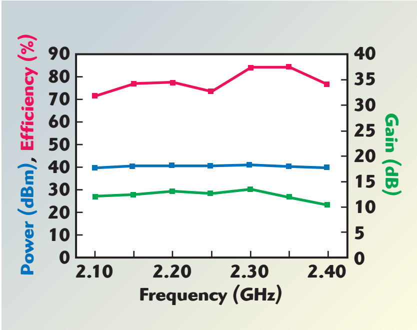

▲ *Fig. 13 Measured performance of the continuous Class F^{-1} PA.*

power, gain and efficiency over the entire bandwidth. The optimized PA is shown in ***Figure 9***.

The frequency band is 2.1 to 2.4 GHz. The fundamental, second and third harmonic admittances at the intrinsic I-gen plane are shown in ***Figure 10***. The figure shows they are well controlled. High efficiency is achieved across the band, as shown by the simulated performance in ***Figure 11***.

FABRICATION AND MEASUREMENT

The PA is implemented with a Cree CGH40010F GaN HEMT mounted on a Taconic RF35 substrate with permittivity of 2.2 and thickness of 20 mils (see ***Figure 12***). The drain bias is 28 V, the gate bias is -3 V and the PA draws a quiescent current of 30 mA.

A single tone continuous wave signal swept from 2.1 to 2.4 GHz with 50 MHz spacing is used for the initial evaluation. Measured performance over the entire bandwidth is shown in ***Figure 13***. The drain efficiency is greater than 71 percent, with a maximum efficiency of 84.3 percent at 2.3 GHz. Output power is 39.7 to 40.8 dBm, and the saturation gain is 10.4 to 13.3 dB.

Two OFDM signals with different bandwidths are used to replicate actual communication systems. The first is a 20 MHz OFDM signal with a PAPR of 8.4 dB and a center frequency of 2.15 GHz. For an average output power of 31.2 dBm, the ACLR is -31.7 dBc (at -20 MHz) and -32.2 dBc (at +20 MHz). To satisfy communication system requirements, linearization is necessary. With DPD, the ACLR is improved to -50.6 dBc (at -20 MHz) and -51.2 dBc (at +20 MHz), as shown in ***Table 1***. In this case, the average efficiency is 29.5 percent. The output power spectrum with and without

TABLE 1

ACLR WITH AND WITHOUT DPD

	ACLR Without DPD		ACLR With DPD	
Signal	**Upper**	**Lower**	**Upper**	**Lower**
Single Carrier OFDM, 20 MHz Bandwidth	–32.2	–31.7	–51.2	–50.6
Five Carrier OFDM, 100 MHz Bandwidth	–32.5	–30.1	–45.9	–46.6

DPD is shown in ***Figure 14a***. To test the performance of PA in broadband systems, the second modulated signal is a 100 MHz OFDM signal with a PAPR of 7 dB. When the average output power is 32.8 dBm with 38 percent drain efficiency, ACLR with DPD is improved to -45.9 dBc (at +100 MHz) and -46.6 dBc (at -100 MHz) from -32.5 dBc (at +100 MHz) and -30.1 dBc (at -100 MHz), as listed in Table 1. The PA meets modern communication systems requirements. The output power spectrum is displayed in ***Figure 14b***.

CONCLUSION

Equations for the continuous Class-F^{-1} mode are modified to extend the range of the third harmonic impedance. The harmonic MN is placed in front of the fundamental MN to achieve better harmonic matching. The harmonic MN is that

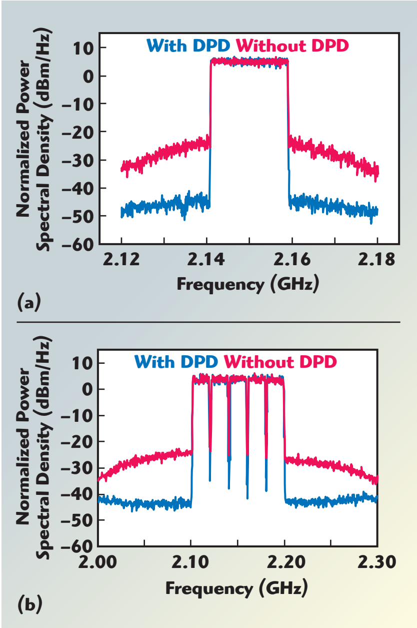

▲ *Fig. 14 Measured output spectrum with and without DPD for 20 MHz, single carrier, OFDM signal (a) and 100 MHz, five carrier, OFDM signal (b).*

of a conventional Class-F^{-1} amplifier, while the fundamental MN is synthesized using the SRFT algorithm. The fabricated PA has a drain efficiency of greater than 71 percent from 2.1 to 2.4 GHz, with a maximum efficiency of 84.3 percent. It produces about 10 W output power with greater than 10 dB gain over the band. Two OFDM signals with different bandwidths are used to evaluate the performance for communication systems. DPD is used for linearization. For a 20 MHz single carrier signal with a PAPR of 8.4 dB, ACLR is below -50 dBc for the upper and lower bandwidth, while the average output power is 31.2 dBm with 29.5 percent drain efficiency. For a 100 MHz, five carrier signal with a PAPR of 7 dB, when the output power is 32.8 dBm and the efficiency is 38 percent, the ACLR is below -45 dBc. The continuous Class-F^{-1} PA has good linearity, suitable for use in modern wideband communication systems. ■

ACKNOWLEDGMENT

The authors would like to acknowledge Dr. Yinjin Sun and Dr. Fan Meng for providing their research group's DPD platform for linearization.

References

1. Y. Woo, Y. Yang and B. Kim, "Analysis and Experiments for High-Efficiency Class-F and Inverse Class-F Power Amplifiers,"

Vector Signals at the touch of a button

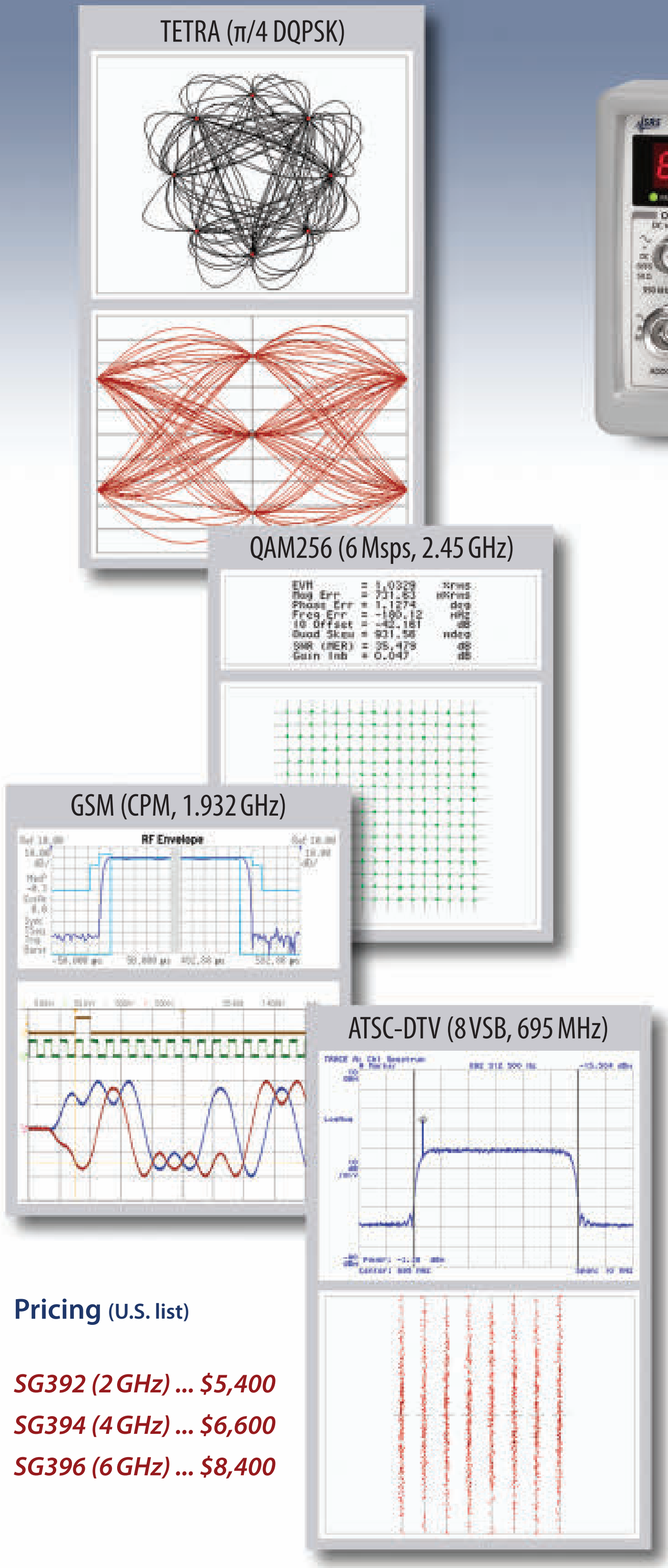

- 2 GHz, 4 GHz & 6 GHz models
- Dual baseband arb generators
- Vector & analog modulation
- I/Q modulation inputs (300 MHz RF BW)
- ASK, FSK, MSK, PSK, QAM, VSB & custom I/Q
- Presets for GSM, EDGE, W-CDMA, APCO-25, DECT, NADC, PDC, ATSC-DTV & TETRA
- GPIB, RS-232 & Ethernet interfaces

The SG390 Series ***Vector Signal Generators*** — taking communications testing to a new level.

The SG390 series has outstanding features and performance: complete vector and analog modulation, dual baseband arb generators, I/Q inputs with 300 MHz RF bandwidth, low phase noise, and an OCXO timebase are all included.

We've also made communications testing quick and easy — everything is available from the front panel of your instrument. Pulse shaping filters, TDMA gating signals, additive white noise, and event markers are all there. Use the built-in pattern or PRBS generators to create data, or upload your own symbol data. Map your symbols to any constellation and transmit at rates up to 6 Msps — it's that simple.

Pricing (U.S. list)

SG392 (2 GHz) ... $5,400
SG394 (4 GHz) ... $6,600
SG396 (6 GHz) ... $8,400

Stanford Research Systems
Tel: (408)744-9040 • www.thinkSRS.com

IEEE Transactions on Microwave Theory and Techniques, Vol. 54, No. 5, May 2006, pp. 1969–1974.
2. J. Kim, G. Jo, J. Oh, Y. Kim, K. Lee and J. Jung, "Modeling and Design Methodology of High-Efficiency Class-F and Class-F^{-1} Power Amplifiers," *IEEE Transactions on Microwave Theory and Techniques*, Vol. 59, No. 1, January 2011, pp. 153–165.
3. F. H. Raab, "Maximum Efficiency and Output of Class-F Power Amplifiers," *IEEE Transactions on Microwave Theory and Techniques*, Vol. 49, No. 6, June 2001, pp. 1162–1166.
4. J. Xia, X. Zhu, L. Zhang, J. Zhai and Y. Sun, "High-Efficiency GaN Doherty Power Amplifier for 100 MHz LTE-Advanced Application Based on Modified Load Modulation Network," *IEEE Transactions on Microwave Theory and Techniques*, Vol. 61, No. 8, August 2013, pp. 2911–2921.
5. V. Carrubba, A. L. Clarke, M. Akmal, J. Lees, J. Benedikt, P. J. Tasker and S. C. Cripps, "The Continuous Class-F Mode Power Amplifier," *European Microwave Conference*, September 2010, pp. 432–435.
6. V. Carrubba, A. L. Clarke, M. Akmal, Z. Yusoff, J. Lees, J. Benedikt, S. C. Cripps and P. J. Tasker, "Exploring the Design Space for Broadband PAs Using the Novel Continuous Inverse Class-F Mode," *European Microwave Conference*, October 2011, pp. 10–13.
7. B. Merrick, J. King and T. J. Brazil, "A Simplified Procedure for the Design of Continuous Class-F Power Amplifiers," *European Microwave Conference*, October 2013, pp. 1479–1482.
8. N. Tuffy, L. Guan, A. Zhu and T. J. Brazil, "A Simplified Broadband Design Methodology for Linearized High-Efficiency Continuous Class-F Power Amplifiers," *IEEE Transactions on Microwave Theory and Techniques*, Vol. 60, No. 6, June 2012, pp. 1952–1963.
9. V. Carrubba, J. Lees, J. Benedikt, P. J. Tasker and S. C. Cripps, "A Novel Highly Efficient Broadband Continuous Class-F RFPA Delivering 74 Percent Average Efficiency for an Octave Bandwidth," *IEEE MTT-S International Symposium Digest*, June 2011, pp. 1–4.
10. R. Tong, S. He, B. Zhang, Z. Jiang, X. Hou and F. You, "A Novel Topology of Matching Network for Realizing Broadband High Efficiency Continuous Class-F Power Amplifiers," *European Microwave Conference*, October 2013, pp. 1475–1468.
11. K. Chen and D. Peroulis, "Design of Broadband Highly Efficient Harmonic-Tuned Power Amplifier Using In-Band Continuous Class-F^{-1}/F Mode Transferring," *IEEE Transactions on Microwave Theory and Techniques*, Vol. 60, No. 12, December 2012, pp. 4107–4166.
12. S. C. Cripps, P. J. Tasker, A. L. Clarke, J. Lees and J. Benedikt, "On the Continuity of High Efficiency Modes in Linear RF Power Amplifiers," *IEEE Microwave and Wireless Components Letters*, Vol. 19, No. 10, October 2009, pp. 665–667.
13. S. C. Cripps, "RF Power Amplifiers for Wireless Communications," *Artech House* Norwood, Mass., 2006.
14. V. Carrubba, R. Quay, M. Schlechtweg, O. Ambacher, M. Akmal, J. Lees, J, Benedikt, P. J. Tasker and S. C. Cripps, "Continuous Class-F3 Power Amplifier Mode Varying Simultaneously First 3 Harmonic Impedances," *IEEE MTT-S Microwave Symposium Digest*, June 2012, pp. 1–3.
15. A. Grebennikov, "High-Efficiency Transmission-Line Inverse Class F Power Amplifier for Active Antenna Arrays," *Asia–Pacific Microwave Conference*, December 2009, pp. 317–320.
16. D. Y. –T. Wu, F. Mkadem and S. Boumaiza, "Design of a Broadband and Highly Efficient 45 W GaN Power Amplifier via Simplified Real Frequency Technique," *IEEE MTT-S International Microwave Symposium Digest*, June 2010, pp. 1090–1093.
17. B. S. Yarman and H. J. Carlin, "A Simplified 'Real Frequency' Technique Applied to Broadband Multistage Microwave Amplifiers," *IEEE Transactons on Microwave Theory and Techniques*, Vol. 30, No. 12, December 1982, pp. 2216–2222.
18. B. S. Yarman, "Design of Ultra Wideband Power Transfer Networks," Wiley, New York, 2010.
19. D. M. Pozar, "Microwave Engineering," Wiley, New York, 2010.

UP TO **100 Watt**

AMPLIFIERS

NOW! 100 kHz to 26.5 GHz

from $995 ea. qty. (1-9)

High-powered performance across wide frequency ranges. Mini-Circuits' class A/AB linear amplifiers have set a standard for wideband high-power performance throughout the RF and microwave industry. Rugged and reliable, they feature over-voltage and over-temperature protections and can withstand opens and shorts at the output! Available with or without heat sinks, they're perfect for demanding test lab environments and for integrating directly into customer assemblies. With standard models covering frequencies from 100 kHz up to 26.5 GHz, chances are we have a solution for your needs in stock. Place your order on minicircuits.com today for delivery as soon as tomorrow! Need a custom model? Give us a call and talk to our engineers about your special requirements!

Model	Frequency (MHz)	Gain (dB)	Pout @ Comp. 1 dB (W)	Pout @ Comp. 3 dB (W)	$ Price* (Qty. 1-9)
NEW! ZVM-273HP+	13000-26500	14.5	0.5	0.5	2195
ZVE-3W-83+	2000-8000	35	2	3	1295
ZVE-3W-183+	5900-18000	35	2	3	1295
ZHL-4W-422+	500-4200	25	3	4	1160
ZHL-5W-422+	500-4200	25	3	5	1670
ZHL-5W-2G+	800-2000	45	5	5	995
ZHL-10W-2G+	800-2000	43	10	12	1295
• ZHL-16W-43+	1800-4000	45	12	16	1595
• ZHL-20W-13+	20-1000	50	13	20	1395
• ZHL-20W-13SW+	20-1000	50	13	20	1445
LZY-22+	0.1-200	43	16	30	1495
ZHL-30W-262+	2300-2550	50	20	32	1995
ZHL-30W-252+	700-2500	50	25	40	2995
LZY-2+	500-1000	47	32	38	2195
LZY-1+	20-512	42	50	50	1995
• ZHL-50W-52+	50-500	50	63	63	1395
• ZHL-100W-52+	50-500	50	63	79	1995
• ZHL-100W-GAN+	20-500	42	79	100	2395
ZHL-100W-13+	800-1000	50	79	100	2195
ZHL-100W-352+	3000-3500	50	100	100	3595
ZHL-100W-43+	3500-4000	50	100	100	3595

Listed performance data typical, see minicircuits.com for more details.

• Protected under U.S. Patent 7,348,854

**Price Includes Heatsink*

Mini-Circuits®

www.minicircuits.com P.O. Box 350166, Brooklyn, NY 11235-0003 (718) 934-4500 sales@minicircuits.com

416 rev AG

MWJ REVIEW BOARD APPROVED

Simplified Feed Prime Focus Reflector Antenna

Li-Jian Zhang, Seong-Gon Choi, Bireng-Chearl Ahn and Jae-Hoon Bang
Chungbuk National University, Cheongju City, South Korea
Dong-Hyun Kim and Young-Tae Choi
NARO Space Center, Korea Aerospace Research Institute

A low cost circular waveguide feed operates from 17.5 to 19.5 GHz with excellent radiation pattern symmetry, low cross polarization and low back radiation. The design consists of a circular waveguide open end with a quarter-wave choke and a pair of E-plane slots. A dielectric slab is employed to improve impedance matching. The feed is energized with a probe at the end of a coaxial cable instead of a conventional circular or rectangular waveguide. The cable introduces a small loss but significantly simplifies the design and reduces fabrication costs.

In recent years, there has been an increasing demand for low cost 25 to 35 dB gain antennas for point-to-point backhaul communication. The prime focus single reflector antenna is very competitive for this application due to its simplicity and low cost. Feeds for the prime focus reflector usually take the form of self-supporting backfire antennas or waveguide open ends. In the latter case, the waveguide is bent in a gooseneck shape and routed to the transceiver unit at the back of the reflector.

If a waveguide open end feed is used, one can replace the gooseneck waveguide with a coaxial cable by attaching the feed to the inside wall of a suitably dimensioned radome, while accepting a small loss introduced by the coaxial cable. In this article, we describe a high performance and low cost coaxially-fed circular waveguide feed suitable for this application.

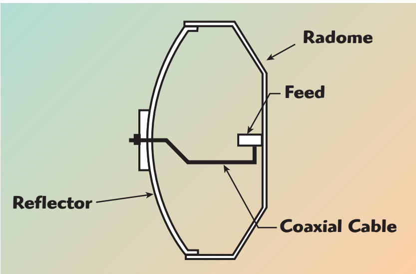

Fig. 1 Feed concept.

FEED DESIGN

Characteristics required of a good prime focus feed include radiation pattern rotational symmetry, sharp gain roll-off beyond the reflector illumination angle, low cross polarization, small back radiation and good impedance matching.

Figure 1 shows the concept. The feed is firmly attached to the inside wall of the reflector's radome. The feed and the radome are dimensioned so that the feed's phase center is exactly at the reflector's focal point. The feed is energized with a probe at the end of a coaxial cable, which is then connected to the transceiver unit. Coaxial cables with low loss (e.g., 1.2 dB/m at 18.5 GHz) are commercially available. A reflector of diameter 290 mm gives 35 dB gain at 18.5 GHz with an efficiency of 71.3 percent. In this case, the cable length of suitably bent shape is about 20 cm, which introduces 0.24 dB loss at 18.5 GHz.

Figure 2 shows the feed cross section. It consists of a circular waveguide of a suitable

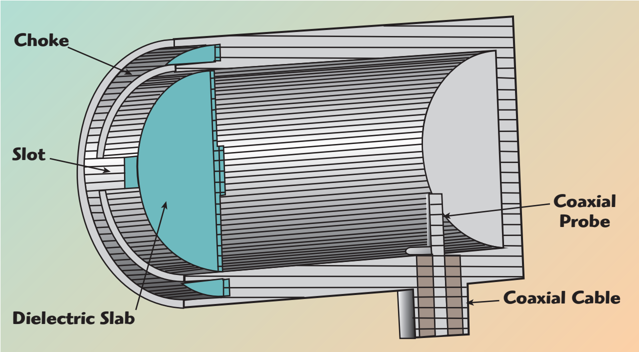

Fig. 2 *Feed cutaway view.*

diameter, a quarter-wave choke, a pair of E-plane slots, a dielectric slab for impedance matching and a coaxial probe. The rotational symmetry of the radiation pattern is dependent on the waveguide diameter with 0.9 to 1.2 λ_0 being optimum.[1] A quarter-wave choke around the aperture wall is added to reduce back radiation as well as to improve the pattern symmetry. A pair of E-plane slots on the "choked" waveguide wall further improves the pattern symmetry;[2] however, because the E-plane slots and the choke increase the feed's reflection coefficient, a dielectric slab (see ***Figure 3***) is added to improve impedance matching.[3]

Figure 4 shows the feed's dimensional parameters. A waveguide diameter of 12 mm (0.74 λ_0 at 18.5 GHz) is chosen to obtain the required 12 dB taper at 65 degrees off boresight. A waveguide wall thickness (t_w) of 2 mm is suitable to contain a choke with a 1 mm gap. Choke length is optimized for the lowest back radiation over the 17.5 to 19.5 GHz band. The optimum value is found to be 3.7 mm (0.228 λ_0 at 18.5 GHz).

Next, a pair of E-plane slots (two rectangular slots 180 degrees apart) are placed so that the aperture's electric field is formed across the slot gap of dimension (h_s). The E-plane slots equalize E- and H-plane patterns by virtually increasing the aperture width in the H plane. The width and length of E-plane slots are optimized for best pattern symmetry: slot length l_{ch} = 3.7 mm and slot gap h_s = 1.88 mm.

The circular waveguide's open end of 0.74 λ_0 diameter does not provide a good impedance match. Further mismatch is caused by the choke and E-plane slots. The match is improved by placing a dielectric slab with thickness (t_{d1}) of 0.5 mm at the base of the choke inside the waveguide. Polycarbonate (PC) with a dielectric constant of 2.7 and loss tangent of 0.002 is used as the dielectric material. The dielectric insert in Figure 3 is composed of two parts, a circular slab for matching and a support ring for attaching the slab to the waveguide. The total thick-

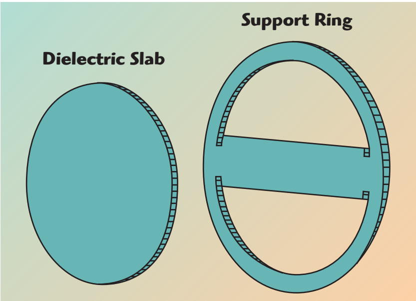

Fig. 3 *Dielectric insert for impedance matching.*

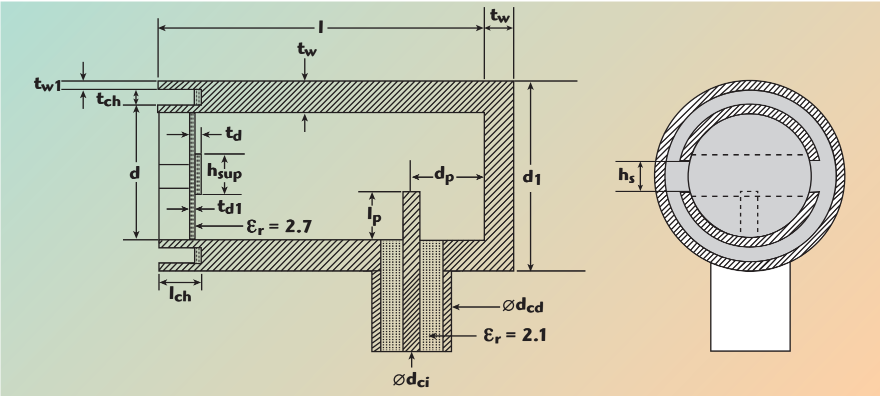

Fig. 4 *Feed dimensional parameters.*

ness t_d of the dielectric insert is 1 mm, including the support ring.

The thickness and location of the dielectric insert are very important in obtaining a good impedance match. The support ring is inserted at the base of the choke gap and then securely bonded so that it does not move or rotate. The combined structure of the slab and the ring is precisely machined. The quarter-wave choke, E-plane slots and dielectric matching structure are all designed for excitation in the dominant TE_{11} mode.

The final design step is optimization of the coaxial probe. The probe diameter is 1.28 mm in an SMA connector. The position from the waveguide back short (d_p) and the length l_p of the probe are optimized using Microwave Studio™ to obtain the lowest reflection coefficient over the 17.5 to 19.5 GHz band. This results in l_p = 3.4 mm and d_p = 6.1 mm. The total length of the feed is $l + t_w$ = 30 + 2 = 32 mm.

Figure 5 shows the feed's E-plane, H-plane and cross-polarized radiation patterns at 18.5 GHz. It has excellent pattern symmetry up to 90 degrees off boresight. Maximum gain is 10 dB with a taper of 12 dB at 65 degrees from the boresight (θ = 65 degrees). At 17.5 GHz and 19.5 GHz, the E- and H-plane gain difference is 1.2 dB and 1.6 dB, and at θ = 65 degrees and maximum gain is 9.6 dB and 10.5 dB, respectively.

The maximum level of the cross polarization in the 45-degree plane is about -27 dB relative to the maximum co-polarized gain. The phase center is 0.6 mm away from the aperture plane toward the reflector surface. With the coordinate origin at the phase center, the far field phase deviations over 0 to 65 degrees off boresight are 1.1 degrees and 4.7 degrees in the E- and H-planes, respectively.

When feeding a 290 mm diameter reflector with F/D = 0.392, the reflector has 35 dB gain with 71.3 percent efficiency, 3 dB beamwidths of 3.94 degrees in the E-plane and 3.84 degrees in the H-plane and sidelobe levels of -26 dB in the E-plane and -23 dB in the H-plane, respectively.

FABRICATION AND MEASUREMENT

Figure 6 shows the fabricated feed antenna. The circular waveguide, choke and E-plane slots are machined out of an aluminum block. A solid piece of polycarbonate material is machined to the dimensions of the dielectric matching plate. The probe of the designed length is placed at the proper position using a panel-mount type SMA connector.

The measured reflection coefficient of the feed is less than -10 dB over 17 to 21 GHz (see ***Figure 7***). The improvement in the impedance matching by the dielectric plate can clearly be seen. ***Figure 8*** shows the E-plane gain pattern of the fabri-

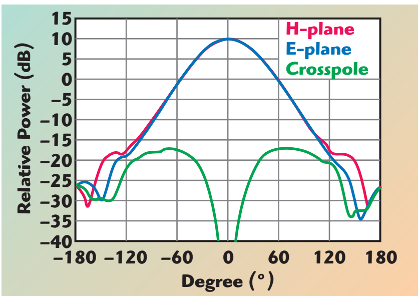

Fig. 5 Simulated far field gain patterns.

cated feed at 18.5 GHz, which agrees well with the simulation. The H-plane gain pattern exhibits similar agreement.

CONCLUSION

A low cost, high performance feed for use in prime focus reflector antennas consists of a circular waveguide, a quarter-wave choke, a pair of slots on the choked wall and a coaxial probe. The feed is connected directly to a coaxial cable that is routed to the transceiver unit at the back of the reflector. The feed demonstrates pattern symmetry, low cross polarization, low back radiation and good impedance matching. Compared to the conventional goose-neck type feed, it has an additional 0.2 to 0.3 dB loss due to the coaxial cable. This is offset by the simplicity of connecting the feed to the transceiver unit.■

ACKNOWLEDGMENT

This work was supported by the Human Resources Development of the Korea Institute of Energy Technology Evaluation and Planning (KETEP) grant funded by the Korean government Ministry of Trade, Industry & Energy (No. 2014020901).

References

1. A.D. Olver, P.J.B. Clarricoats, A.A. Kishk and L. Shafai, "Microwave Horns and Feeds," IEEE, New York, 1994.
2. L. Shafai, "Broadening of Primary Feed Patterns by Small E-Plane Slots," *Electronic Letters*, Vol. 13, No. 4, February 1977, pp. 102–103.
3. J.J. Lee and R.S. Chu, "Aperture Matching of a Dielectric Loaded Circular Waveguide Element Array," *IEEE Transactions on Antennas and Propagation*, Vol. 37, No. 3, March 1989, pp. 395–399.

▲ *Fig. 6 Fabricated feed.*

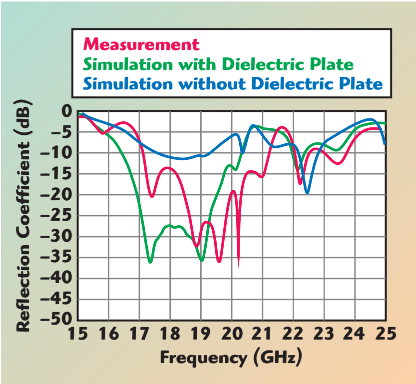

▲ *Fig. 7 Reflection coefficient of the fabricated feed.*

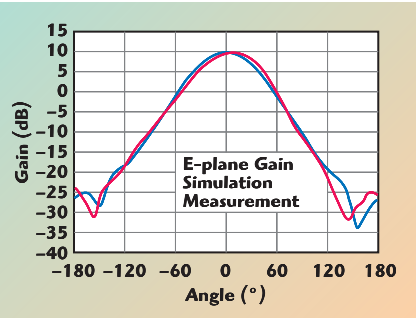

▲ *Fig. 8 E-plane gain pattern of the fabricated feed.*

Ultra Stable Low Power OCXOs Based on IHR Technology

Igor Abramzon and Vadim Tapkov, Magic Xtal Ltd.
Omsk, Russia

Modern trends in the development of high accuracy timing and frequency control systems are placing increased demands on the stability and phase noise of the reference oscillators. For battery supply applications requiring precise synchronization and timing in GPS denied environments such as underwater clocks, high-end mobile radio and portable test equipment, the requirement is for the best frequency stability along with the smallest size and lowest power consumption. Conventional oven controlled oscillators (OCXO) provide acceptable frequency stability and phase noise but consume too much (>1 W) power and cannot be considered adequate for these applications.

One of the most promising recent approaches has been the chip scale atomic clock technology (CSAC) that has a combination of the "atomic" long-term stability with the OCXO style packaging and very low power consumption (130 mW). However, the disadvantage of this approach is poor short-term stability (or Allan variance) determined by the temperature compensated crystal oscillator (TCXO) embedded in the CSAC structure that considerably restricts its wide use. This shortcoming was overcome with the low noise CSAC version (LNCSAC) that employed a miniature low power OCXO based on the internally heated resonator technology (IHR) of the TCXO. Incorporation in the atomic clock of the high stability crystal oscillator has ensured a radical improvement in its short-term stability; however, at the expense of significant increase in the size and doubling of the power consumption[1].

Meanwhile recent improvements of the IHR technology have enabled the creation of new OCXO designs with considerably improved frequency stability, almost to the level of high-end conventional OCXOs and achieved with very low power consumption and a much

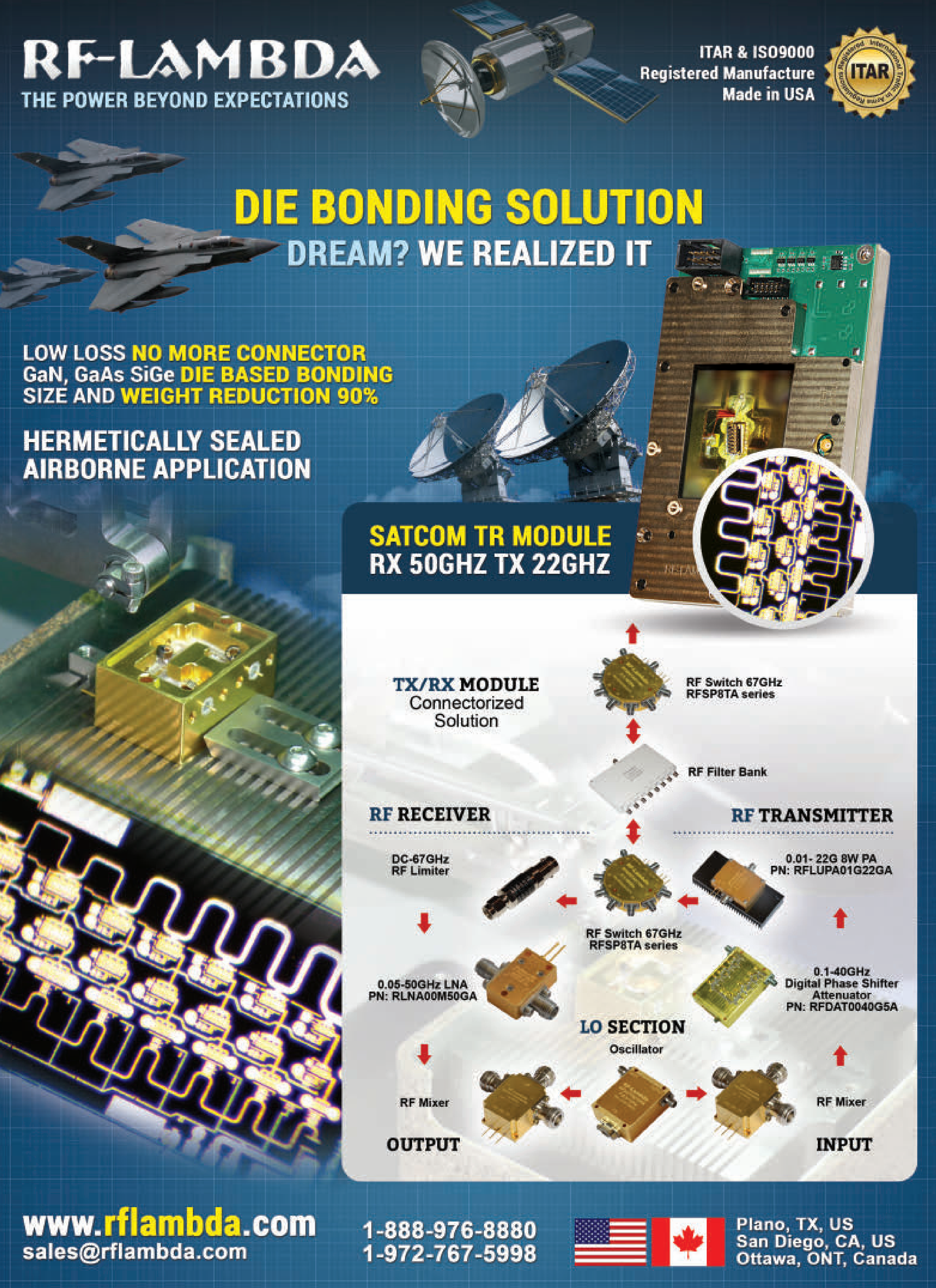
RF-LAMBDA
THE POWER BEYOND EXPECTATIONS
ITAR & ISO9000
Registered Manufacture
Made in USA
ITAR
DIE BONDING SOLUTION
DREAM? WE REALIZED IT
LOW LOSS NO MORE CONNECTOR
GaN, GaAs SiGe DIE BASED BONDING
SIZE AND WEIGHT REDUCTION 90%
HERMETICALLY SEALED
AIRBORNE APPLICATION
SATCOM TR MODULE
RX 50GHZ TX 22GHZ
TX/RX MODULE
Connectorized
Solution
RF Switch 67GHz
RFSP8TA series
RF Filter Bank
RF RECEIVER
RF TRANSMITTER
DC-67GHz
RF Limiter
0.01- 22G 8W PA
PN: RFLUPA01G22GA
RF Switch 67GHz
RFSP8TA series
0.05-50GHz LNA
PN: RLNA00M50GA
0.1-40GHz
Digital Phase Shifter
Attenuator
PN: RFDAT0040G5A
LO SECTION
Oscillator
RF Mixer
RF Mixer
OUTPUT
INPUT
www.rflambda.com
sales@rflambda.com
1-888-976-8880
1-972-767-5998
Plano, TX, US
San Diego, CA, US
Ottawa, ONT, Canada

smaller size. Significant improvement in the performance has become possible due to the minimization of two fundamental factors limiting frequency instability of the IHR oscillators. The first is the non-uniform heating of the crystal plate in the miniature oven structure enclosed in less than a 1 cm^3 IHR holder, resulting in noticeable thermal gradients in the plate varying with the ambient temperature changes. The other factor affecting OCXO stability is the temperature sensitivity of the surrounding circuitry arranged outside the ovenized volume at ambient temperature conditions.

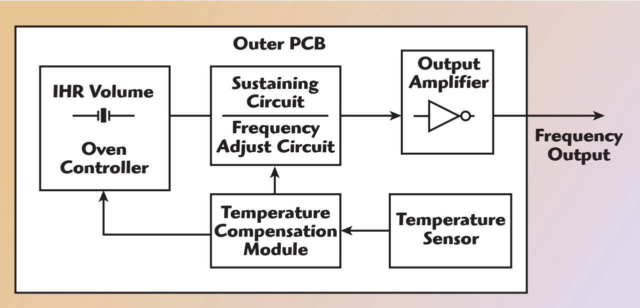

▲ *Fig. 1 Structure of the IHR OCXO with temperature compensation circuitry.*

Significant reduction of the causes of instability has required a new technique for frequency versus temperature stabilization. It assumes that besides physical minimization of temperature sensitivity of the IHR and the sustaining circuitry, the device can eliminate the remaining frequency deviations with the compensation circuitry, correcting the operating temperature and output frequency in accordance with ambient temperature changes. The structure of the new oscillator is schematically depicted in ***Figure 1***.

The new OCXO design consists of the IHR (internally heated resonator with the crystal plate and oven controlled system integrated in the TO-8 vacuum holder) and the electronic circuitry arranged on the outer PC board. The circuitry, except the sustaining stages, electronic corrector and output amplifier, contains the external temperature sensor generating a voltage output linear with the ambient temperature changes. The voltage from the temperature sensor passes to the compensation module producing a correction bias on the oven controller and the electronic corrector minimizing the temperature error of IHR and temperature sensitivity of the sustaining circuitry.

Such a combination of the oven control and electronic compensation techniques has enabled the reduction of the temperature instability factors to almost “zero” enhancing the stability of the IHR devices near the level of double-oven OCXOs. The long-term frequency stability (aging) of the OCXOs is almost entirely determined by aging of the crystal resonator that is mostly caused by mechanical stresses and contamination on the crystal plate surfaces. To minimize the aging factors, the high-overtone crystal plates with small surface-to-volume ratio are utilized in the IHR construction. Together with a very clean manufacturing process, this ensures stability of 10 MHz oscillators to less than 0.1 ppb/day and 15 ppb/year aging rate.

TABLE 1

PARAMETERS OF THE IHR OCXOS WITH DIP8 AND DIP14 COMPATIBLE SIZES

Performance	10 MHz OCXO	100 MHz OCXO
Stability (ppb), -40° to +85°C	2	10
Aging (ppb/day)	0.1	2
Allan Variance (10^{-12})	3	10
Power Consumption (mW)	<170	
Packaging and Size	MXO37/8  15 mm × 15 mm × 9 mm	MXO37/14 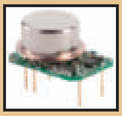 15 mm × 21 mm × 9 mm

TABLE 2

MXO37/R COMPARED TO A DOUBLE OVEN OCXO AND LNCSAC

Typical Performances at 10 MHz	*MXO37/R*	*Double OCXO*	*LNCSAC*
Operating Temperature Range (°C)	–40° to +85°		–10° to +35°
Temperature Stability in the Range (ppb)	0.5	0.2	0.5
Aging Rate (ppb) Per Day Per Month	 0.1 2		 0.01 0.3
Allan Variance, TAU = 1 s, (10^{-12})	2	1	20
Phase Noise (dBc/Hz) at: 1 Hz 10 Hz 1 kHz 10 kHz	 –105 –135 –160 –170		 –88 –120 –145 –150
Input Voltage (V)	3.3 to 5		3.3
Power Consumption (W)	< 0.17	1.5	0.26
Packaging Volume (ccm)	5	16	45

Integration of the whole oven control system with the crystal plate inside the TO-8 resonator package and arrangement of the oscillator circuitry on outer PC board under the TO-8 base has enabled the creation of the smallest devices in this class with DIP8 and DIP14 compatible sizes and pins-out. ***Table 1*** summarizes basic parameters of these OCXOs operating at 10 and 100 MHz frequencies.

The new IHR oscillators provide the temperature stability and aging similar to high-end conventional OCXOs consuming much lower power and occupying less than 2 cm^3. Further improvement of the temperature stability and Allan variance has been achieved with the OCXO design enclosed in the 20 mm × 20 mm × 12.6 mm steel case. This packaging enables operation of the device in harsh environmental conditions and minimizes temperature mismatch between the resonator and the circuitry at non-uniform or transient ambient temperature. The temperature stability of the packaged MXO37/R model significantly exceeds that of the "packageless" MXO37/8 and MXO37/14 oscillators approaching the level of the double-oven OCXOs.

Table 2 shows the primary performance specifications of the MXO37/R oscillators in comparison to double-oven OCXOs and LNCSACs. The MXO37/R model yields somewhat to the double OCXOs in the temperature stability and Allan variance but has the same aging with much smaller size and lower power consumption. As compared with the LNCSAC, the IHR devices exhibit considerable advantages in most performance parameters except long-term stability where the atomic clocks are superiority.

The new generation of the IHR OCXO is well suited for various applications requiring high frequency stability of the reference oscillator with small size and low power consumption. Realized in the DIP8 and DIP14 compatible sizes, these oscillators provide high performance that was previously only available in high-end conventional OCXOs. Packaged in the 20 mm × 20 mm × 12.8 mm case, the IHR devices exhibit an unmatched combination of low power and small size with excellent frequency stability at the level of the double-oven OCXOs.

Although long-term stability of the IHR OCXOs is currently limited to 0.1 ppb/day rate for some applications, especially in harsh environmental conditions, they can be an attractive alternative to CSACs with the same or less power consumption and smaller size, providing better temperature stability, phase noise and Allan variance.

Reference

1. Peter Cash, Dan Boschen, Ramesh Gandham and David Mailoux, "Low Noise Chip Scale Atomic Clock," 2014 IEEE International Frequency Control Symposium.

Magic Xtal Ltd.
Omsk, Russia
www.magicxtal.com

RF Switch with 10 Million Cycle Life and 0.03 dB Repeatability

Dow-Key Microwave has released a high performance and long life SPDT switch, the first in a new line called Reliant Switch™. Covering DC to 26.5 GHz, the bidirectional coaxial switch has a maximum insertion loss of 0.42 dB up to 4 GHz and 0.80 dB at 26.5 GHz. Repeatability of the insertion loss is guaranteed to be 0.03 dB across the entire operating band. Maximum VSWR is 1.15:1 up to 4 GHz and 1.50:1 at 26.5 GHz. The switch has high isolation: 85 dB at 4 GHz and no less than 60 dB at 26.5 GHz. It was designed to have an extended life of 10 million switching cycles for each position, a 10× improvement over a typical RF switch.

The Reliant Switch™ line is being developed to withstand repeated and long life testing of devices under test (DUT). The switches allow easy switching between I/O ports without having to disconnect and reconnect the RF cables to the DUT. More importantly, the consistency of RF measurements requires extremely repeatable insertion loss with long switch life. The Reliant Switch products meet these requirements to help assure the quality and reliability of RF test and measurement systems.

To support a wide range of test and measurement setups and signal switching configurations, Dow-Key Microwave's Reliant Switch™ is offered with latching actuators, optical position indicators and SMA connectors. The 1×2 switch operates in break-before-make mode and will handle 150 W CW input power at 3 GHz when cold switched; in hot-switching applications, a maximum of 2 W CW can be applied to the input across the full frequency range.

VENDORVIEW

Dow-Key Microwave
Ventura, Calif.
www.dowkey.com

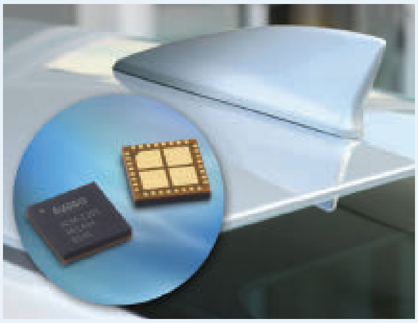

Miniature LNA-Filter Module Improves Car SDARS Coexistence

Automotive satellite radio services like SiriusXM® were introduced in North America in the early 2000s. Technically known as satellite digital audio radio service (SDARS), the system uses a band at 2.3 GHz to broadcast multiple audio channels from satellites to terrestrial radios. Like other commercial signals broadcast by satellites, such as GPS and GNSS, the low level SDARS signal can be difficult to receive, depending on receiver sensitivity and the amount of RF interference at the receiver. Especially in today's heterogeneous wireless environment, it is challenging for SDARS to operate in the presence of nearby large signals, like 4G/LTE and Wi-Fi. Without proper filtering and amplification at the RF front-end, the SDARS signal can go undetected or be disrupted by nearby interferers.

Avago Technologies has developed a miniature LNA-filter RFIC module that addresses the wireless coexistence and car antenna footprint challenges faced by SDARS. The ALM-2203 supports both SDARS and GPS/GNSS applications, integrating three PHEMT LNAs with an FBAR filter in a 5 mm × 5 mm × 0.95 mm package. The highly integrated module reduces BOM cost, PCB area and design time. The front-end module combines 0.83 dB noise figure, enhancing SDARS receiver sensitivity, with high out-of-band input P1dB, enabling SDARS coexistence with cellular, Wi-Fi, Bluetooth and GPS signals. The module, designed to retrofit existing GPS/GNSS LNA-filter systems used in today's shark-fin type car antennas, is approved by SiriusXM.

Avago Technologies
www.avagotech.com

Omni Antennas with Integrated RF Goosenecks for Diversity Applications

With the increasing popularity of radio systems that utilize antenna diversity for improved data throughput and link reliability, selecting the proper antenna is more important than ever. A high performance antenna can help to ensure quality data transmission, especially for applications in urban areas where both the transmitter and receiver may be moving and experiencing difficult transmission environments. Upgrading antennas on an existing product is an easy way to improve performance without the expense of a complete system redesign.

Southwest Antennas has pioneered a new line of rugged omni antennas designed to work with diversity radio systems, multiple-input-multiple-output (MIMO) radios and single antenna systems to overcome the challenges presented by dynamic operating conditions. These antennas combine a rugged, high performance omnidirectional antenna with an integrated RF coaxial gooseneck to provide mounting flexibility. The integrated RF coaxial gooseneck allows each antenna to be positioned for optimal performance, rather than simply conforming to the orientation of the antenna mount. This allows operators to easily reposition the antenna as environmental RF conditions change. To provide performance over the entire operating frequency of each antenna, Southwest Antennas developed proprietary design techniques to ensure the antenna's radiating pattern is not influenced by "common mode" radiation from the integrated gooseneck. Users can also utilize the integrated RF coaxial gooseneck to secure the antenna through MOLLE gear or web gear for dismounted or body-worn applications.

Available in many operating frequencies covering UHF, L-, S- and C-Bands. With a variety of RF connector options, Southwest Antennas' line of integrated RF coaxial gooseneck omni antennas serves a wide range of commercial, government, military and law enforcement markets. Stand-alone RF coaxial gooseneck assemblies with custom RF connector options are available for unique applications.

VENDORVIEW

Southwest Antennas
San Diego, Calif.
sales@southwestantennas.com
www.southwestantennas.com

Software and Mobile Apps

Mobile Device App

VENDORVIEW

AR RF/Microwave Instrumentation's mobile app is available as a free download from Apple iTunes and Google Play. This application is a quick and easy tool to access a variety of content from AR. The home screen icons allow easy navigation to view basic and full product descriptions, app notes, AR's literature library, YouTube videos, contact information and social media activity — all from your mobile device. To download the app, visit www.arww-rfmicro.com/html/ar-moblie-app.asp.

AR RF/Microwave Instrumentation
www.arworld.us

COMSOL Multiphysics 5.2

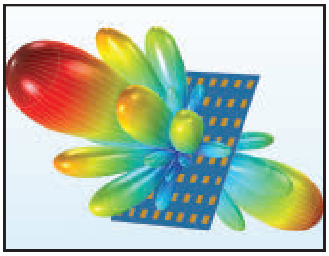

As we work toward 5G and the Internet of Things (IoT), designers of RF and microwaves devices will benefit from multiphysics modeling and simulation of antennas and circuits. The latest version of COMSOL Multiphysics with its Application Builder gives engineers a competitive advantage to deliver the best design solutions by building custom applications that allow anyone on their team or other departments to test different operating conditions and configurations — leaving them free to develop new concepts.

COMSOL Inc.
www.comsol.com

MIPI Receiver Test Software

VENDORVIEW

The Keysight M8085A MIPI C-PHY receiver test solution is designed for engineers in semiconductor and IP vendor companies who need to perform conformance and margin tests. The MIPI C-PHY 1.0 standard supports camera and display applications. The standard comprises multilevel, non-NRZ, non-differential signaling. The M8085A software provides the industry's first complete and standard-conformant routines for calibration of signal parameters and physical layer (PHY) receiver tests. Users can achieve results and gain insight without the need to become experts in the MIPI standard or on using arbitrary waveform generators.

Keysight Technologies Inc.
www.keysight.com

Equiripple Group Delay Filters

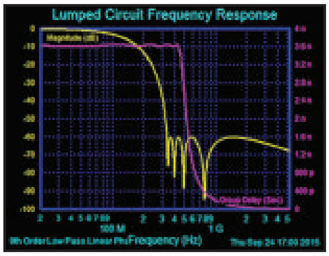

There is a new topology now available for download in FilterSolutions® version 14.3.1—Fully user-definable Elliptic style stopband with Bessel, Linear Phase, or Gaussian style group delay. Both equiripple and single point ripple stopbands are supported. The new feature also works in arithmetic bandpass mode to make wide band, equalized group delay filters. The perpetual license for the lumped element module can be purchased as part number 1301 as a node-locked, or 21301 for the dongle-locked version. The price for either version is $3,900.

Nuhertz Technologies LLC
www.nuhertz.com

PADS 3D Tool

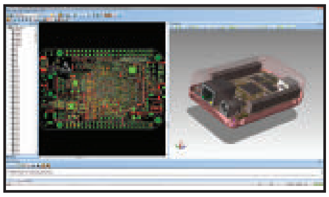

Mentor Graphics announced new PADS® 3D tool capabilities plus major usability enhancements to the PADS flow for printed circuit board (PCB) design. The new technology provides visualization, placement, and design rule checking in 3D, minimizing iterations with mechanical and manufacturing teams. Schematic design and layout enhancements improve usability across the flow for increased user productivity. The powerful 3D engine within the PADS product enables full 3D visualization, placement, design rule checking and PDF creation. Available in a variety of configurations. For more information visit www.pads.com.

Mentor Graphics Corp.
www.mentor.com

Sonnet Suites 16 (V16)

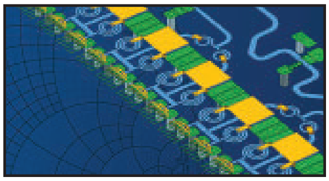

Sonnet® Suites 16 (V16) enables integration with the Modelithics® CLR Library for Sonnet, along with speed increases in larger projects, and new features that give users more control and automation for their designs. The V16 release adds features enabling compatibility with the soon to be released Modelithics CLR Library for Sonnet — a collection of over 270 simulation models for vendor-specific component families, representing nearly 9,000 individual components. The models offer multiple scalability features, including substrate, part-value and pad dimension scaling, plus seamless electromagnetic co-simulation within the Sonnet design environment.

Sonnet Software Inc.
www.sonnetsoftware.com

eLEARNING center

Presented by: Microwave Journal

February Short Course Webinars

Innovations in EDA

5G Physical Layer Modeling: A Communication System Architect's Guide

Presented by: Keysight Technologies

Live webcast: 2/4/16

Technical Education Training

RF and Microwave Heating Simulation and Application Design

Sponsored by: COMSOL

Live webcast: 2/18/16

Technical Education Training

Large Signal Device Characterization for RF Power Amplifier Design

Sponsored by: National Instruments

Live webcast: 2/23/16

Register to attend at mwjournal.com/webinars

Scan page using layar app

Past Webinars On Demand

Technical Education Training Series

- Critical Aspects of Dielectric Constant Properties for High Frequency Circuit Design
- Demystifying MIMO Radar and Conventional Equivalents
- Passive Intermodulation (PIM) in Printed Circuit Boards: Mechanisms and Mitigation
- Port Tuning – EM Accuracy and Circuit Theory Speed
- Antenna Simulation with COMSOL
- Breakthroughs in Phased Arrays and Radars
- Very-Near-Field Scanning Solutions for Pinpoint Diagnosis of EMC Compliance Problems
- GaN Technology in Mainstream RF Energy Applications
- RF PCB Design
- VCO Fundamentals
- Preview of FEKO 14.0 Under Altair HyperWorks
- Highly Integrated Silicon ICs – A Disruptive Technology for Phased Arrays
- Microwave and Millimeter-Wave High Frequency Circuit Material Performance (up to 110 GHz)
- Reducing VNA Test Costs and Decreasing Test Times
- Simulation of Radio Frequency Interference (RFI) in our Wireless World
- Developing Flexible & Reusable, Automated Test Systems with Fast Turnaround Times
- Addressing Electrically Large Antenna System Design with ANSYS HFSS Hybrid Simulation

CST Webinar Series

- Hybrid Simulation for Electrically Large Aerospace Platforms
- Simulation of Implanted Medical Devices
- Advanced PCB Rule Checking for Signal Integrity and EMC
- Graphene-Enhanced Devices: Simulation-based Design from Microwave to Optical Frequencies
- Precise High Frequency Modeling of SMD Components
- Electromagnetic Simulation Supporting Aircraft Certification
- Phased Array, FSS and Polarizer Design

RF/Microwave Training Series

Presented by: Besser Associates

- Passive Components: Dividers, Couplers, Combiners
- Introduction to Radar
- RF Components for Aerospace & Defense

Innovations in EDA

Presented by: Keysight Technologies

- Designing X-Band PAs Using SMT Plastic Packaged GaN Transistors
- How to Design Broadband Impedance Matching Networks
- How to Design Power Electronics: HF Power Semiconductor Modeling

Keysight Technologies Webcast

- Best Practices to Optimize Power Meter Sensor Measurements
- 5G Channel Sounding Challenges and Test Approaches
- Achieving Fast, Accurate Multi-Channel Power Measurements Over a Wide Dynamic Range

NEW PRODUCTS

FOR MORE NEW PRODUCTS, VISIT WWW.MWJOURNAL.COM/BUYERSGUIDE
FEATURING VENDORVIEW STOREFRONTS

COMPONENTS

S-Band Bandpass Cavity Filter

VENDORVIEW

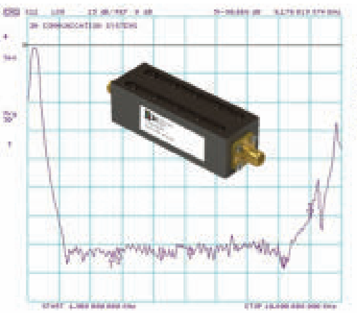

3H Communication Systems announced its new high performance S-Band bandpass cavity filter with >90 dB attenuation. The filter offers low in-band insertion loss of <0.50 dB max. and >90 dB attenuation out to 9 GHz with no need for a lowpass filter. The filter is available in a connectorized package of 3.58"L × 1.0"W × 1.0"H with average power handling of 100 W. This filter meets Mil-Std-202 conditions.

3H Communication Systems
www.3Hcommunicationsystems.com

Cavity Bandpass Filter for Wi-Fi Hotspots

Anatech Electronics introduced the AB5745B579, a 5745 MHz cavity bandpass filter designed for use in Wi-Fi hotspots that delivers high rejection, low insertion loss and can handle RF power levels up to 30 W CW. The AB5745B579 has a center frequency of 5745 MHz, passband of 40 MHz, passband insertion loss of 1.75 dB (± 0.75 dB), rejection of at least 20 dBc, group delay variation of 4 ns over any 0.5 MHz range within the passband, and operates over a temperature range of -45° to +85°C.

Anatech Electronics
www.anatechelectronics.com

RoHS Compliant Flange Mount RF Termination

VENDORVIEW

Barry Industries introduced an RoHS compliant flange mount RF termination, T50R0-1750-1X, which dissipates 1750 W with favorable return loss over a DC to 1 GHz bandwidth. Barry Industries is an ISO9001:2008 certified, ITAR registered manufacturer of high quality thick film resistors, terminations, attenuators and high temperature co-fired ceramic (HTCC) packaging. The thick film on beryllium oxide (BeO) T50R0-1750-1X termination, with its internally matched circuit architecture, exhibits 20 dB or better return loss from DC to 1 GHz.

Barry Industries
www.barryind.com

Digital Step Attenuator

DS Instruments introduced the DAT32H, a compact, full featured RF step attenuator that covers 100 MHz to 13 GHz. The minimum step size is 0.5 dB. Attenuation can be manually via front panel controls, or remotely programmed from a PC over the range of 0 to 31.5 dB with USB SCPI commands. Typical insertion loss at 3 GHz is 5 dB. Input/output VSWR is typically 1.3:1. Maximum input power is +22 dBm. The DAT32H has a complete front panel user interface displaying current attenuation value and confirming device settings. The USB port is configured as power source and industry standard COM port requiring no additional drivers.

DS Instruments
www.dsinstruments.com

2 × 2 Switch Matrix Assembly

Ducommun Inc. RF Products presents a high reliability 2 × 2 redundancy switch matrix for space applications. The operating frequency range is from DC to 5 GHz with an input power of 5 W CW. The operating voltage is from 24 to 34 VDC (28 VDC normally) at extreme temperatures of -20° to +60°C (minimum). The 2 × 2 switch matrix is a latching type switch equipped with suppression diodes, telemetry circuitry, and 50 ohm terminations. Ducommun Inc. RF Products design engineers can create custom versions for your specific applications. Contact them at (310) 513-7256 or (310) 513-7200 for more information.

Ducommun Inc.
www.ducommun.com

24-Bit 2 Msps SAR ADC

VENDORVIEW

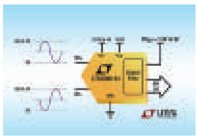

Linear Technology Corp. introduced the LTC2380-24, a breakthrough no latency 24-bit 2 Msps successive approximation register (SAR) analog-to-digital converter (ADC). The LTC2380-24 features an integrated digital filter that averages 1 to 65,536 conversion results real time, dramatically improving the dynamic range from 101 dB at 1.5 Msps to 145 dB at an output data rate of 30.5 sps. This makes the LTC2380-24 ideal for seismic, medical and many other applications demanding high dynamic range. Using an on-chip digital filter to average conversion results, the LTC2380-24 eliminates the processing burden from the digital host, conserving digital resources and the associated power.

Linear Technology Corp.
www.linear.com

Cavity Filters

MCV Microwave cavity filters are available from 10 MHz to 40 GHz and with bandwidth from 0.1 percent to over 66 percent. Cavity filters offer very high Q and low insertion loss, steep skirt selectivity, and narrower bandwidths. MCV combline cavity and waveguide filters include cavity bandpass filters, cavity band reject filters, cavity multiplexers, dual cavity duplexers, combline bandpass filters, interdigital filters, waveguide bandpass filters and dielectric resonator loaded cavity filters.

MCV Microwave
www.mcv-microwave.com

100 W Low PIM Attenuators

VENDORVIEW

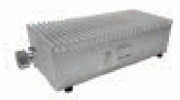

MECA's line of 50 W low PIM attenuators is offered within series and between series in: 4.1/9.5, 4.3/10.0, 7/16 DIN and Type N connectors. With PIM spec of -160 dBc typ, while handling full rated power to +85°C with no power deration over temperature. Covering 0.698 to 2.7 GHz frequency bands and weatherproof IP67 rated. Products are verified for RF performance and PIM tested to the industry standard consisting of 2 × 20 W tones at 25°C in both cell and PCS bands.

MECA Electronics Inc.
www.e-MECA.com

Block Frequency Converter

VENDORVIEW

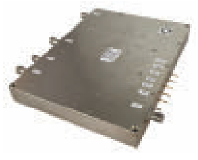

Introducing a new Norden block frequency converter product to extend 40 GHz ELINT systems to 70 GHz. RF input 1 accepts 40 to 60 GHz with a band switch at 50 GHz, RF input 2 accepts 60 to 70 GHz. The single common IF output covers between 2.4 and 17.6 GHz. The

NewProducts

unit operates with an external LO signal of 14.4 GHz or 16 GHz (depending on band). To save DC power unused portions of the unit are turned off, and the unit also has a power down command. It has less than 16 dB noise figure, 5 to 10 dB gain, IIP3 of 0 dBm, and in-band LO to IF leakage of less than -105 dBm.
Norden Millimeter
www.nordengroup.com

Solder for Capacitor Assemblies

VENDORVIEW

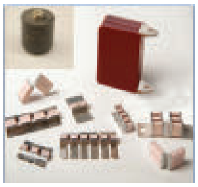

Passive Plus Inc. now provides its customers with the option of specifying capacitor assemblies with SAC 305 solder, which is 100 percent lead free. Previous to this breakthrough, engineers were limited to specifying capacitor assemblies that typically utilized a high lead based solder to attach the leads to the capacitors. PPI has qualified this lead free solder option to enable engineers to design 100 percent RoHS compliant capacitor assemblies, supporting the increasing demands for 100 percent lead free products.
Passive Plus Inc.
www.passiveplus.com

Waveguide Frequency Mixers

VENDORVIEW

Pasternack's new waveguide mixers, also referred to as waveguide converters, are a key building block component of mmWave receivers used to down-convert very high frequency signals to usable RF frequencies for cost effective signal processing. They are also very useful for test and measurement applications to convert signals to frequency levels that can be measured with available equipment. Similarly, these mixers can be used to efficiently up-convert RF signals to millimeter wave frequencies for point-to-point radio and mmWave radar applications.
Pasternack
www.pasternack.com

Switchable RF Attenuator

VENDORVIEW

PMI Model No. SAA-218-6-093-013542 OPT. HERM is a switchable RF attenuator for six signal paths operating from 2 to 18 GHz. Designed to be switched between a low loss state (2 dB loss typical) and a high loss state (20 dB loss typical). The settings will be selected by six digital control bits.

Planar Monolithics Industries Inc.
www.pmi-rf.com

IF Bandpass Filter

VENDORVIEW

The 4C10-70-0.4N11 narrowband IF bandpass filter is centered at 70 MHz with a

3 dB bandwidth of only 450 kHz. This unit offers 40 dB of unwanted signal attenuation only 1.2 MHz away from the center frequency and can be fitted with most any RF connector required. Reactel manufactures a wide variety of filters, multiplexers and multifunction assemblies, contact them today with your requirements.
Reactel Inc.
www.reactel.com

Compact 100 W Termination

Response Microwave Inc. announced the availability of its new compact size termination for use in high power ATE or production applications. The new RMTE.12000Nf100 provides DC to 12 GHz coverage with maximum VSWR of 1.20:1. The 100 W average power is handled via a small package measuring 2.3" × 1.3" × 0.8". Units are standard with N female connectors but options are available with TNC as well. Unit housings are made from clear iridite aluminum with stainless/passivate connectors. For more information on this new line or to discuss your application specific requirement, please contact Response Microwave at (978) 772-3767.
Response Microwave Inc.
www.responsemicrowave.com

Ultra Linear SPDT

VENDORVIEW

RFMW Ltd. announced design and sales support for the PE42422 UltraCMOS SPDT RF switch from Peregrine Semiconductor. The enhanced frequency range of the PE42422 pushes down to 5 MHz providing broadband performance from 5 to 6000 MHz. Typical insertion loss of 0.25 dB at 1000 MHz with 44 dB isolation is maintained. This reflective switch from Peregrine integrates on-board CMOS control logic requiring no external components and supports a wide supply voltage range of 2.3 to 5.5 V. IIP2 of 115 dBm highlights the PE42422's performance. Housed in a 2×2 mm QFN package, ESD tolerance is 4 kV HBM on the RF pins.
RFMW Ltd.
www.rfmw.com

Terminated SP7T/8T Switches

RLC Electronics introduced terminated SP7T and SP8T switches that operate to 34 GHz. These switches are much smaller in size and lighter, and also have the benefit of exhibiting lower current draw than RLC's standard switches. The switch also features extremely low insertion loss and VSWR over the entire DC to 34 GHz range, while maintaining high isolation. The switch can be provided in latching self-cutoff or pulse latching mode, in addition to



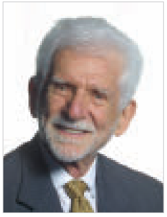

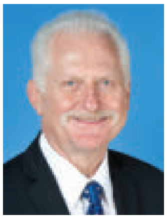

failsafe which is standard on all RLC switches. The DC to 26 GHz version of the switch comes with SMA connectors, while the DC to 34 GHz version is available with K connectors.
RLC Electronics
www.rlcelectronics.com

Digital Isolators

Silicon Labs introduced a new family of multi-channel digital isolators featuring a high-voltage isolation barrier designed to withstand 10 kV surge hits. Based on Silicon Labs' proprietary capacitive isolation technology, the new Si86xxxT digital isolator family provides robust protection against secondary lightning strikes and increases system reliability in a wide range of demanding industrial applications.
Silicon Labs
www.silabs.com

1.5 to 20 GHz Absorptive Pin-Switch

VENDORVIEW

UMCC model SR-GS70-1S is an absorptive SPST pin-switch with a TTL-driver. The switch

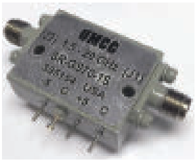

features 4.3 dB insertion loss at 20 GHz, 90 dB min isolation, 1.9:1 VSWR, 25 ns rise/fall time, +24 dBm operating power and +5/-5 V supplies.
Universal Microwave Components Corp.
www.umcc111.com

Power Metal Strip® Resistor

Vishay Intertechnology Inc. announced a new surface-mount Power Metal Strip® current sense resistor featuring a Kelvin 4-terminal connection that reduces TCR down to 35 ppm and enables tight tolerances down to 0.1 percent for increased measurement accuracy. The Vishay Dale WSK1206 combines tight tolerance and low TCR with extremely low resistance values down to 0.01 ohm in the compact 1206 case size. With its 4-terminal construction, the device reduces system errors while eliminating the need for system calibration. The advanced construction of the WSK1206 incorporates a solid metal nickel-chrome or manganese-copper resistive element with low TCR (< 20 ppm/°C).
Vishay Intertechnology Inc.
www.vishay.com

PolyVent High Airflow Series

W. L. Gore & Associates introduced the next generation of its PolyVent High Airflow, which advances the performance capabilities of GORE® Protective Vents screw-in series. Engineered to handle the large pressure differentials caused by extreme weather conditions, the new GORE® PolyVent High Airflow provides twice the airflow, with the same reliable ingress protection as Gore's prior generation of "HA" (High Airflow) units.
W. L. Gore & Associates
www.gore.com

50 dB Dual Directional Coupler

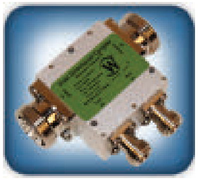

Full 700 to 6000 MHz Bandwidth. 500 W CW. The Model C10364, a 50 dB dual directional coupler, is designed Mismatch Tolerant®, capable of operation, at rated power, into a severe load mismatch condition. Measuring just 2.15" × 2" × 1.36", the C10364 operates with less than 0.2 dB of insertion loss and better than 15 dB of directivity.
Werlatone
www.werlatone.com

CABLES & CONNECTORS

SMA Phase Adjusters

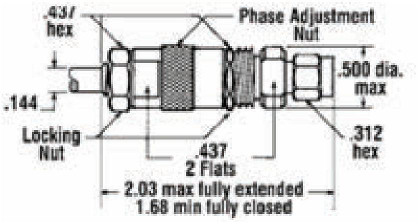

Coaxicom's SMA phase adjusters are designed for high performance and low insertion loss. The 3993 series is just one of a number of quality components all made in the U.S., in stock and ready for quick delivery most often with 24 hours. Features include a means of phase adjustment over frequency ranges up to 18 GHz, an adjustment range of over 180° and a maximum VSWR of 1.30:1, and a phase-adjustable SMA plug (male) direct solder connector for RG405 (0.085" semi-rigid) or Coaxicom's ultra-flex and blue-flex cables.
Coaxicom
www.coaxicom.com

Ultra-Miniature Cable Assemblies

Fairview Microwave Inc. introduced a brand new family of ultra-miniature UMCX, WMCX and HMCX32 cable assemblies. Commonly used to connect an external antenna to a mini-PCB, these flexible micro-coax jumpers operate from DC to 6 GHz and are ideal for use in wireless communications systems. Additional wireless applications include antennas for GPS and other radio systems, Wi-Fi, wireless LAN, Bluetooth, ZigBee, LTE, mini-PCI and PDA/PCS/cellular handset applications. Fairview Microwave's new UMCX and WMCX cable assemblies are compatible with Hirose® U.FL™ and W.FL™ connectors respectively, and feature miniature snap-on connectors with mated connection heights ranging from only 1.2 to 2.5 mm.
Fairview Microwave
www.fairviewmicrowave.com

NewProducts

AMPLIFIERS

25 to 100 W, 1 to 6 GHz Amplifier

VENDORVIEW

Models 25S1G6AB, 50S1G6AB, 100S1G6AB are solid-state; 25, 50 and 100 W Class AB amplifier designs that

instantaneously cover the 1 to 6 GHz frequency band in a single benchtop unit. These amplifiers provide 25, 50 or 100 W output power, depending on model, in approximately half the size of a traditional Class A design with increased efficiency at a more economical price.

AR RF/Microwave Instrumentation
www.arworld.us/post/100S1G6AB.pdf

Balanced LNA

VENDORVIEW

Custom MMIC is now offering a new, low noise amplifier (LNA) that is perfect for EW and communication systems where small size and low power consumption are critical — the CMD223 9 to 18 GHz balanced low noise amplifier. The CMD223 features a low noise figure, high-gain, broadband performance, excellent return losses, and single positive supply voltage. At 13.5 GHz the CMD223 delivers greater than 22 dB of gain with a corresponding output 1 dB compression point of +13.5 dBm and a noise figure of 1.5 dB.

Custom MMIC
www.custommmic.com

2 W W-Band Solid-State Power Amplifier

VENDORVIEW

QuinStar Technology introduced state-of-the-art performance in W-Band power amplifiers, now offering the QPN-94043330 a 92 to 96 GHz SSPA with 33 dBm Pout and 30 dB gain, the QPW-75A52125 a 75 to 105 GHz SSPA with 21 dBm Pout and 26 dB gain, as well as the QLW model LNA's offering 3.5 dB from 80 to 98 GHz, 4 dB from 70 to 85 GHz, and 5 dB from 75 to 110 GHz. Many other models exist from 18 to 140 GHz and are available upon request.

QuinStar Technology Inc.
www.QuinStar.com

SYSTEMS

W-Band Receiver

VENDORVIEW

Model SSR-9630831560-10-S1 is a W-Band receiver. The receiver has a typical conversion

gain of 15 dB with a typical RF input power of -60 dBm in the frequency range of 92 to 100 GHz and an IF output frequency range of DC to 4 GHz. The required LO power and frequency range are +5 dBm and 16 GHz. The LO and IF port are both equipped with female SMA connectors and the RF port is a WR-12 waveguide with a UG-387/U flange.

SAGE Millimeter Inc.
www.sagemillimeter.com

SOURCES

Signal Generator

VENDORVIEW

The Model 845-26 is a low noise and fast-switching microwave signal generator covering a continuous frequency range from 100 kHz up to 26 GHz. The 845-26 has 0.001 Hz frequency resolution, fast switching (only

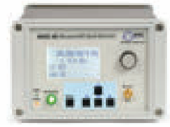

400 µs frequency), excellent phase noise (-108 dBc/Hz at 10 GHz and 20 kHz offset) and a high power output. The Model 845-26 operates with an ultra-stable temperature compensated 100 MHz reference (OCXO) and can be phase-locked to any external reference from 1 to 250 MHz.

Berkeley Nucleonics
www.berkeleynucleonics.com

Low Energy Front-End Modules

VENDORVIEW

Skyworks offers two low-power Bluetooth® low energy (BLE) front-end modules (FEM) for connected home, wearable and industrial

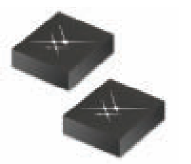

applications. The SKY66110-11 and SKY66111-11 FEMs operate between 2.4 and 2.485 GHz, with power consumption of only 10 mA in transmit mode. They are suitable for products operating from coin cell batteries including sensors, beacons, smart watches, thermostats, smoke and carbon dioxide detectors, wireless cameras and audio headphones, hearing aids and medical pendants. The FEMs more than double the range when compared to a stand-alone system on chip solution. The SKY66111-11 FEM features adjustable output power.

Skyworks Solutions Inc.
www.skyworksinc.com

Miniature Optimized Band Surface-Mount VCO

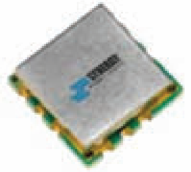

This miniature size VCO model DCO432493-3 operates from 4325 to 4950 MHz over an 11 V tuning range with only a +3 V bias. Key features include a planar resonator construction, an output power of -2 dBm (min.), a harmonic suppression of 18 dB (Typ.) and low phase noise performance, -87 dBc/Hz at 10 kHz (typ.) and -112 dBc/Hz (typ.) at 100 kHz offsets. Housed in an RoHS surface-mount package measuring just 0.3" × 0.3" × 0.100" (L x W x H), this low power consumption product is ideal for handheld and battery driven applications.

Synergy Microwave Corp.
www.synergymwave.com

CLV Series VCOs

VENDORVIEW

The CLV Series VCOs utilize a microstrip topology that is based on a patented high-Q distributed resonator design which delivers low phase noise and linear tuning spanning over a wide range of frequency bands covering 400 MHz to 4 GHz. They exhibit excellent tuning linearity and superior harmonic suppression making them the ideal choice for test equipment and satellite communication applications.

Z-Communications Inc.
www.zcomm.com

SOFTWARE

Wireless InSite® Propagation Software

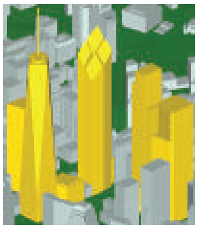

Remcom announced a new version of Wireless InSite®, its site-specific radio propagation software for the analysis of wireless communication systems. This version, Release 2.8, supports the import of KMZ and COLLADA geometry files. It also provides several other enhancements, including significant speed improvements to the processing of terrain and city geometry, enabling simulations that include larger or more complex urban scenes. The ability to import and create KMZ (.kmz) and COLLADA (.dae) geometry files is particularly useful for adding single structures, such as bridges, high resolution buildings, or new construction to a scene.

Remcom
www.remcom.com

ANTENNAS

3D RF Tracking-Antenna Array

VENDORVIEW

Aaronia's new 3D RF Tracking Antenna IsoLOG 3D includes a high density, customizable LPDA sector array. A total of at least 8 and up to 36 LPDA antennas, for horizontal and for vertical polarization can be integrated. Additionally 8 or 16 specialized low frequency antennas can be added to extend the

frequency range down to 9 kHz. In total, up to 52 independent antennas can be equipped. The antennas are protected by an included radom which can be ordered in any color and optional prints. The radom is watertight, shock- and heat-proofed to withstand the harshest conditions.

Aaronia AG
www.aaronia.com

S- and C-Band Omni Antennas

VENDORVIEW

Southwest Antennas offers an innovative line of S- and C-Band Omni Antennas with an integrated sealed spring base, which is stiff enough to keep the antenna oriented vertically but can bend and flex if pushed, reducing the chance of damage to the antenna or attached radio equipment. These antennas are an ideal solution for wireless cameras/ broadcast video or mobile handheld radios used by first responders.

Southwest Antennas
www.southwestantennas.com

TEST EQUIPMENT

Coaxial Probe

The T-Probe is a coaxial probe that offers one signal pin on center and several fixed pitch ground contacts with low inductance. The probe is claimed to provide excellent electrical performance for applications having test points with adjacent grounds. It has pitch ranges of 0.8/1.5/2.5 mm from signal to ground contact and is produced by a precision manufacturing process. It is available for signal probing tests in applications such as RF and microwave module signal insertion/output measurement, high speed digital and high frequency circuit board analysis.

Withwave
www.with-wave.com

MICRO-ADS

Introduction to RF and Microwave Passive Components

Richard Wallace and Krister Andreasson

Richard Wallace and Krister Andreasson wrote an introduction and overview of RF, microwave and millimeter wave passive components for those seeking a broad, non-mathematical explanation of the circuits commonly found in wireless systems, whether commercial, industrial or military. Technicians, field service, sales and marketing staff entering the industry, as well as digital and systems engineers, will find the information helpful in developing an understanding to illuminate the “black magic” of RF systems.

The book begins with a discussion of frequency bands and what frequencies are considered “microwaves,” then touches on applications that rely on them — mobile communications and GPS, for example. Chapter 2 introduces the need to consider signal propagation, the interplay of transmitted and reflected signals, and the various transmission lines used to connect circuit components (e.g., coax, waveguide, planar media). Chapter 3 treats antennas and feed networks. Rather than covering millimeter wave frequencies in the first chapter, the authors chose a separate chapter to define the frequency range, applications and transmission media for millimeter wave signals. After addressing these fundamentals, the second half of the book (Chapters 5 through 8) reviews the passive components that are used in microwave and millimeter wave systems: isolators, circulators and other ferrite circuits; hybrids and their applications; power dividers and combiners; and filters.

Both authors have extensive careers in the industry and have taught courses for those working in the field. This is reflected in the book, which is intentionally pragmatic. Wallace’s career includes Ericsson, Infineon and Texas Instruments, as well as teaching since 2002. Andreasson has taught since 1987, and his industrial experience includes LGP Telecom and Microdata Telecom.

If you want to gain a deep technical understanding of any of the passive components covered in this text, this is not the book you need. However, if you seek a basic understanding, the material provides a solid introduction and, since it covers a broad range of components, is a good reference.

To order this book, contact

Artech House
www.artechhouse.com
ISBN: 978-1-63081-008-5
390 pages
$149 for the hardcover edition
Also available in eBook format

AdvertisingIndex

Advertisers in blue are enabled with the layar app

Sales Representatives

Microwave Journal
Frequency Matters.

Eastern and Central Time Zones
Chuck Boyd
Northeast Reg. Sales Mgr.
(New England, New York, Eastern Canada)
685 Canton Street
Norwood, MA 02062
Tel: (781) 619-1942
FAX: (781) 769-5037
cboyd@mwjournal.com

Michael Hallman
Eastern Reg. Sales Mgr.
(NJ, Mid-Atlantic, Southeast, Midwest, TX)
4 Valley View Court
Middletown, MD 21769
Tel: (301) 371-8830
FAX: (301) 371-8832
mhallman@mwjournal.com

Pacific and Mountain Time Zones
Brian Landy
Western Reg. Sales Mgr.
(CA, AZ, OR, WA, ID, NV, UT, NM, CO, WY, MT, ND, SD, NE & Western Canada)
144 Segre Place
Santa Cruz, CA 95060
Tel: (831) 426-4143
FAX: (831) 515-5444
blandy@mwjournal.com

International Sales
Richard Vaughan
International Sales Manager
16 Sussex Street
London SW1V 4RW, England
Tel: +44 207 596 8742
FAX: +44 207 596 8749
rvaughan@horizonhouse.co.uk

Germany, Austria, and Switzerland (German-speaking)
WMS.Werbe- und Media Service
Brigitte Beranek
Gerhart-Hauptmann-Street 33,
D-72574 Bad Urach
Germany
Tel: +49 7125 407 31 18
FAX: +49 7125 407 31 08
bberanek@horizonhouse.com

Korea
Young-Seoh Chinn
JES Media International
2nd Floor, ANA Bldg.
257-1, Myungil-Dong
Kangdong-Gu
Seoul, 134-070 Korea
Tel: +82 2 481-3411
FAX: +82 2 481-3414
yschinn@horizonhouse.com

China
Shenzhen
Michael Tsui
ACT International
Tel: 86-755-25988571
FAX: 86-10-58607751
michaelt@actintl.com.hk

Shanghai
Linda Li
ACT International
Tel: 86-21-62511200
lindal@actintl.com.hk

Beijing
Oasis Guo
ACT International
Tel: 86-13011108861
oasisg@actintl.com.hk

Hong Kong, Taiwan, Singapore
Mark Mak
ACT International
Tel: 852-28386298
markm@actintl.com.hk

Japan
Katsuhiro Ishii
Ace Media Service Inc.
12-6, 4-Chome,
Nishiiko, Adachi-Ku
Tokyo 121-0824, Japan
Tel: +81 3 5691 3335
FAX: +81 3 5691 3336
amskatsu@dream.com

Ed Kiessling Traffic Manager/Inside Sales • 685 Canton Street Norwood, MA 02062 • Tel: (781) 619-1963 FAX: (781) 769-6178 • ekiessling@mwjournal.com

FABS and LABS

LPKF Continues to Make a Global Name for Itself

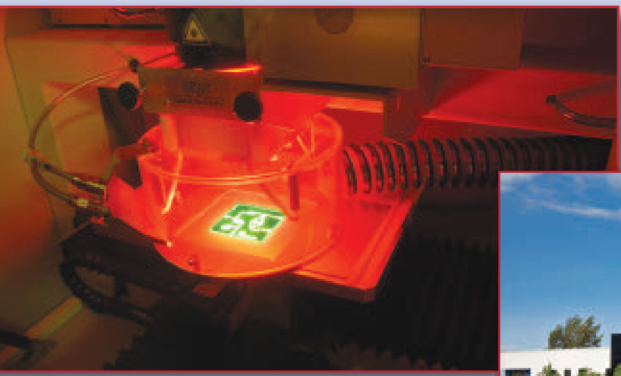

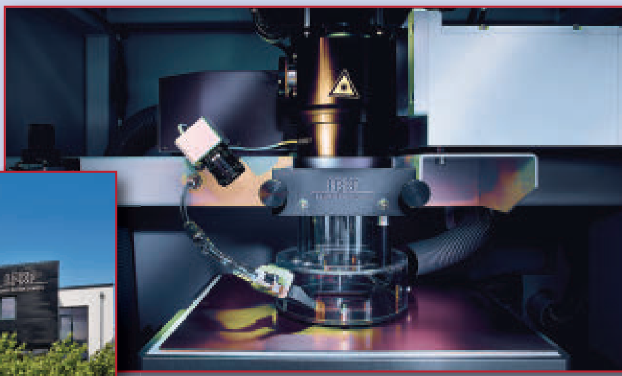

Those familiar with LPKF, the technology it uses and the products it manufactures would be justified in thinking that the first two letters of the name might stand for 'Laser' and 'Prototyping'. In fact, LPKF stands for Leiterplatten-Kopierfräsen, which translated means circuit board copy milling and refers to the establishment of the company in 1976 when it began to make a name for itself with its unorthodox procedures for the prototyping of printed circuit boards, establishing its CAD controlled milling technology as an efficient and pollution free alternative to etching.

Headquartered in Garbsen, Germany, LPKF Laser & Electronics AG has continued to innovate and expand its horizons, both technically and geographically. Currently the company boasts around 800 employees, serving customers worldwide via subsidiaries and/or commercial representatives. Around 20 percent of the workforce is engaged in research and development.

Microwave Journal readers are likely to be most familiar with LPKF's PCB prototyping capability. They use high-energy light as a tool and offer very advanced capabilities. Modern lasers can work in the 50 µm/15 µm range, which is put into perspective by the fact that a human hair is approximately 120 µm thick!

There are different mechanisms for laser machining: The laser vaporizes tiny amounts of material with each pulse. It can also heat up partitions, expose light sensitive layers or even weld parts by melting them. The one thing that LPKF processes have in common is that the micro-machining process puts high demands on precision, with less emphasis on pure laser power.

As the main site for PCB production systems and Rapid Prototyping (RP) systems, the Garbsen headquarters is staffed by approximately 300 people. It houses the R&D centers for different business units, several laboratories for material and applications tests, the business development division, which is geared up to recognize and meet market requirements, as well as the production and service departments.

In 1994 LPKF set up a wholly owned subsidiary in Slovenia, which is responsible for producing and developing PCB and SMT systems, working in conjunction with the team in Garbsen. The facility also develops and produces laser sources exclusively for its own prototyping and production systems.

LPKF has key branches in U.S., Japan and South Korea and recognized the potential and significance of the China market by establishing LPKF Tianjin Co. Ltd. as a new subsidiary in 2000. Since then China has become LPKF's largest service location, positioned in six different cities as well as Hong Kong. Almost 100 service technicians and sales representatives are employed to attend to installed systems and the needs of customers. LPKF offers 24/7 services all around the world and runs a customs warehouse with spare parts.

On the heels of its 40th anniversary, LPKF can celebrate significant development since its inception and its ambitions do not stop there. The company has set a goal of freeing laser technology from its image as an expensive, elite product, and establishing it as an economical production technology. LPKF is entering new markets and evolving to cater for the latest technologies. For instance, any modern smartphone uses Laser Direct Structuring (LDS) parts for connection purposes or as antenna. The progression from CAD controlled milling continues.

www.lpkf.com

WERLATONE®

Celebrating 50 Years of High Power Passive Components

Mismatch Tolerant®

Test & Measurement Couplers

- **Up to 1000:1 Bandwidth**
- Low Insertion Loss
- Power Levels of 20 W CW to 20 kW CW
- Designs for Laboratory use Worldwide
- **Covering Full DC - 6000 MHz!**

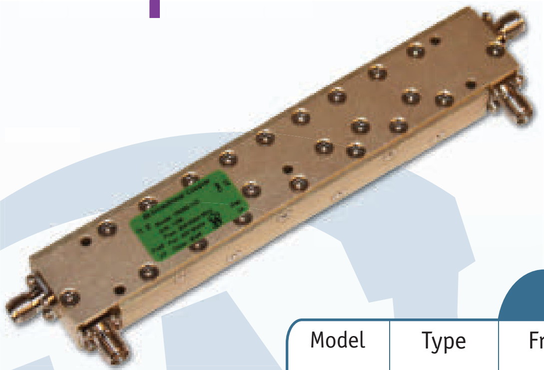

NEW

Directional Couplers

Model	Type	Frequency (MHz)	Power (W CW)	Coupling (dB)	Insertion Loss (dB)	VSWR (ML)	Size (Inches)
C6021	Dual	0.01-1000	500	40	0.45	1.30:1	6.7 x 2.27 x 1.69
C5725	Dual	0.1-1000	500	40	0.5	1.25:1	5.2 x 2.67 x 1.69
C9688	Dual	1-1000	800	40	0.5	1.20:1	6 x 2.2 x 2.2
C7734	Dual	30-2500	100	43	0.35	1.25:1	3.5 x 2.6 x 0.7
C8188	Uni	30-3000	20	20	2.4	1.35:1	6 x 1.5 x 1.1
C3910	Dual	80-1000	200	40	0.2	1.20:1	3 x 3 x 1.09
C8373	Bi	100-2500	200	20	0.8	1.25:1	9.58 x 1.48 x 0.88
C7711	Dual	100-3000	100	40	0.35	1.25:1	3 x 2.2 x 0.7
C7058	Bi	200-2000	200	10	0.3	1.25:1	6.4 x 1.6 x 0.72
C8060	Bi	200-6000	200	20	1.1	1.40:1	4.8 x 0.88 x 0.5
C7248	Bi	300-3000	100	6	0.35	1.25:1	6 x 2 x 0.85
C8000	Bi	600-6000	100	30	0.4	1.25:1	1.8 x 1 x 0.56
C8214	Bi	700-2500	100	6	0.35	1.25:1	6 x 2 x 0.85
C10462	Dual	700-4200	250	40	0.2	1.30:1	2 x 2 x 1.06
C10525	Dual	700-4200	700	50	0.2	1.35:1	2.15 x 2 x 1.36
C10536	Dual	700-4200	1000	50	0.2	1.35:1	2.15 x 2 x 1.36
C10006	Dual	700-4200	2000	50	0.2	1.35:1	3 x 3 x 1.59
C10117	Dual	700-6000	250	40	0.2	1.30:1	2 x 2 x 1.06
C10364	Dual	700-6000	500	50	0.2	1.35:1	2.15 x 2 x 1.36
C8644	Bi	1800-6100	60	20	0.4	1.25:1	1.1 x 0.75 x 0.48

Mismatch Tolerant® Designed to operate, at rated power, into Severe Load Mismatch Conditions

Werlatone, Inc.®
17 Jon Barrett Road
Patterson, NY 12563
T 845 278 2220
F 845 278 3440
sales@werlatone.com
www.werlatone.com

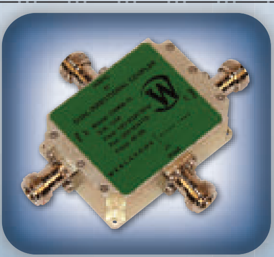

Directional Couplers

0° Combiners/Dividers

90° Hybrid Couplers

180° Hybrid Combiners

Absorptive Filters